Università degli studi di Salerno

Dipartimento di Chimica e Biologia "Adolfo Zambelli"

Tesi di dottorato in Chimica

XXX Ciclo

New metal catalysts for the synthesis of polyolefins and bioderived polymers

Tutor: Dr Stefano Milione

Co-Tutor: Prof. Alfonso Grassi

Coordinatore: Prof. Gaetano Guerra

Candidato

Rosita Lapenta

Anno Accademico 2016-2017

A Paolo

Abstract

This doctoral thesis is mainly focused on the development of new metal catalysts active in the polymerization of α-olefins and polar monomers from renewable sources. The attention is focused on the chemistry of Group IV metals and zinc for their low toxicity, good control of the polymerization, high thermal stability and biocompatibility. This work is divided into 5 Chapters, herein, shortly summarized.

Chapter 1 provides an overview on the chemistry of biodegradable polyesters in term of chemical and physical properties, synthetic processes and potential applications.

Chapter 2 describes the synthesis and the characterization of new Group IV complexes (**1-5**, Chart 1) bearing a tetradentate (OSSO)-type ligands (**L1-3**, Chart 1). The ROP of *rac*-lactide catalyzed by **1-5** showed a good polymerization control and high activities. In presence of hexogen alcohols, as ^{i}PrOH or ^{t}BuOH, polymerization proceeds with an "activated monomer" mechanism alternative to the classic "coordination-insertion" process.

Chapter 3 regards the preparation and the characterization of three titanium complexes of general formula (OSSO)TiCl$_2$ (**6-8**, Chart 1) All complexes are active in ethylene and propylene polymerization in presence of MMAO or [(Ph$_3$C)B(C$_6$F$_5$)$_4$] activators; high molecular mass polyethylene (HDPE) and oligopropylene samples were obtained.

Chapter 4 reports the synthesis of a dinuclear zirconium complex bearing a 1,5-*m*-xylene-diyl- bridged calix[8]arene ligand (**L5**, Chart 1) and

catalytic screening in the ROP of *rac*-lactide, ε-caprolactone and β-butyrolactone, leading to the selective production of macrocyclics. The complex (**9**) is the first case in which the cooperative effect of the metal centers in dinuclear Group IV catalyst, yields a highly selective formation of cyclic oligomers.

Chapter 5 is aimed at introducing the copolymerizations of cyclohexene oxide (CHO) or propylene oxide (PO) with succinic anhydride (SA) using dinuclear zinc-N-heterocyclic carbene complexes (**10-12**, Chart 1) under solvent free and high temperature. The catalytic performances are comparable to the most active complexes reported so far for similar reactions, producing copolymers with controlled microstructure.

.

Table of Contents

Chart 1

Ligands reported in thesis

OSSO$_{t\text{Bu}}$**-H**
(L1)

OSSO$_{\text{cum}}$**-H**
(L2)

OSSO$_{\text{Cl}}$**-H**
(L3)

OSSO$_{t\text{Bu}}$**-H**
(L4)

1,5-*m*-xylene-diyl-bridged calix[8]arene (L5)

Complexes reported in thesis

(1)

(2)

(4)

(3)

(5)

(6)

(7)

(8)

(9)

(10)

(11)

(12)

13
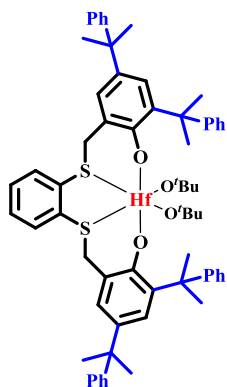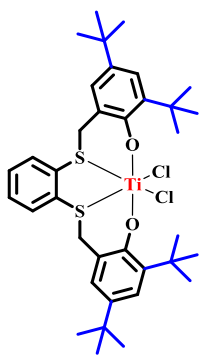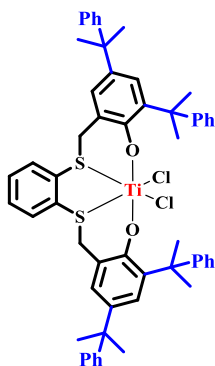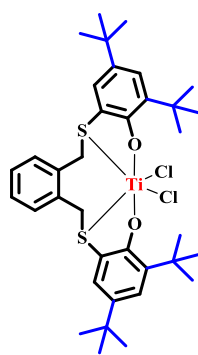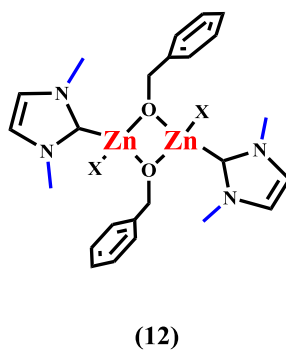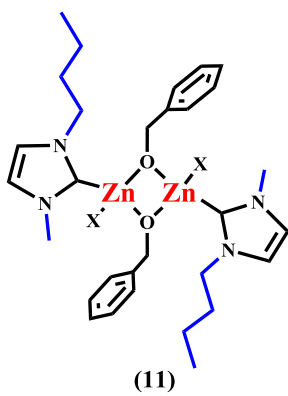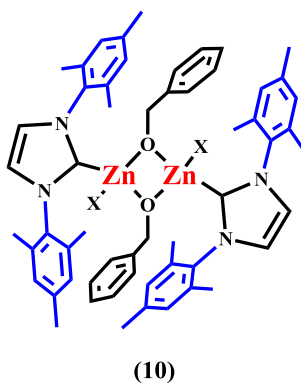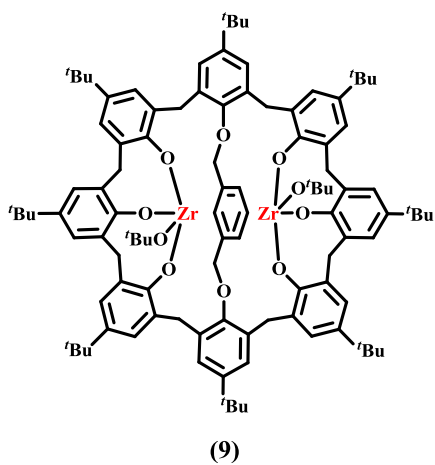
Chart 2

General structures of bis(phenolato) ligands

ONNO structure with substituents R_1, R_2, R_3, R_4, two N atoms bridging, and OH groups.

OSSO structure with substituents R_1, R_2, R_3, R_4, two S atoms bridging, and OH groups.

ONSO structure with substituents R_1, R_2, R_3, R_4, N and S atoms bridging, and OH groups.

Salan

Salen

Salalen
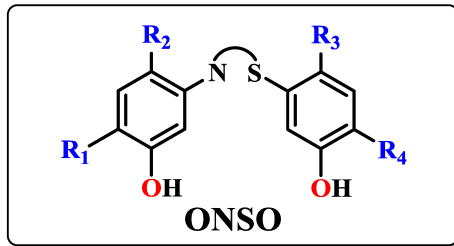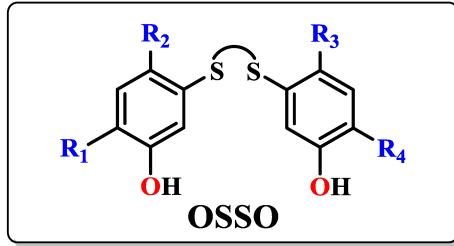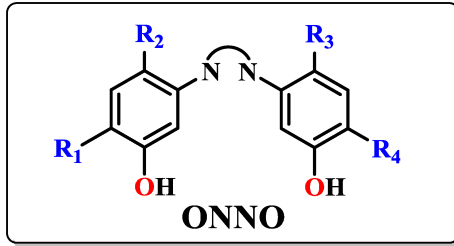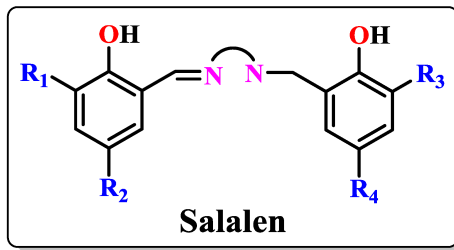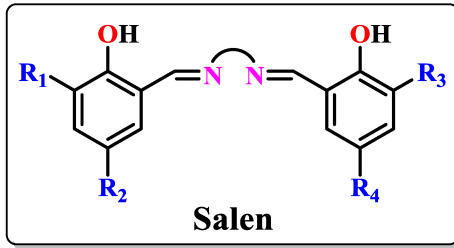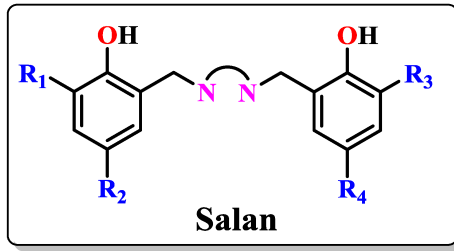
List of abbreviations

Ad: Adamantyl

br: broad signal

CHO: cyclohexene oxide

d: doublet

DMAP: 4-Dimethylaminopyridine

DSC: differential scanning calorimetry

ESI-MS: Electrospray Ionization Mass Spectrometry

Et: ethyl

GPC: gel permeation chromatography

I: Initiator

IMe: imidazolium salt

^{i}Pr: iso-propyl

J: coupling constant (NMR)

Lact: lactate

M: Monomer

m: multiplet

MALDI-MS-TOF: Matrix-assisted laser desorption/ionization time-of-flight

Me: methyl

MMAO: modified methylaluminoxane

Mw: weight-average molar mass

NaHMDS: sodium bis(trimethylsilyl)amide

NMR spectroscopy: Nuclear magnetic resonance spectroscopy

Oct: octanoate

P3HB: poly(3-hydroxybutyrate)

PDI: Polydispersity index

PO: propylene oxide

P_r: Probability of heterotactic enchainment

PSB: polybutene succinate

rac-LA: *rac*-lactide

ROCOP: ring-opening copolymerization

ROP: ring-opening polymerization

s: singlet

SA: succinic anhydride

TBACl: tetrabutylammonium chloride

*t*Bu: *tert*-butyl

TOF: turnover frequency ($M_{product}/t \cdot mol_{cat}$)

β-BL: β-butyrolactone

δ: chemical shift (NMR)

ε-CL: ε-caprolactone

Chapter 1

INTRODUCTION

1.1 Sustainable Polymers from renewable resources

Biodegradable polymer indicates, according to IUPAC definition, "polymer susceptible to degradation by biological activity, with the degradation accompanied by a lowering of its molar mass".[1] Factors affecting biodegradation are the polymer structure (presence of hydrolyzable linkages), polymer morphology (atactic or semicrystalline) and molecular weight.

Biodegradable polymers are natural or synthetic. The first ones (such as starch, proteins and cellulose) arise from plants and animals, while the second ones can be synthesized by homo or copolymerization of renewable monomers, obtained from the fermentation of natural carbohydrates. Polylactide is derived by the fermentation of starch, while poly(butylene succinate) is prepared from sucrose (Figure 1.1.1)[2] It is possible to modulate the reaction conditions and the choice of the monomers, to obtain polyesters with fixed chemical and physical properties.
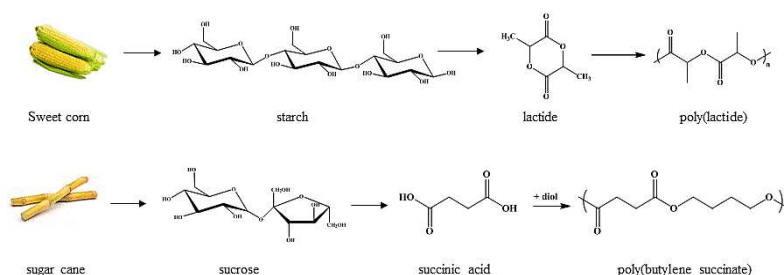
Figure 1.1.1. Alternative process to prepare biodegradable polymers

Biodegradable polymers are widely used in the medical field (for surgical implant devices, artificial skin and drug delivery systems), in agriculture, packaging, hazardous waste removal and in the automotive and paper industries. The growing environmental responsibility has led the government of China and Germany to encourage the use of biodegradable materials in order to reduce the volume of wastes in landfills.[3] Also multinational companies, as LEGO and COCA COLA, are aiming to create products completely formed with biopolymers by 2030. A recent market study of the Nova-Institute in Germany estimated the worldwide production of biopolymers of 2% in 2020.[4]

Figure 1.1.2. Bottle in bioPET (100% made from plants)

1.2 Polylactide (PLA)

Aliphatic polyesters are an important class of biodegradable and biocompatible polymers extremely interesting in a variety of applications.[5] Among these, polylactides (PLA), polycaprolactone (PCL) and polyhydroxybutyrate (PHB) are the most investigated.

PLA, discovered by Carothers in 1932, can be synthetized for polymerization of lactide, the cyclic dimer of lactic acid (Figure 1.2.1). In 1960, poly-(*L*)-lactide was indicated as biocompatible and biodegradable material and its copolymers (especially with glycolide) were at the basis of medical devices or other body implants. The most popular example of bio-absorbable sutures was the device provided by Vicryl, a lactide-glycolide copolymer (poly[L-LA (8%)-co-GA (92%)]).[6]
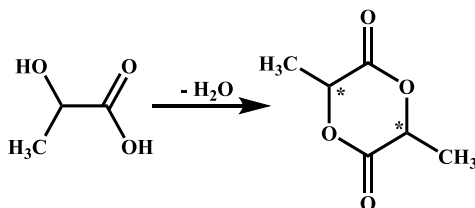
Figure 1.2.1. Synthesis of lactide monomer

PLA can be considered a sustainable polymer at the basis of the twelve principles of Green chemistry, well-described by Warner and Anastas in "Green Chemistry: Theory and Practice";[7] in fact, PLA is prepared from cheap raw materials and after its lifetime can be recycled by hydrolysis of the ester linkages by enzymes or using low toxic alkaline catalysts. Life cycle assessment (LCA) is an important methodology to determine environmental impacts of a process, evaluating every single stage of life cycle (Figure 1.2.2).
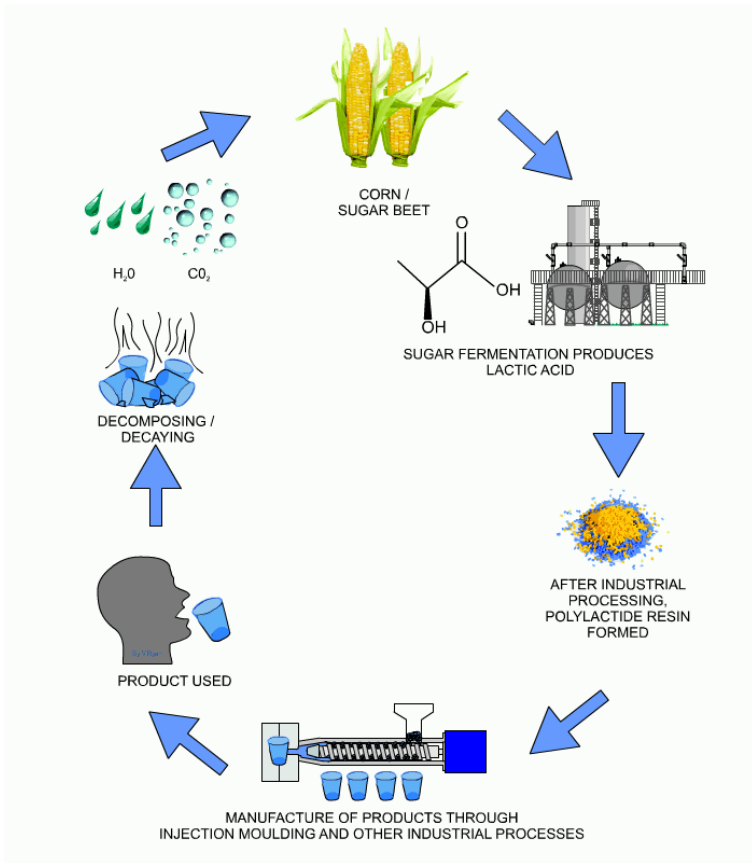
Figure 1.2.2. Life cycle of lactide polymers[8]

In this cycle, PLA production starts from the corn starch fermentation to obtain lactic acid, which is polymerized, under high temperature, to polymer pellets. Through injection moulding or other industrial processes, a specific product can be prepared (such as coffee cup). When the product is discarded (waste), it will be decomposed by enzymatic process. During biodegradation, the amount of CO_2 produced is equal to the amount absorbed by plant for its growth.[9]

In addition, PLA can be also recycled through mechanical or chemical processes. The mechanical recycling proceeds through eight stages, schematically reported in Figure 1.2.3; during the process about 4 % of polymer is loss and PLA is recycled only once.

RESIDUAL PLA
SEPARATION → GRINDING → WASHING → DRYING
RECYCLED PLA ← SIEVING ← GRANULATION ← COOLING ← EXTRUSION
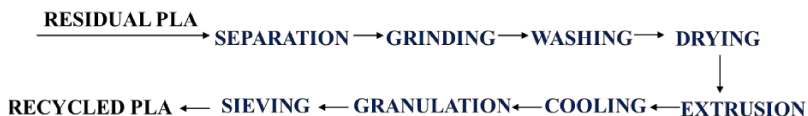
Figure 1.2.3. PLA mechanical recycling

The chemical recycling of PLA consists in the hydrolysis to the monomer or oligomers and subsequent polymerization. Depolymerization of PLA is carried out in bath at 180°C for 2 h; then, the resulting lactic acid is cooled, and solution filtered to remove the unreacted PLA and catalyst (Sn^{II}). Finally, the clean solution of lactic acid is used to produce lactide (Figure 1.2.4). To promote the synthesis of polymer, in the reactor containing lactide is added tin ethanoate as catalyst, which through ring opening polymerization mechanism induce the formation of desired PLA. 1 kg of lactic acid solution results in 0.7 kg of recycled PLA.[10]

RESIDUAL PLA $\longrightarrow$ **SEPARATION** $\longrightarrow$ **GRINDING** $\longrightarrow$ **WASHING** $\xrightarrow[\text{weight}]{\text{PLA } 40\%}$ **REACTOR** $\xleftarrow{}$ water

$\longrightarrow$ **COOLING**

COOLING $\xrightarrow[\text{(180°C)}]{\text{Lactic acid}\\ + \text{impurities}}$ **DECANTATION and FILTRATION** $\xleftarrow{}$ precipitation agent

DECANTATION and FILTRATION $\longrightarrow$ impurities

DECANTATION and FILTRATION $\xrightarrow[\text{(180°C)}]{\text{Lactic acid}\\ + \text{impurities}}$ **EVAPORATION**

EVAPORATION $\xrightarrow{\text{Concentrated}\\ \text{lactic acid}}$
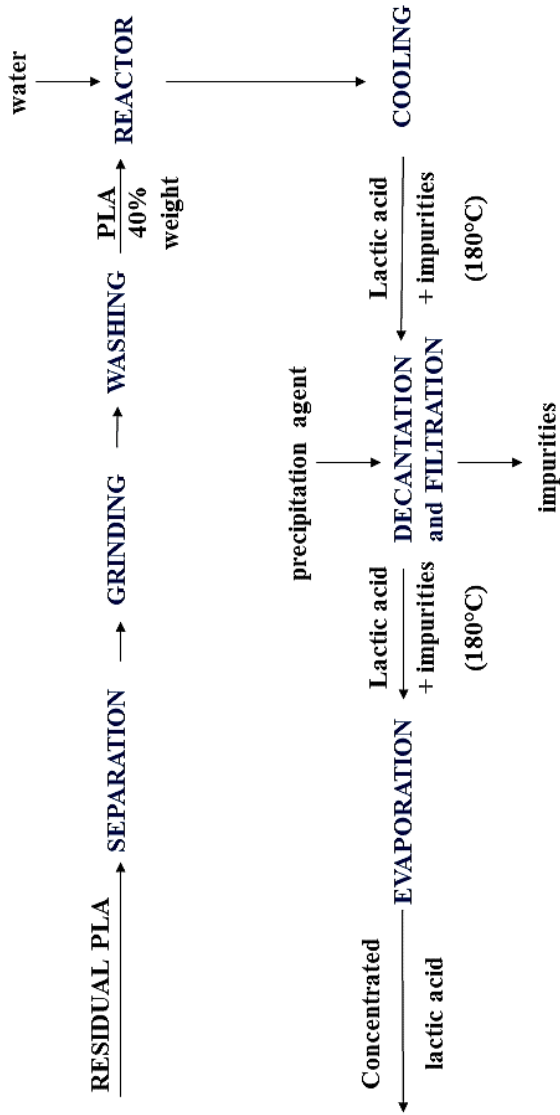
Figure 1.2.4. PLA chemical recycling: hydrolysis
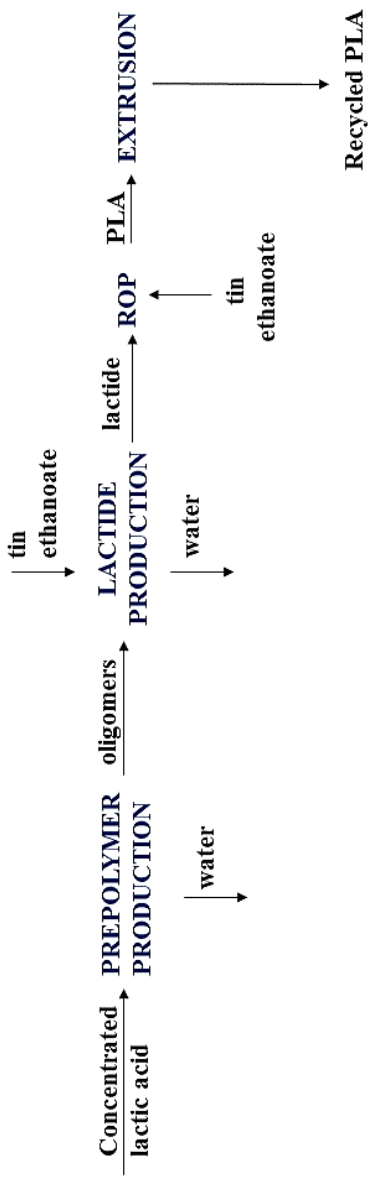
Figure 1.2.5. Polymerization step during polylactide chemical recycling

Hydrolysis and biodegradation of a polymer can be influenced by molecular weight, microstructure and macromolecular architecture that in turn depend on the reaction conditions in which this is obtained (synthesis, nature of the monomer, etc.).

Three different stereoisomers are known for LA: L-lactide (S, S), D-lactide (R,R) and *meso*-lactide (S, R); *rac*-lactide is a mixture 50:50 of L- and D-lactide (Figure 1.2.6).
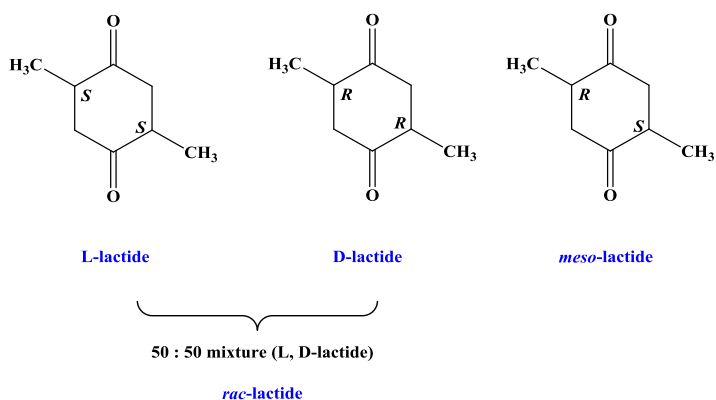
Figure 1.2.6. Stereoisomers of *rac*-lactide

In absence of epimerization reactions, the polymerization of L- or D-lactide gives isotactic poly(L-lactide) or poly(D-lactide). From *rac*-lactide, three different polymers could result: 1) racemic mixture of isotactic poly(L-lactide) and poly(D-lactide); 2) isotactic stereoblock of PLA, in which regular sequences $(RR)_m(SS)_n$ or $(SS)_m(RR)_n$ are present; 3) heterotactic PLA $(RRSS)_n$. The polymerization of *meso*-lactide gives syndiotactic PLA.[11] All possible microstructures are shown in Figure 1.2.7.
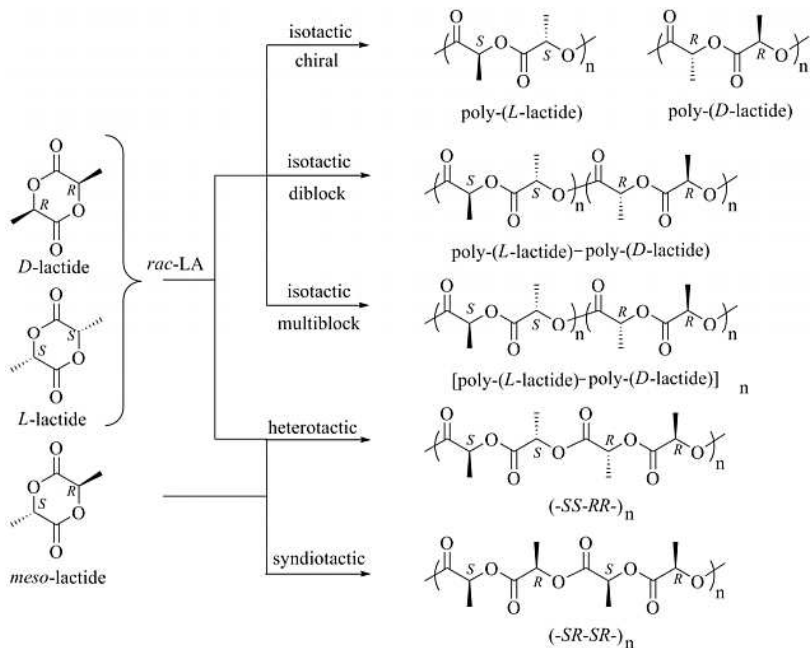
Figure 1.2.7. Microstructures of PLA

The physical properties depend on the tacticity of the polymer. Isotactic PLA is semicrystalline with a melting point (T_m) of 170 °C and glass transition temperature (T_g) of about 60°C; the corresponding syndiotactic polymer is characterized by a T_m of about 150 °C. Differently, the stereocomplex of PLLA and PDLA (1:1) shows a T_m of 230 °C; for the stereoblock T_m is 205°C. Finally, atactic and heterotactic PLA are amorphous and perfectly soluble in solvents as acetonitrile, toluene, chloroform and tetrahydrofuran.[12]

1.3 Mechanisms of ring opening polymerization (ROP) of cyclic esters

The lactide polymerization is an example of ring-opening polymerization (ROP). It offers many advantages in term of polymerization control, mild conditions, solvent free polymerization and possibility to achieve end-functionalization.[13]
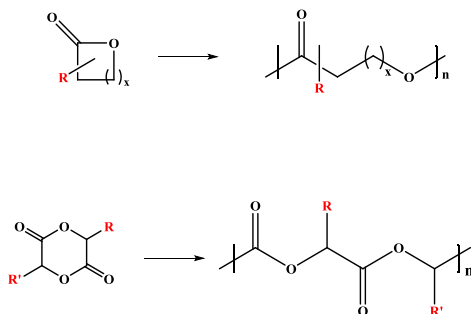
Figure 1.3.1. Ring-opening polymerization of lactone and lactides.

ROP can proceed through different mechanisms, e.g. cationic, anionic, radical, coordination-insertion and activated monomer mechanism.

The cationic ROP of cyclic esters is, generally, promoted by Lewis acids, protic acids and alkylating agents. The polymerization proceeds by the protonation or alkylation of a carbonyl group of lactone, which becomes positively charged. Then, the nucleophilic attack of an additional monomer breaks the O-CH bond, producing an another electrophilic carbenium ion (see Figure 1.3.2). During this process, high temperature values can induce racemization of lactide units. To minimize this undesired process, the polymerizations are carried out at about 50°C.[14]
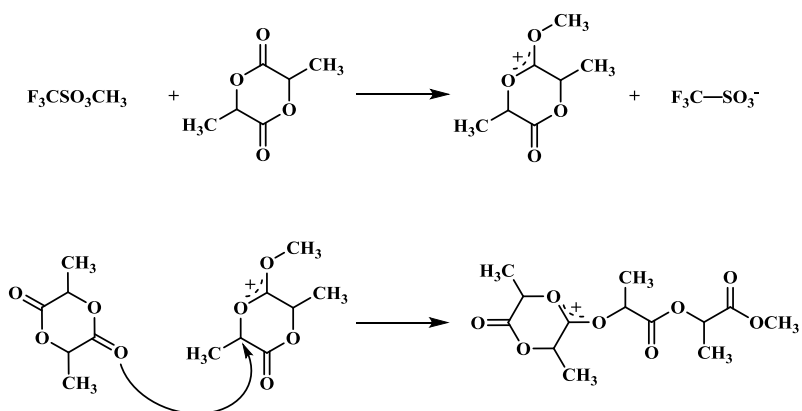
Figure 1.3.2. Cationic ROP of lactide

The anionic ROP occurs when a nucleophilic anion of the initiator attacks the carbonyl group of the lactone, producing a cleavage of the C-O single bond. The derived alkoxide specie promotes the propagation step. (Figure 1.3.3).
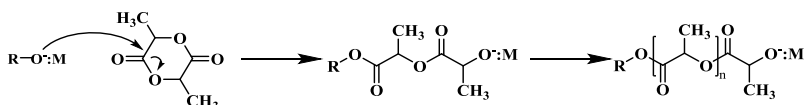
Figure 1.3.3. Anionic ROP of lactide

The ring opening polymerization through the coordination-insertion mechanism is the most efficient synthetic route for the preparation of polyesters with specific properties and controlled microstructures, in terms of molecular weights, end groups and stereoregularity. The metal catalyzed ROP of LA is typically initiated by an alkoxide metal complex and the mechanism (see Figure 1.3.4) proceeds via coordination of the monomer to the metal center, followed by the attack of the alkoxide group to the activated carbonyl carbon. Successively, the intermediate undergoes acyl

bond cleavage to generate a new metal alkoxide species. The reaction is terminated by hydrolysis of L_nM-O bond, which forms a hydroxyl end-group of the polymeric chain.[15]
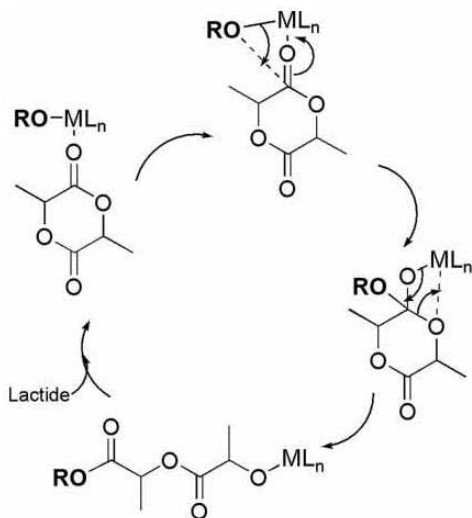
Figure 1.3.4. "Coordination-Insertion" Polymerization

The coordination compounds can promote the ROP of lactide through an alternative route designed as "activated monomer" mechanism. In this case, the nucleophilic attack to the carbonyl group of lactone, which is preventively activated by an interation with metal complex, is carried out by an exogenous alcohol (Figure 1.3.5). This mechanism is also promoted by organocatalysts like N-heterocyclic carbenes or H-bond donors.[16]
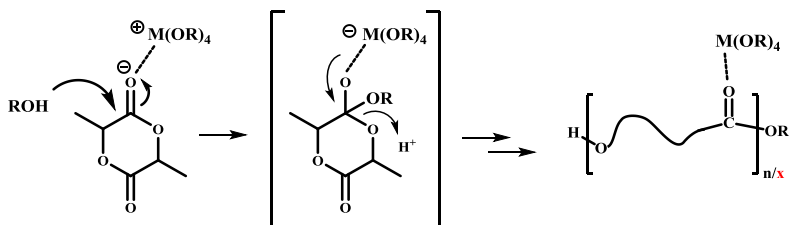
Figure 1.3.5. Activated Monomer Mechanism

Transesterification reaction (also designated as back-biting reaction).is the main side reaction during the ROP and can be intramolecular or intermolecular. The intramolecular transesterification leads to the formation of mixture of linear and cyclic polymers, while the intermolecular process consists in a chain redistribution resulting in a broadening of the molecular weight distribution (Figure 1.3.6).[11]
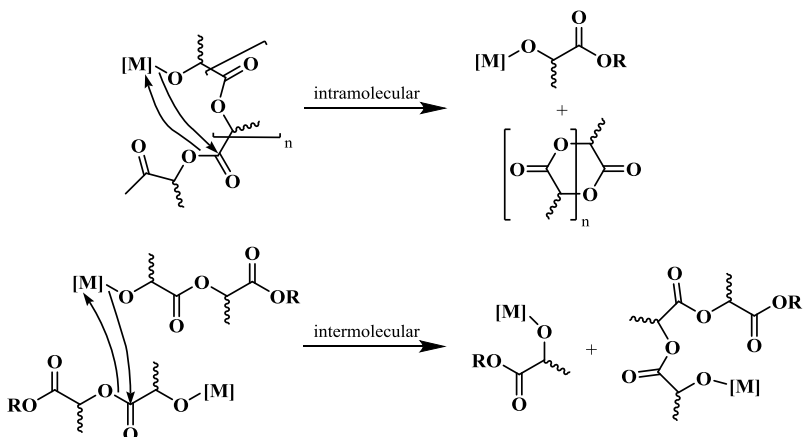
Figure 1.3.6. Schematic representation of intra- and inter-molecular transesterification

1.4 Initiators in the ROP of lactide: brief history

Among the large variety of complexes investigated in the ROP of lactide, the homoleptic "first generation" catalysts (SnOct$_2$, Al(O^{i}Pr)$_3$, Zn(Lact)$_2$) are widely used under industrial conditions. However, they can produce undesired aggregation phenomena and subsequently promote collateral reactions (intra- or inter- molecular transesterifications), inhibiting the propagation.[17] Efforts to obviate these problems were focused on the development of new heteroleptic complexes with formula L$_n$MX$_m$, where L represents the ligand, M is the metal center and X is an initiator group. This new family of complexes is called "second generation" and allow a better control, activity, and selectivity of the polymerization reaction.[18] A large variety of metals have been tested in the ring opening polymerization of cyclic esters including examples like litium, sodium and potassium from Group 1, calcium and magnesium from Group 2, titanium, zirconium and hafnium from Group 4, aluminum and indium from Group 13 and finally rare-earth metals.[19] Among these metal complexes investigated as initiators, Group 4 metal complexes have been shown to be particularly attractive thanks to their low toxicity and good control over polymerization process.[20]

1.5 Aim of the PhD Project

The PhD project is focused on the development of new metal catalysts active in the polymerization of polar monomers and α-olefins. Among the class of polydentate ligands, the attention is devoted to the tetradentate OSSO-type bis(phenolato) ligands for their easy preparation and high affinity to Group IV metals. The group IV alcoholates are known as powerful initiators in the ROP of cyclic esters (*rac*-lactide, ε-caprolactone and β-butyrolactone). The influence of steric and electronic properties of the ligand will be investigated using three different OSSO-type ligands substituted by *tert*-butyl, cumyl and chlorine atoms (**L1-4,** Chart 1) and the corresponding Group IV metal complexes of general formula $(OSSO)M(OR)_2$ which are tested in the polymerization of *rac*-lactide (Figure 1.5.1).
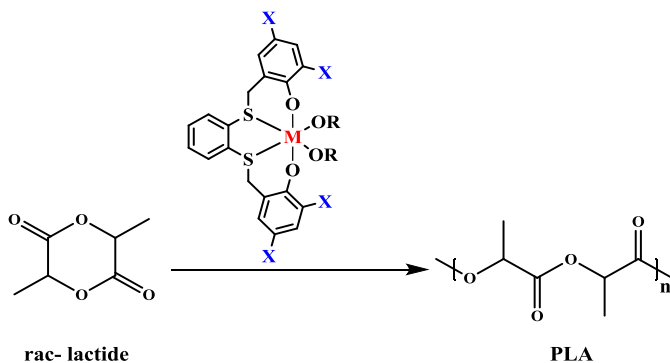
Figure 1.5.1. $(OSSO)M(OR)_2$ tested in the ROP of *rac*-lactide

(OSSO)-type bis(phenolato) complexes are a versatile class of catalysts, as matter of fact the corresponding chloro derivates have been found active in the polymerization of α-olefins. The catalytic performances of the chloro complexes of general formula $(OSSO)TiCl_2$ will be investigated in the polymerization of ethylene and propylene (Figure 1.5.2).
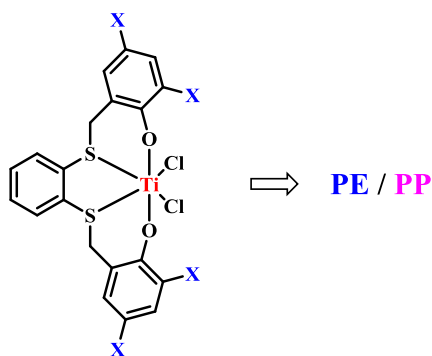
Figure 1.5.2. (OSSO)MCl$_2$ for ethylene and propylene polymerization

Although mononuclear Group IV metal complexes are widely explored in the ROP of lactones, few examples of corresponding dinuclear complexes have been studied until now. As part of our interest in developing Group IV metal catalysts for the ROP of cyclic esters, we turned focus on the zirconium calixarene complex. In particular, we explored the synthesis of a di-zirconium complex **9** featuring *p-tert*-butylcalix[8]arene 1,5-bridged with m-xylene diyl functionality and its use in the ROP of *rac*-lactide, ε-caprolactone and β-butyrolactone.
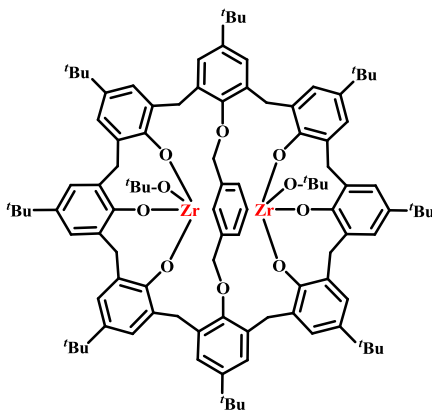
Figure 1.5.3. Schematic representation of dinuclear complex **9**

An alternative approach to prepare biodegradable and biocompatible polyesters consists in the ring opening copolymerization (ROCOP) of cyclic anhydrides with epoxides. This reaction allows to modulate the physical and chemical properties of the desired polyester, choosing appropriately the substituents on the monomers. Among the most active catalysts, there are dinuclear zinc complexes that are interesting for their high control of polymerization and activity.[21] For these fascinating advantages, we plan to synthetize a new class of dinuclear zinc complexes bearing a monodentate N-heterocyclic carbene ligands (**10-12**, Chart 1) for catalytic screening in the copolymerization between succinic anhydride (SA) and propylene oxide (PO) or cyclohexene oxide (CHO).
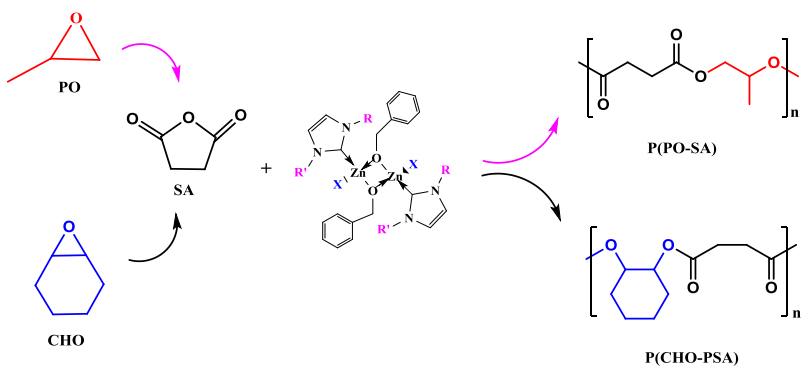
Figure 1.5.4. ROCOP of SA and CHO or PO by **10-12**

1.6 References

[1] PAC, **2004**, *76*, 889; doi:10.1351/pac200476040889.

[2] Zhu, Y.; Romain, C.; Williams, C. K. *Nature*, **2016**, *540*, 354-362.

[3] Kumar, A. A.; Karthick. K, and Arumugam, K. P. *International Journal of Bioscience, Biochemistry and Bioinformatics*, **2011**, *1*, 173-176.

[4] http://biovalue.dk/bioplastic-seminar-2016/

[5] a) Middleton, J. C.; Tipton, A. J. *Biomaterials* **2000**, *21*, 2335−2346. b) Nair, L. S.; Laurencin, C. T. *Prog. Polym. Sci.* **2007**, *32*, 762−798. c) Ikada, Y.; Tsuji, H. *Macromol. Rapid Commun*. **2000**, *21*, 117−132.

[6] a) Lewis D. H. *Biodegradable polymers as drug delivery systems,* **1990***, 1-41; b) Albertsson, A.-C.; Varma, I. K. *Degradable Aliphatic Polyesters*, 1-40.

[7] Anastas, P. T.; Warner, J. C.; *Green Chemistry: Theory and Practice,* Oxford University Press, New York, USA, **1998**.

[8] From http://www.technologystudent.com/pdf7/poly2.pdf

[9] Buggy, M. *Natural Fibres, Biopolymers, and Biocomposites (Eds. Mohanty, A.; Misra, M.; Drzal, L.)* CRC Press, Taylor & Francis Group, New York, **2005**.

[10] de Andrade, M. F. C.; Souza, P. M. S.; Cavalett, O.; Morales, A. R. J *Polym Environ*. **2016**, *24*, 372-384.

[11] Dechy-Cabaret, O.; Martin-Vaca, B.; Bourissou, D. *Chem. Rev*. **2004**, *104*, 6147-6176.

[12] Kricheldorf, H. *Chemosphere* **2001**, *43*, 49-54.

[13] Tong, R. *Ind. Eng. Chem. Res*. **2017**, *56*, 4207–4219.

[14] a) Duda, A.; Penczek, S. *Thermodynamics, kinetics and mechanisms of cyclic esters polymerisation. In Polymers from Renewable Resources: Biopolyesters and Biocatalysis; Scholz, C.; Gross, R. A., Eds.; ACS*

Symposium Series; Oxford University Press: Washington, DC, **1996**; Vol. 5, 317-343. b) Tang, Z.; Chen, X.; Liang, Q.; Bian, X.; Yang, L.; Piao, L.; Jing, X. *J Polym Sci Part A Polym Chem* **2003**; *41*,1934–1941.

[15] Platel, R. H; Hodgson, L. M.; Williams, C. K. *Polymer Reviews* **2008**, *48*, 11-63.

[16] a) Ajella, N.; Carpentier, J.-F.; Guillaume, C.; Guillaume, S. M.; Helou, M.; Poirier, V.; Sarazin, Y.; Trifonov, A. A. *Dalton Trans*., **2010**, *39*, 8363-8376. b) Sarazin, Y.; Poirier, V.; Roisnel, T.; Carpentier, J.-F. Eur. J. *Inorg. Chem.*, **2010**, 3423-3428. c) Sarazin, Y.; Liu, B.; Roisnel, T.; Maron, L.; Carpentier, J.-F. *J.A.C.S.*, **2011**, *133*, 9069-9087.

[17] a) Degee, P.; Dubois, P.; Jerome, R.; Jacobsen, S.; Fritz, H.-G. *Macromol. Symp*. **1999**, 144, 289; b) Duda, A.; Penczek, S. *Macromolecules* **1998**, 31, 2114. c) Chabot, F.; Vert, M.; Chapelle, S.; Granger, P. *Polymer* **1983**, *24*, 53. d) Schwach, G.; Coudane, J.; Engel, R.; Vert, M. *Polym. Int.* **1998**, *46*, 177.

[18] Thomas, C. M. *Chem. Soc. Rev*., **2010**, *39*, 165–173.

[19] a) Yang, X.; Wang, L.; Yao, L.; Zhang, J.; Tang, N.; Wang, C.; Wu, J. *Inorg. Chem. Commun*. **2011**, *14*, 1711−1714. b) Dutta, S.; Hung, W. C.; Huang, B. H.; Lin, C. C. *Adv. Polym. Sci*. **2012**, *245*, 219. **c)** Chuck, C. J.; Davidson, M. G.; du Sart, G. G.; Ivanova-Mitseva, P. K.; Kociok-Kohn, G. I.; Manton, L. B. *Inorg.Chem.*, **2013**, *52*, 10804-10811.

[20] a) Sauer, A.; Kapelski, A.; Fliedel, C.; Dagorne, S.; Kol, M.; Okuda, J. *Dalton Trans*. **2013**, *42*, 9007–9023. b) Della Monica, F.; Luciano, E.; Roviello, G.; Grassi, A.; Milione, S.; Capacchione, C. *Macromolecules* **2014**, *47*, 2830-2841.

[21] a) Wu, L.-y.; Fan, D.-d.; Lu, X.-q.; Lu, R. Chin. J. Polym. Sci. 2014, 32, 768−777. b) Saini, P. K.; Romain, C.; Zhu, Y.; Williams, C. K. *Polym. Chem.*, 2014, 5, 6068-6075

Chapter 2

2.1 Group 4 Metal Complexes of the (OSSO)-type ligands as initiators in the ROP of lactide

In the last twenty years, a new series of Group IV metal complexes bearing tetradentate bis(phenolato) ligands were prepared. The term bis(phenolato) is, generally, used to describe linear tetradentate ligands formed by two phenoxide groups linked with bridge comprising two additional neutral donor atoms in ortho or benzyl positions; depending on the type of heteroatoms, they are called *ONNO*, *ONSO* and *OSSO* type bis(phenolato) ligands (Figure 2.1.1).
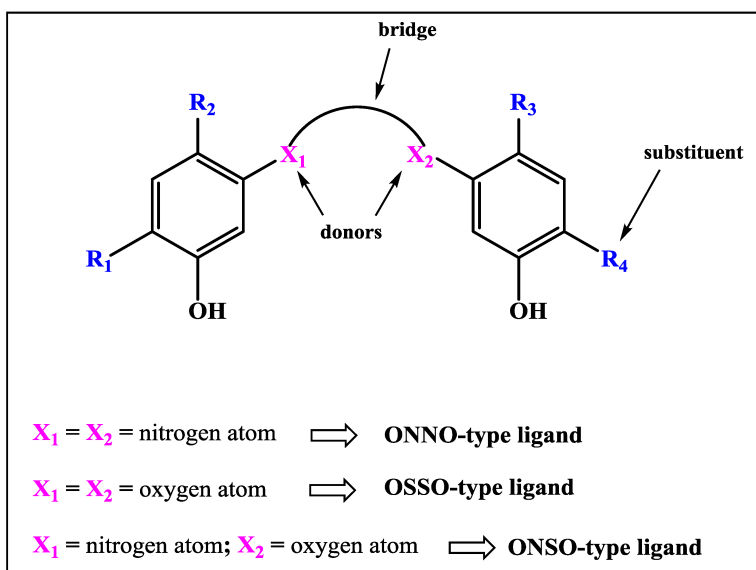
Figure 2.1.1. General structure of bis(phenolate) ligand

Group IV metal complexes of salan-type (see Chart 2) ligand showed a high activity in the ROP of lactide, producing isotactic enriched PLA (Figure 2.1.2).[22]
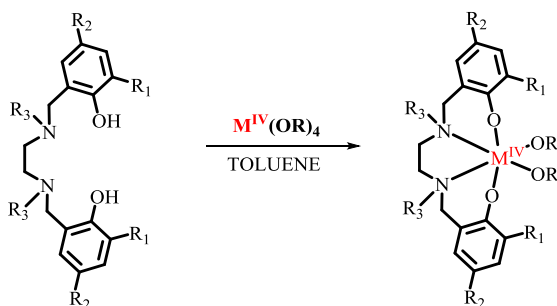
Figure 2.1.2. Group 4 complexes bearing salan ligands

Chakraborty et al. observed that polynuclear complexes of zirconium and hafnium bearing salen-type ligand (see Chart 2) promoted fast polymerization of *rac*-lactide under solvent-free conditions (200 eq. converted in 60 min), producing polymer with a molecular weight of 30 KDa (Figure 2.1.3).
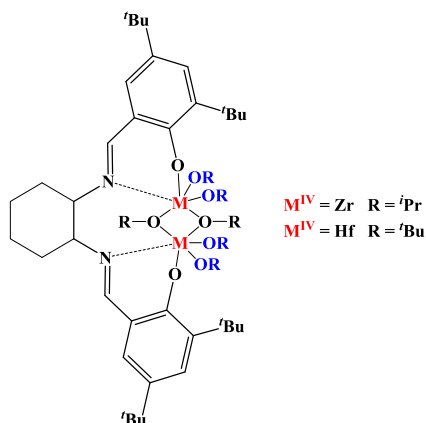
Figure 2.1.3. Dinuclear Group IV metal complexes bearing salen ligand[23]

In 2010 Mahon prepared of a series of unsymmetrical Group IV salalen (Chart 2) complexes active in the ROP of lactide (Figure 2.1.4).
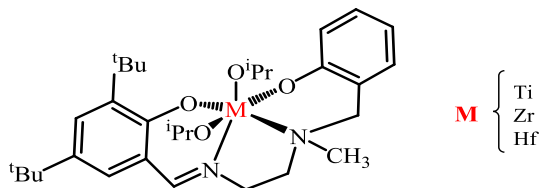
Figure 2.1.4. Group IV salalen complexes.[24]

These complexes converted 300 equivalents of *rac*-lactide in 15 min under bulk condition, and in 2 h in toluene solution. Unexpectedly, the analogous hafnium catalyst displayed lower activity (98 % conv. in 24 h, toluene); the resulting PLA is isotactic.

Titanium and zirconium complexes of phenylenediamine bis(phenolato) ligand (Figure 2.1.5) displayed extremely high activity in lactide polymerization. The titanium complex converted 300 eq. of *rac*-lactide into 2 min, yielding heterotactic PLA; the heteroselective polymerization may result from the fluxional character of the catalysts in solution.
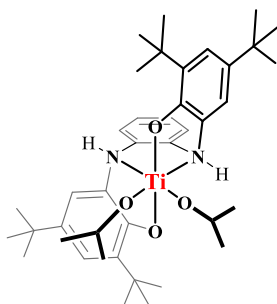
Figure 2.1.5. Titanium salan complex active in the ROP of *rac*-LA[25]

Recently, Kol et al. have introduced another class of Group IV complexes with ONSO-type ligands; they are similar in the structure to the ONNO-type ligand, but the rigid imine link is replaced by a more flexible thioether linkage. The reaction of the protonated ligand with $Zr(^tBuO)_4$ gave $(ONSO)Zr(O^tBu)_2$ complexes, which are active in the polymerization of L-lactide and *rac*-lactide. The poly-*rac*-lactide obtained using this fluxional catalyst are heterotactic enrichment, whereas the polymer prepared by the rigid catalyst is prevalently isotactic (Figure 2.1.6).
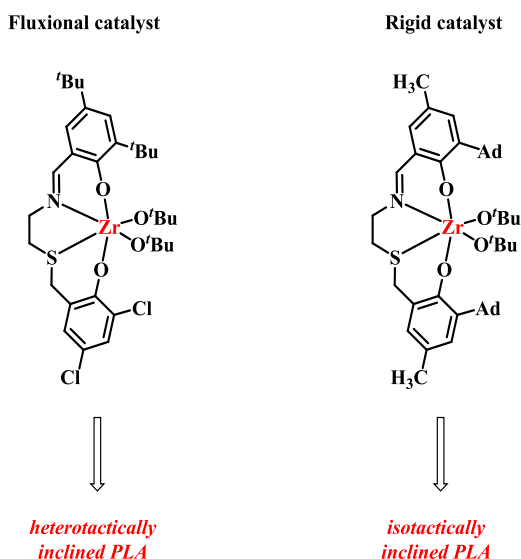
Figure 2.1.6. Zirconium Complexes of (ONSO) Ligands[26]

Finally, in 2010, Kol reported the first examples of syndiotactic PLA from *meso*-lactide using (OSSO)-type titanium complexes and heterotactic poly(*meso*-lactide) using similar zirconium complexes; the schematic representation of the catalysts is reported in Figure 2.1.7.

$M = Ti; X = O^iPr$

$M = Zr; Hf; X = O^tBu$
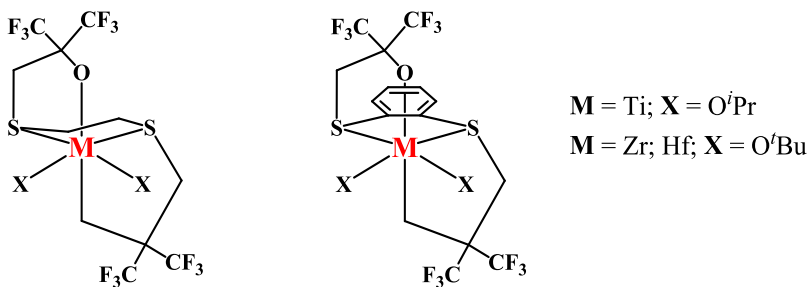
Figure 2.1.7. Group 4 Complexes bearing dithiodiolate ligands[27]

The major contribution in the chemistry of Group IV complexes supported by OSSO-type bis(phenolato) was given by Okuda who described the synthesis of new zirconium catalysts based on 1,ω-dithia-alkanediyl-bridged bis(phenolato) (OSSO)-type ligands extremely active in the polymerization of *meso*-lactide to give heterotactic polylactides (Figure 2.1.8).

$(CH_2)_2$

$(CH_2)_3$
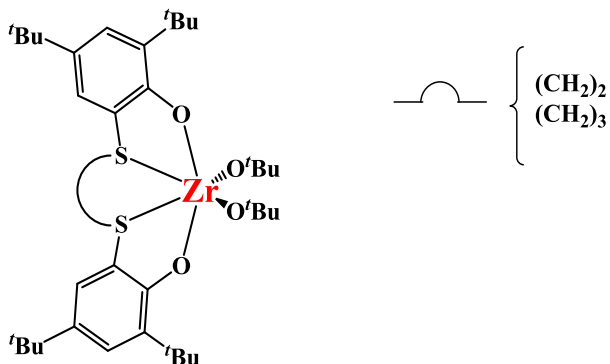
Figure 2.1.8. Zirconium initiators for the polymerization of *meso*-lactide[28]

In an effort to further study the catalyst structure-activity and structure-selectivity correlations in the ROP of *rac*-lactide, we prepared a new series of Group IV complexes bearing *o*-phenylene-bridged bis(phenolato) ligands of general formula $(OSSO_X)M(OR)_2$ (**1-5**), in detail, studied in the Section 2.2.[29]

2.2 Synthesis and characterization of the OSSO-type ligands and of the corresponding Group IV metal complexes (1-5)

The *o*-phenylene-bridged bis(phenolato) ligands were synthesized by reaction between benzene-1,2-dithiol and 2 equivalents of 2-(bromomethyl)phenol in dry THF (Scheme 2.2.1).[30]
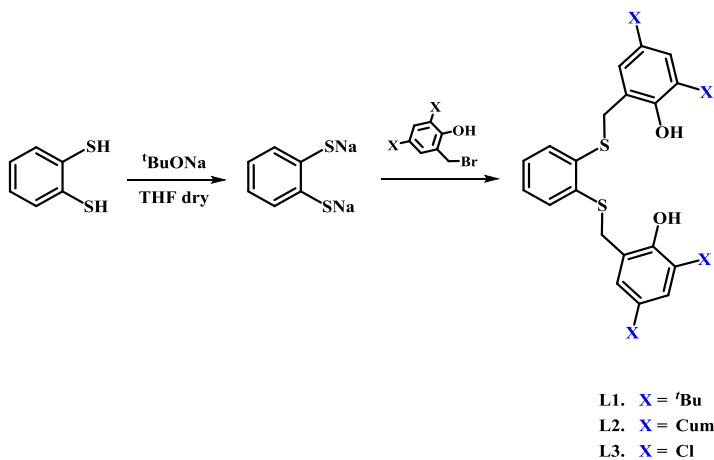
Scheme 2.2.1. Synthetic Route for the OSSO-type (bispenolato) ligands used for the preparation of complexes **1-5**

To explore the influence of electronic and steric parameters of the ligands, we prepared three different ligands substituted by *tert*-butyl or cumyl groups and chlorine atoms (**L1-3**, Scheme 2.2.1); the ligands were obtained as white solids in good yields (50-80%). **L1** and **L2** were purified by recrystallization from petroleum ether at room temperature. **L3** is poorly soluble in petroleum ether or *n*-hexane at room temperature and was purified by crystallization from cold toluene. All the ligands were fully characterized by NMR spectroscopy and elemental analysis. The

assignments of the resonances were based on previously reported data. In all the spectra, the signal of the methylene groups appears as a sharp singlet in the range 3.96- 4.13 ppm (CDCl$_3$, rt, Figure 2.2.1). In detail, the ^{1}H NMR spectrum of **L1** displays at δ 1.21 and 1.41 ppm two singlets corresponding to 36 protons assuming the *tert*-butoxide groups as internal standard. The signal of the methylene groups (s, 4 H, δ 4.13 ppm) are followed by the singlet of hydroxide groups (2 H) at 6.09 ppm. The aromatic protons (8H) are detected in the range between 6.85-7.36 ppm. It is worth noting that in the ^{1}H NMR spectrum of the **L2**, the methyl groups of the two different cumyl substituents give rise to a single signal.
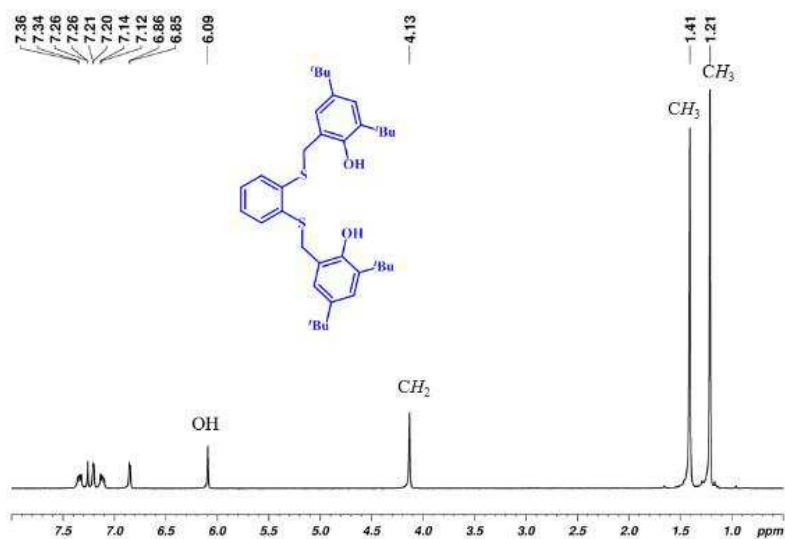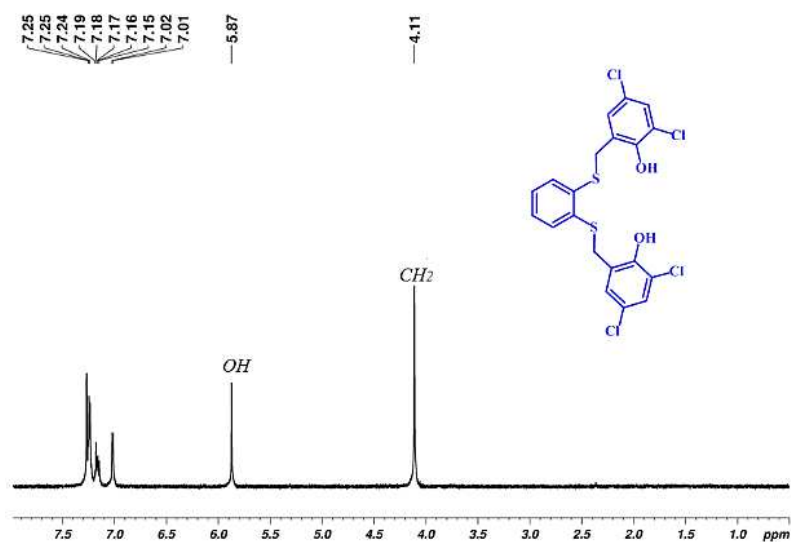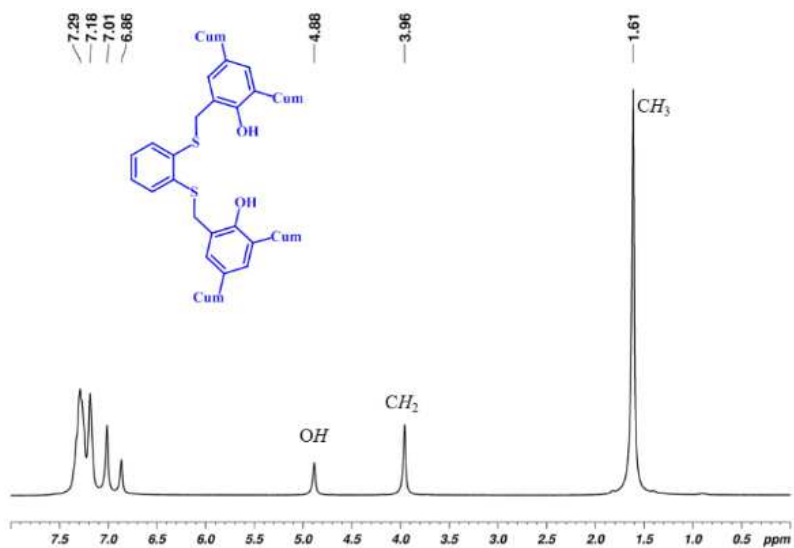
Figure 2.2.1. ^{1}H NMR spectra of **L1-3** (CDCl$_3$, 300 MHz, 25°C).

Recrystallization of **L2** from toluene/THF afforded crystals suitable for X-ray analysis. The X-ray molecular structure is shown in Figure 2.2.2, in which one thiophenoxo unit is depicted in purple for sake of clarity (thermal ellipsoids at the 30% probability level). The bond lengths and angles are in the range observed for similar OSSO-type ligands reported in literature[30].
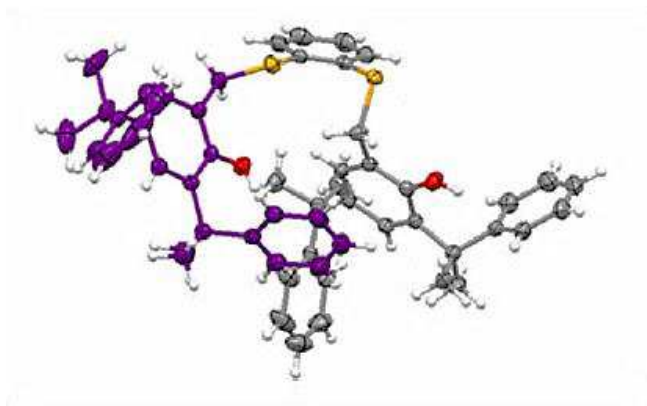
Figure 2.2.2. Molecular structure of OSSO$_{Cum}$-*H* resolved by single-crystal X-ray diffraction

The corresponding group 4 metal complexes of general formula (OSSO$_X$)M(OR)$_2$ (X = R = ^{t}Bu, M = Zr (**1**); X = cumyl, R = ^{t}Bu, M = Zr (**2**); X = cumyl, R = ^{i}Pr, M = Ti (**4**); X = cumyl, R = ^{t}Bu, M = Hf (**5**)) were prepared by reaction of the proligand with the appropriate homoleptic metal precursor (Zr(OtBu)$_4$, Hf(OtBu)$_4$ and Ti(O^{i}Pr)$_4$) in toluene at 25°C (Scheme 2.2.2).The crude products were washed with *n*-hexane and isolated as pale yellow solids in good yields (65-70 %). The ^{1}H NMR monitoring of the reaction displayed a complete evolution of the reagents into the desired complexes in few minutes.

X = ^{t}Bu,	M = Zr,	R = ^{t}Bu	**(1)**
X = Cum,	M = Zr,	R = ^{t}Bu	**(2)**
X = Cum,	M = Ti,	R = ^{i}Pr	**(4)**
X = Cum,	M = Hf,	R = ^{t}Bu	**(5)**
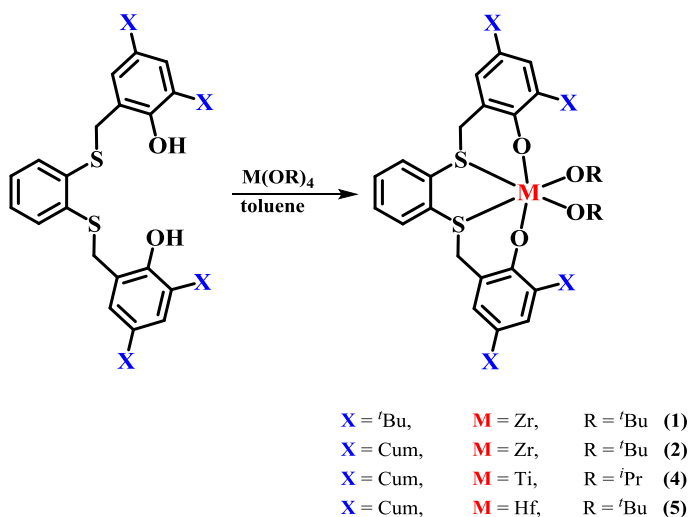
Scheme 2.2.2. Synthesis of heteroleptic Group IV metal complexes

Except for **L3**, the heteroleptic complexes $(OSSO_X)M(OR)_2$ were obtained in pure form. Surprisingly, the reaction of **L3** with $Zr(O^tBu)_4$ led to the homoleptic complex $(OSSO_{Cl})_2Zr$ (**3**) regardless of the [ligand]/[Zr] molar ratio and the experimental conditions (temperature, solvent, order of addition of the reagents used), likely as result of the high acidity of the ligand and low steric encumbrance offered by chloro substituents (Scheme 2.2.3). The homoleptic complex **3** was isolated as pure solid after the direct reaction of $Zr(O^tBu)_4$ with 2 equivalents of the proligand in toluene solution at the temperature of 25°C, as shown in Figure 2.2.3.
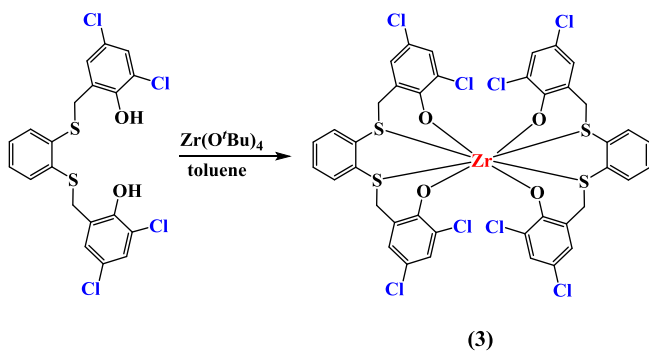
Scheme 2.2.3. Synthesis of (OSSO$_{Cl}$)$_2$Zr complex
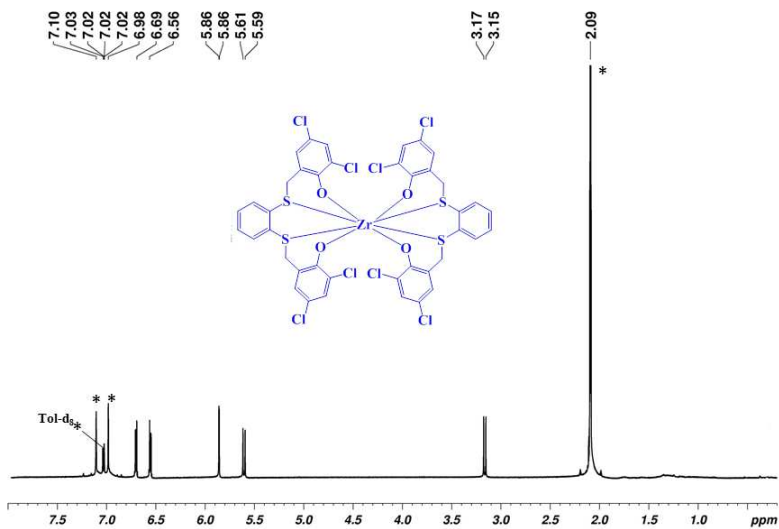
Figure 2.2.3. ^{1}H NMR spectrum of (OSSO$_{Cl}$)$_2$Zr (3) (Tol-d$_8$, 600 MHz, 25°C).

In principle the tetradentate OSSO-type ligands can wrap the Group IV metal center in an octahedral environment producing three different stereoisomers, named as *mer–mer (trans), fac–fac (cis-α)* or *fac–mer* (*cis-β*), showing C$_S$, C$_2$ and C$_1$ symmetry, respectively. The *cis-α* and *cis-β*

isomers exist in two stereoisomeric forms (Λ and Δ), in which the stereogenic center is the metal. All the described coordination modes were summarized, below, in the Figure 2.2.4.
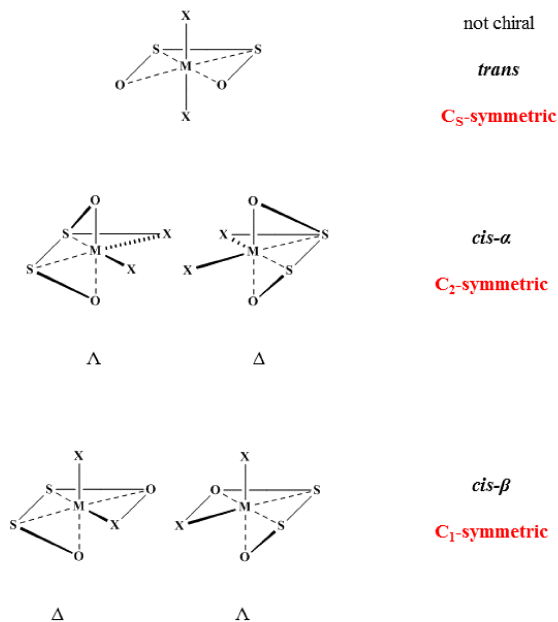
Figure 2.2.4. Coordination modes of tetradentate OSSO ligands in octahedral environment

The ^{1}H NMR spectrum of $(OSSO_{tBu})Zr(O^tBu)_2$ complex (**1**) indicates the presence of a single stereoisomer in solution (Figure 2.2.4, benzene-d_6). The methylene protons give rise to a signal with an AB pattern (3.32 and 4.22 ppm) revealing the C_2-symmetric arrangement for the complex. The *tert*-butoxide protons appeared at 1.59 ppm as singlet, while resonances of the *tert*-butyl *o*-substituted were observed at δ 1.11 and 1.83 as narrow singlets. In the range between 6.11 and 7.36, the aromatic protons were clearly detected (Figure 2.2.5).
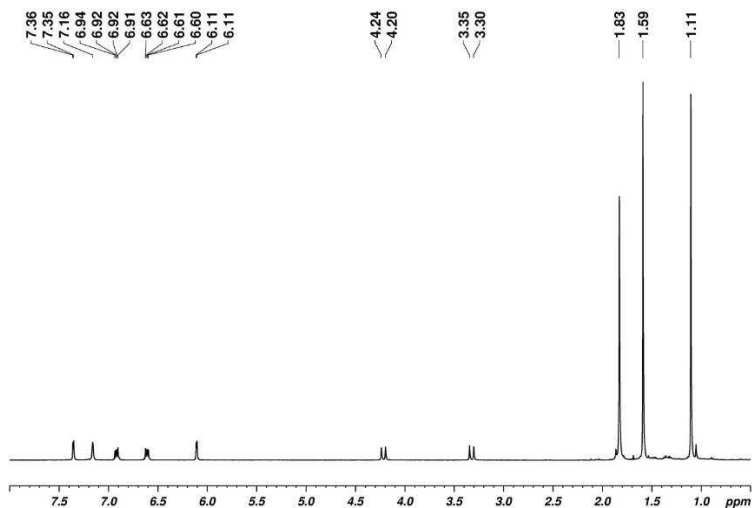
Figure 2.2.5. ^{1}H NMR of (OSSO$_{tBu}$)Zr(O^{t}Bu)$_2$ (**1**) (600 MHz, C$_6$D$_6$, 25°C)

In order to explore the configurationally stability of complex **1**, the ^{1}H NMR spectrum was acquired in the range from 20°C to 100°C. The variable temperature ^{1}H NMR (VT-NMR) spectra are reported Figure 2.2.6. The configuration of complex **1** resulted highly stable; as matter of fact, coalescence of the resonances resulting from a fast enantiomer (Δ - Λ) interconversion was not observed in the explored range of temperature.

It is worth noting that the analogous OSSO zirconium complex is rigid at room temperature and become fluxional upon warming; the coalescence of the diastereotopic protons is observed at 85°C. [31]
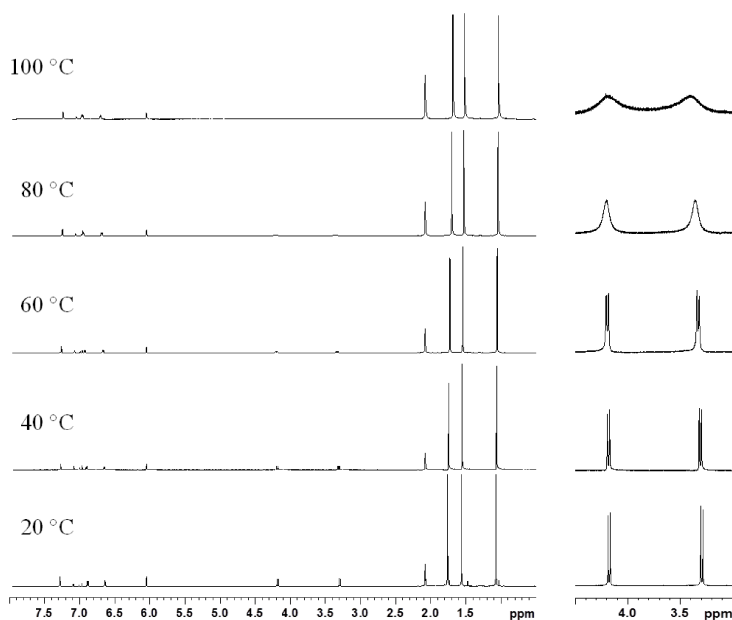
Figure 2.2.6 Variable-temperature ^{1}H NMR spectra of complex **1** (600 MHz, Tol-d8, 25°C)

EXSY experiment allows recording dynamic processes (as chemical exchange) occurring in a slow exchange regime on the NMR time scale. The EXSY experiment for the complex **1** in benzene-d$_6$ at 60°C (Figure 2.2.6) showed positive crosspeaks correlating the methylene signals proving the existence of the Λ-Δ interconversion. The intensity of this peak permitted to calculate the rate constant for the exchange ($k_{exchange}$) of 0.27 s^{-1}, the corresponding free energy of activation ($\Delta G^{\ddagger}$) was 20.4 kcal mol^{-1}.

Similar results were observed for (OSSO$_{Cum}$)Zr(O^{t}Bu)$_2$ (**2**) and (OSSO$_{Cum}$)Hf(O^{t}Bu)$_2$ (**5**). The Λ-Δ interconversion was slower and the value of $k_{exchange}$ was 0.05 s^{-1} corresponding to $\Delta G^{\ddagger}$ of 21.6 kcal mol^{-1}, for both complexes.

The ^{1}H NMR spectrum of **3** indicates a highly symmetric structure, in which the methylene protons resulted in the AB pattern and one of the two doublets are downfield shifted at 5.59 ppm (Figure 2.2.7).
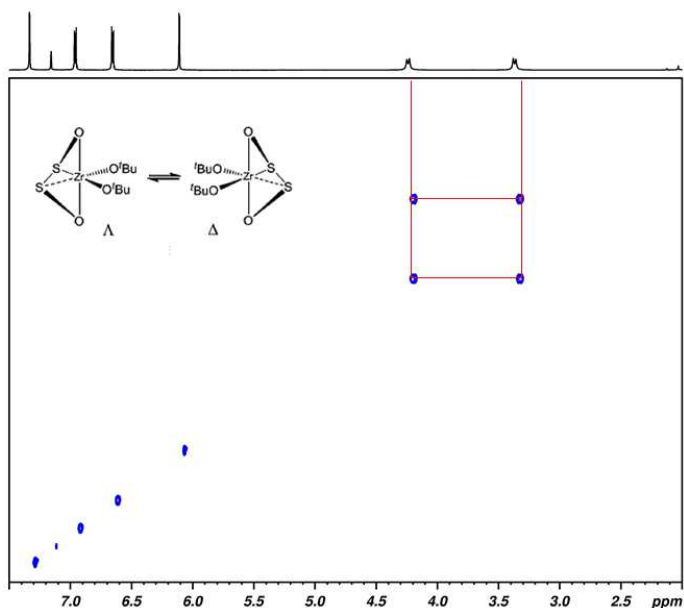
Figure 2.2.7. ^{1}H-^{1}H EXSY spectrum of **3** (C$_6$D$_6$, 60°C, mixing time 0.400 s, 600 MHz)

Differently, the ^{1}H NMR spectrum of (OSSO$_{Cum}$)Ti(O^{i}Pr)$_2$ (**4**) revealed, already at room temperature, fast fluxional behavior producing a broad singlet at 3.62 ppm for the S-CH$_2$ protons. The smaller size of titanium atom and the weaker interaction between the soft sulfur atom and the hard titanium ion likely influenced the configurational rigidity of **4** (Figure 2.2.8).

The solution structure of (OSSO$_{Cum}$)Ti(O^{i}Pr)$_2$ complex (**4**) was also monitored by variable temperature NMR in the range between -40°C to

30°C in CD$_2$Cl$_2$. The broad resonance of the S-CH$_2$ groups resolved in the typical AB pattern, after the coalescence at 0°C. The isopropoxide groups produced a doublet at 1.06 ppm and a septet at 4.38 ppm. The signals relative to the aromatic protons were observed in the range 6.03 - 7.40 ppm.
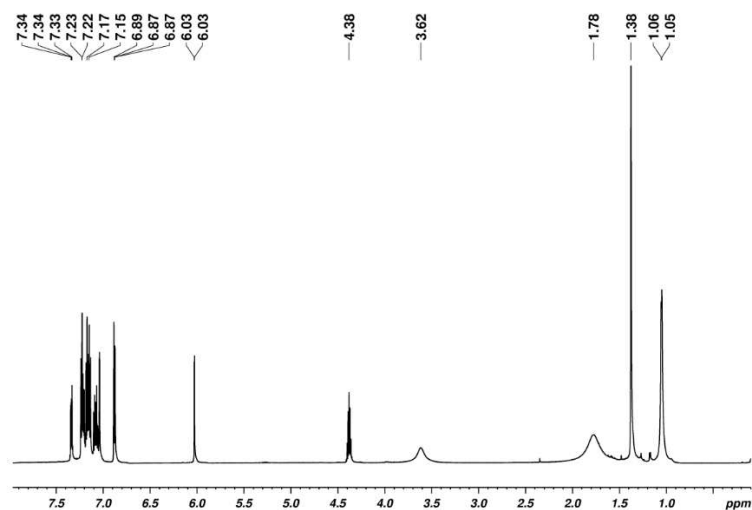
Figure 2.2.8. ^{1}H NMR of (OSSO$_{Cum}$)Ti(O^{i}Pr)$_2$ (**4**) (600 MHz, Tol-d$_8$, 25°C)

Kinetic parameters were calculated using line-shape analysis of the ^{1}H NMR spectra measured in the temperature range from -40 to 30 °C. The free energy of activation for the fluxional processes was calculated as $\Delta G^{\ddagger}$ = 13.4 ± 0.1 kcal mol^{-1} at 293 K. The activation parameters were $\Delta H^{\ddagger}$ = 11.9 ± 0.3 kcal mol^{-1} and $\Delta S^{\ddagger}$ = −5 ± 1 cal mol^{-1} K^{-1}.
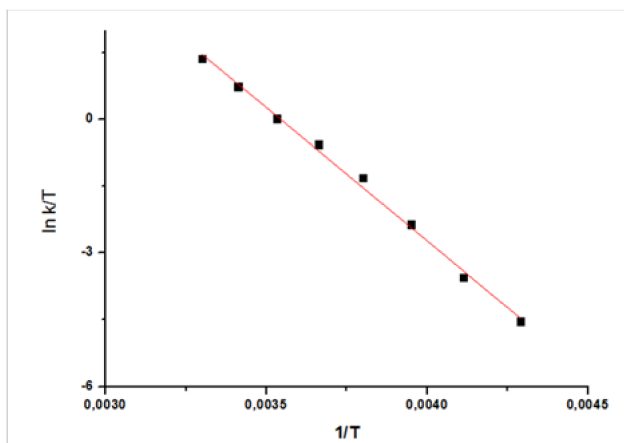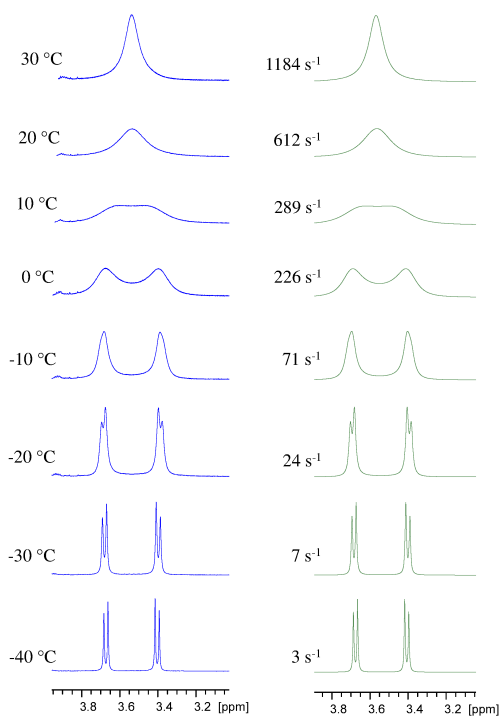
Figure 2.2.9. Variable-temperature ^{1}H NMR spectra of $(OSSO_{Cum})Ti(O^{i}Pr)2$ (**4**) and Eyring plot for the Δ-Λ enantiomer interconversion

The X-ray analysis of the complex $(OSSO_{Cum})Zr(O^tBu)_2$(**2**) confirmed the C_2-symmetric structure, in which the zirconium center is in octahedral environment resulting from the *fac-fac* coordination of the tetradentate ligand (Table 2.2.1). The bond length Zr-S (2.87 Å) are longer than the typical bond observed in this class of complexes with a consequent steric congestion around the Zr atom. Moreover, the distances of Zr- alkoxy groups (1.92Å) and Zr-O1 (2.03 Å) were paragonable to the analogous complexes of this family reported in literature.[31]
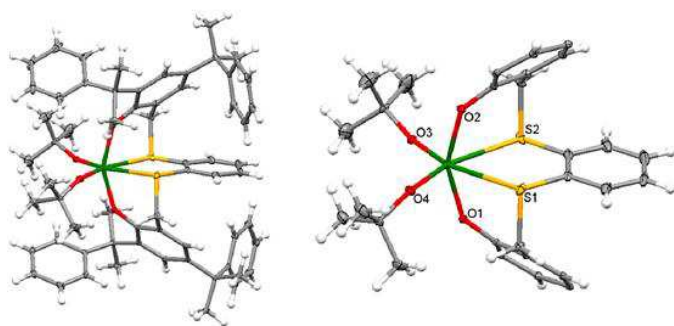
Figure 2.2.10. ORTEP drawing of $(OSSO_{Cum})Zr(OtBu)_2$

	Selected bond lengths (Å) and bond angles (°)
Zr−S1	**2.8704 (5)**
Zr−S2	**2.8797 (5)**
Zr−O1	**2.0309 (14)**
Zr−O2	**2.0380 (14)**
Zr−O3	**1.9263 (14)**
Zr−O4	**1.9420 (15)**
S1−Zr1−S2	**70.928 (18)**

Table 2.2.1.Selected bond lengths (Å) and bond angles (°) for $(OSSO_{Cum})Zr(O^tBu)_2$ as determined by single-crystal X-ray diffraction.

2.3 Ring Opening Polymerization of rac-Lactide catalyzed by 1-5

The complexes **1-5** were tested in the polymerization of *rac*-lactide in toluene (2.4 mL) at 100°C using the initiator to monomer molar ratio of 100.
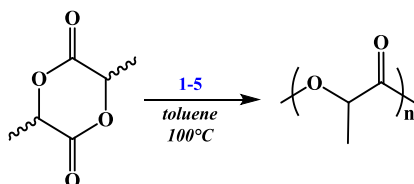
Figure 2.3.1. ROP of lactide catalyzed by **1-5**

The main results are reported in the Table 2.3.1. At specified time intervals, a small amount of the polymerization mixture was sampled by a pipette and quenched in wet CDCl₃ to evaluate the conversion through ^{1}H NMR spectroscopy.

Table 2.3.1. ROP of rac-lactide catalyzed by 1-5

Entry[a]	Initiator	t/h	Conv.%[b]	TOF/h^{-1c}	$M_{n(th)}$[d]	$M_{n(expt)}$[e]	PDI[e]
1	**1**	24	88	3.7	12.7	14.0	1.12
2	**2**	24	96	4.0	13.8	17.1	1.12
3	**3**	24	0	-	-	-	-
4	**4**	72	90	1.3	6.5[f]	6.3	1.13
5	**5**	24	94	3.9	13.5	15.4	1.32

[a]All reactions were carried out in 2.4 mL of toluene; $[I]_0 = 5.0$ mM, $[LA] = 0.52$ M, $[LA]/[I]_0 = 100$, and T = 100 °C. [b]Molecular conversion determined by ^{1}H NMR spectroscopy (CDCl₃, 298 K). [c]TOF = $mol_{LA}/(mol_I \ h)$. [d]Calculated molecular weight using M_n(th) (kg mol^{-1}) = (144.13×($[LA]_0/[I]_0$)×(LA conversion))/1000. [e]Experimental molecular weight M_n(expt) (kg mol^{-1}) and polydispersity (PDI) determined by GPC in THF using polystyrene standards and corrected using the factor 0.58. [f]Mn(th) (kg mol^{-1}) = (144.13 × ($[LA]_0/[2 \times I]_0$)×(LA conversion))/1000.

Complexes **1** and **2** showed a moderate activity, leading to high monomer conversion in 24 h; the turnover frequencies (TOF) are of 3.7 and 4.0 h^{-1}, respectively. The complex **3** was inactive, differently by similar homoleptic group IV metal complexes reported in literature[20] that are effective initiators for the ROP of lactide. Changing the metal center from zirconium (**2**) to hafnium (**5**), the catalytic performances were not influenced, obtaining high monomer conversion in 1 day. As expected, **4** was less active than the corresponding zirconium complexes **1** and **2**, leading to 90 % conversion in 72 h.

To investigate the mechanism of polymerization, **2** was selected for the kinetic investigations, via ^{1}H NMR spectroscopic analysis. At 100°C, the polymerization reaction displayed an induction period of 6 h after which the polymerization proceeded with a first-order dependence with respect to the monomer concentration. The semilogarithmic plot of $\ln([rac\text{-LA}]_0/[rac\text{-LA}]_t)$ versus time (h) was linear with a slope of 0.147 ± 0.008 h^{-1}. At 80°C, the catalytic activity decreased and a longer induction time was observed, as reported in Figure 2.3.2. In this last case, k$_{obs}$ was of 0.0371 ± 0.0009 h^{-1}.
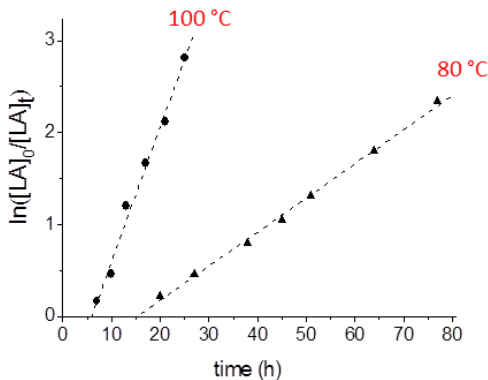
Figure 2.3.2. Kinetic of *rac*-LA polymerization by **2** at 100 °C (●) and 80 °C (▲). (k$_{obs}$ (100 °C) = 0.147 ± 0.008 h^{-1} R^2 = 0.986; k$_{obs}$ (80 °C) = 0.0371 ± 0.0009 h^{-1} R^2 = 0.996).

The origin of this induction time can be related to the genesis of the catalytic species. To identify the active species in the polymerization process, the reaction of **2** with *rac*-LA was monitored by ^{1}H NMR spectroscopy. The intensity of the signals of **2** decreased producing new patterns of proton signals, but it was not possible to identify the products in the reaction mixture.

The PLA samples by **2** showed narrow distributions of molecular weight ($1.12 \leq PDI \leq 1.32$) and a good agreements between the experimental and theoretical Mn values were observed in all samples by zirconium and hafnium catalysts. As reported in Figure 2.3.3, the experimental Mn*s* increase linearly with the monomer conversion. The polymers, obtained by titanium complex **4**, displayed experimental molecular weights in agreement with the corresponding theorical Mn*s*, assuming the growth of two chains per metal center. The PLAs obtained by **1-5** were atactic.
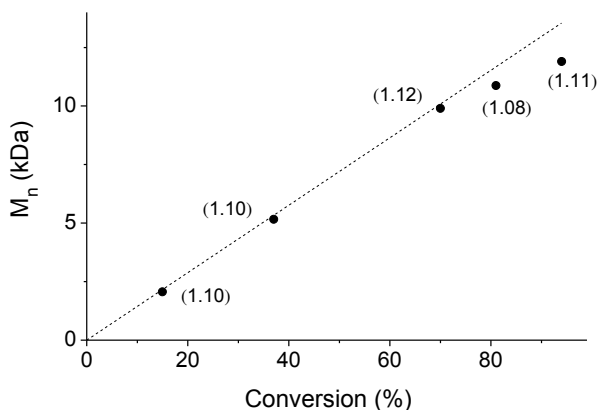
Figure 2.3.3. Plot of number-averaged molecular weights Mn(expt) (dot) vs conversion (%) with theoretical Mn(th) (dash line) using 2 as an initiator at 100 °C, M_w/M_n values are in parentheses.

Finally, the obtained PLA*s* were characterized by NMR spectroscopy and ESI mass spectrometry. The ^{1}H NMR spectrum of the sample by **2**, in CDCl$_3$, showed the signals relative to the *tert*-butoxide end group at 1.46 ppm, indicating a coordination-insertion mechanism (Figure 2.3.4). ESI MS analysis displayed a peak distribution relative to oligomers end terminated with tert-butoxide and hydroxyl groups [OCH(CH$_3$)C(=O)]$_n$-O^{t}Bu, in agreement with the NMR data. A second series of peaks was also detected due to the presence of cyclic oligomers. Both distributions were characterized by peaks separated by m/z of 72 corresponding to half monomer unit for effect of intramolecular and intermolecular transesterifications.
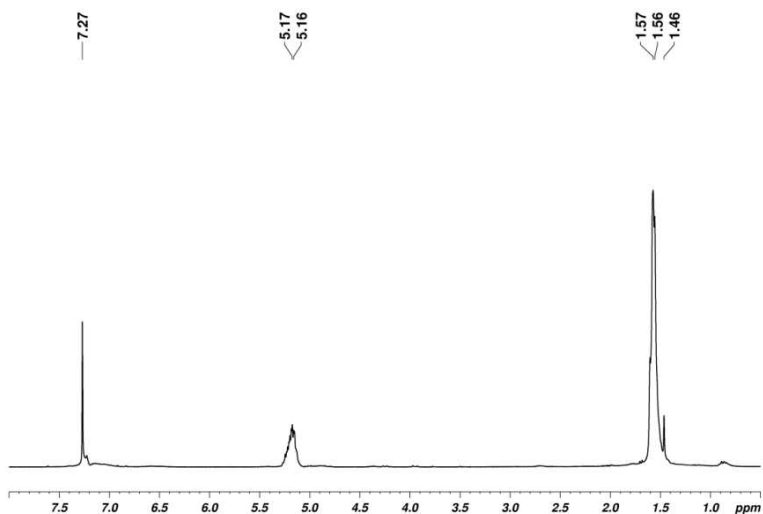
Figure 2.3.4. ^{1}H NMR spectrum of PLA by **2** (CDCl$_3$,400 MHz, 298 K)
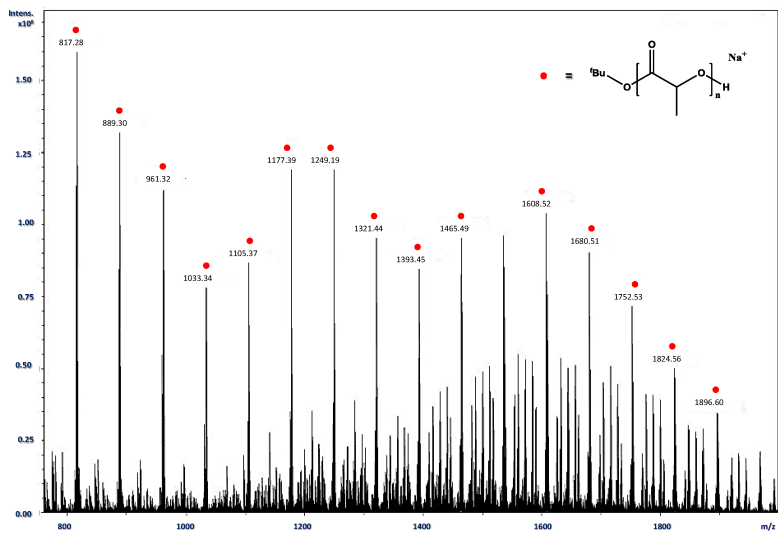
Figure 2.3.5. ESI-MS spectrum of oligomer of PLA by **2** as initiator.

2.3.1 Polymerization of rac-lactide in presence of isopropanol

The addition of an exogenous alcohol (ROH) has a benefical effect on the performances of the catalyst.[16] During the ring opening polymerization process, in absence of ROH, the number of growing polymer chain is equal to the number of the active sites, possibly the number of metal atoms of the precatalyst. The introduction of a nucleophilic species, as an alcohol (ROH), results in chain transfer between growing and dormant macromolecules. The number of growing polymer chains is, in this case, equal to ROH and higher than the metal atoms; this process is known as "immortal ROP" (Scheme 2.3.1.1).
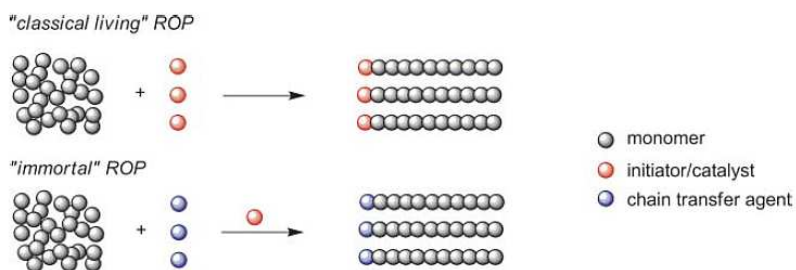
Scheme 2.3.1.1. Schamatic representation of ROP in presence of ROH

Recently, Carpentier reviewed the ROP of cyclic esters using cationic complexes in presence of exogen alcohols.[32] The cationic complexes were classified in three different categories named type-I, type-II and type-III. Type-I indicates metal complexes bearing nucleophilic ancillary ligand that are reactive toward the incoming cyclic monomer; type-II represents complexes with the nucleophilic groups inert toward the monomer and type-III where there is no nucleophile. The polymerization promoted by type-I complexes lead to only one growing chain per metal atom and the chain length is defined by the [monomer]$_{converted}$/[number of catalyst]$_0$ ratio *(m/n)* (Figure 2.4.1, *left*). In presence of one molecule of type-I or type-II complex and an excess of alcohol, the number of growing polymer chain is equal to

the molecules of alcohol and the chain length is dipendent of [monomer]$_{converted}$/[protic nucleophile]$_0$ ratio *(m/p)*. A fast transfer between growing and dormant macromolecules induce changing on the chain length defined as *m/(p+1)*. The overell process is reported in Figure 2.3.1.2.
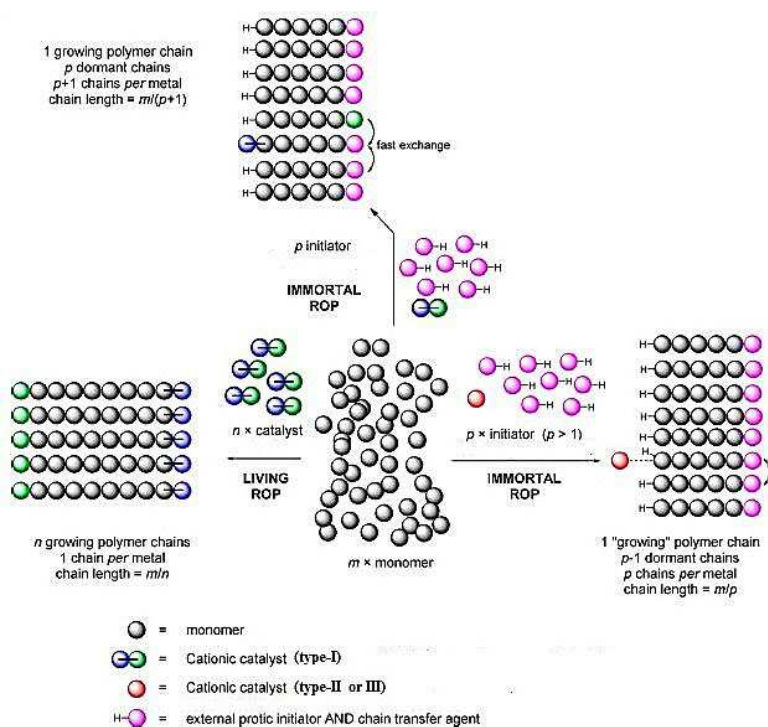
Figure 2.3.1.2 Living and Immortal ROP Processes[32]

To improve the performances of the complexes **1-5**, *i*PrOH (5 equiv.) was added to the mixture reaction; the main results are in the Table 2.3.1.1.

Table 2.3.1.1. ROP of *rac*-lactide in presence of exogenous alcohol

Entry[a]	Initiator	Temp.	alcohol	t/h	Conv.%[b]	TOF/h^{-1c}	$M_{n(th)}$[d]	$M_{n(expt)}$[e]	PDI[e]	P_r[f]
1	**1**	100	*i*PrOH	5	80	1.6×10^1	2.3	3.8	1.10	0.51
2	**2**	100	*i*PrOH	0.5	94	1.9×10^2	2.7	2.3	1.16	0.55
3	**2**	80	*i*PrOH	1.5	97	6.5×10^1	2.8	1.9	1.10	0.56
4	**2**	50	*i*PrOH	45	71	1.6	2.0	2.2	1.10	0.57
5	**3**	100	*i*PrOH	24	72	3.0	2.2	2.2	1.19	0.57
6	**4**	100	*i*PrOH	2	92	4.6×10^1	2.6	1.3	1.11	0.52
7	**5**	100	*i*PrOH	0.5	95	1.9×10^2	2.7	1.8	1.20	0.58
8	**2**	100	*t*BuOH	0.17	95	5.6×10^2	2.7	4.8	1.21	0.58
9	**2**	80	*t*BuOH	0.33	94	2.8×10^2	2.7	3.8	1.10	0.66
10	**2**	50	*t*BuOH	24	95	4.0	2.7	4.7	1.09	0.66

[a]All reactions were carried out in 2.4 mL of toluene, $[I]_0 = 5.0$ mM, $[LA] = 0.52$ M, $[ROH] = 25.0$ mM; $[LA]_0:[I]_0:[ROH]_0 = 100:1:5$. [b]Molecular conversion determined by ^{1}H NMR spectroscopy (CDCl$_3$, 298K). [c]Calculated molecular weight using $M_{n(th)}$ (Kg mol^{-1}) = (144.13 × ([LA]$_0$/[ROH]$_0$) × LA-conversion)/1000. [d]Experimental molecular weight $M_{n(expt)}$ (Kg mol^{-1}) and polydispersity (PDI) determined by GPC in THF using polystyrene standards and corrected using the factor 0.58. [e]Probability of racemic linkages as determined by homodecoupled ^{1}H NMR spectroscopy.

At 100°C, **1** converted 100 equivalents of monomer in 5 hours, whereas **2** showed high monomer conversion in only 30 min (TOF = 1.9 x 10^2 h^{-1}). The complex **5** consumed 95 mol % of *rac*-lactide in 0.5 h and the titanium complex **4** allowed 92 mol % conversion in about 2 h. In presence of isopropanol, **3** became active in the ROP of lactide. The PLAs produced by **1-5** are atactic. The polymerization promoted by complex **2** in presence of isopropanol was monitored at 80°C through ^{1}H NMR spectroscopy, observing a first-order kinetics with an apparent rate constant of 2.32±0.05 h^{-1}. The good agreement between the theoretical and experimental molecular weigths, calculated considering the growing of one chain for molecule of isopropanol, indicated an efficient control of the polymerization process. All the polymers exhibit a monomodal distribution of the molecular weigth with the PDI values in the range of 1.1-1.2 (Figure 2.3.1.3).
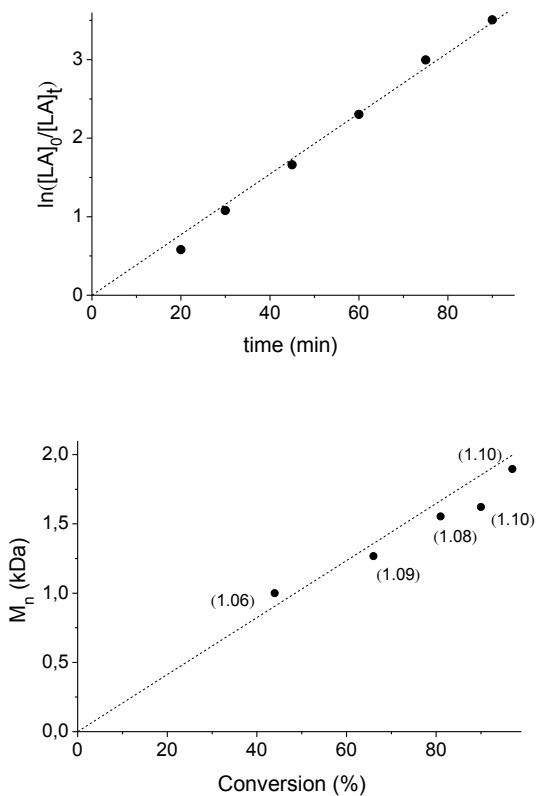
Figure 2.3.1.3 (up) Kinetic of *rac*-LA polymerization promoted by catalyst **2**/^{i}PrOH. (down) Plot of number-averaged molecular weights $M_{n(expt)}$ (dot) *vs* monomer conversion (%) with theoretical $M_{n(th)}$ (dash line) using the catalyst **2**/^{i}PrOH,

The ^{1}H NMR spectrum of PLA displays a polymer chain terminated with isopropoxide (C*H* at 4.35 ppm as heptet and C*H₃* at 1.69 ppm as doublet) and hydroxide end groups (Figure 2.3.1.4). The ESI MS spectrum confirmed the existence of linear oligomers with –O^{i}Pr end-groups (Figure 2.3.1.5).
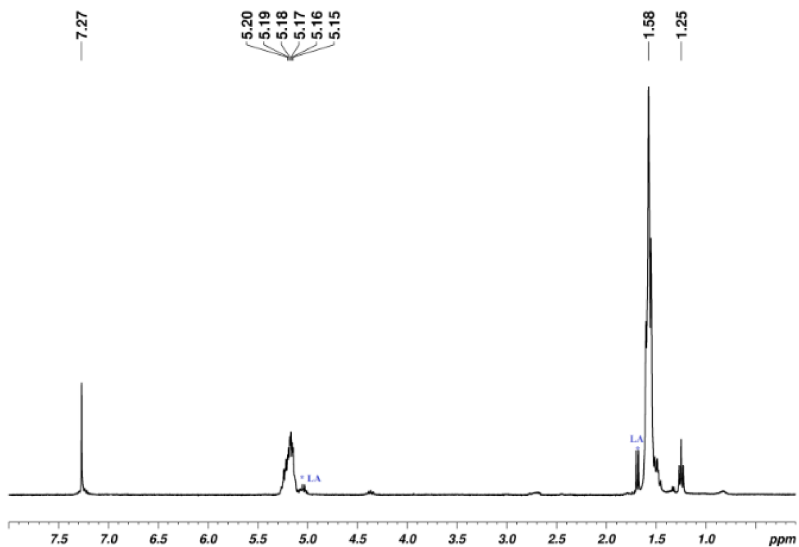
Figure 2.3.1.4. ^{1}H NMR spectrum (400 MHz, CDCl$_3$, 298 K) of PLA by **2**/iPrOH
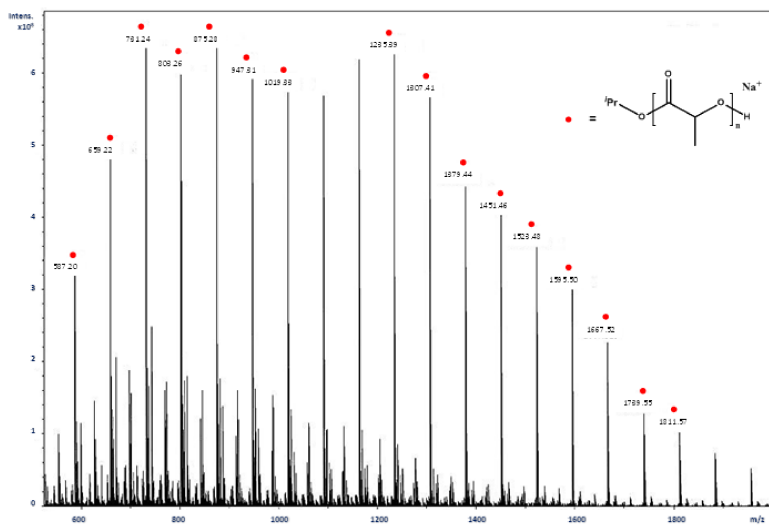
Figure 2.3.1.5. ESI-MS spectrum of PLA by **2**/iPrOH

Different monomer/initiator molar ratios were explored to test the living character of complex **2** in presence of 5 equiv. of ^{i}PrOH. In the range from 100 to 1000, the experimental molecular weights increase linearly as expected for the theoretical values; the distribution of Mns are monomodal and the PDI values are in the range 1.1-1.2 (Figure 2.3.1.6).
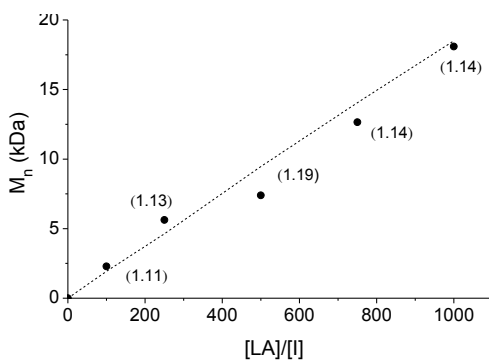
2.3.1.6. Plot of $M_{n(expt)}$ (dot) *vs* $M_{n(th)}$ (dash line) using **2**/^{i}PrOH.

With the aim to investigate the polymerization mechanism, the reaction of the catalyst (OSSO)$_{tBu}$Zr(O^{t}Bu)$_2$ (**1**) with isopropanol was monitored by ^{1}H NMR spectroscopy in NMR tube, using benzene-d$_6$ at 25°C. The NMR spectrum displayed a quantitative conversion of **1** into the corresponding isopropoxide derivate [(OSSO)$_{tBu}$Zr(O^{i}Pr)$_2$] with the concomitant production of ^{t}BuOH (Figure 2.3.1.7).
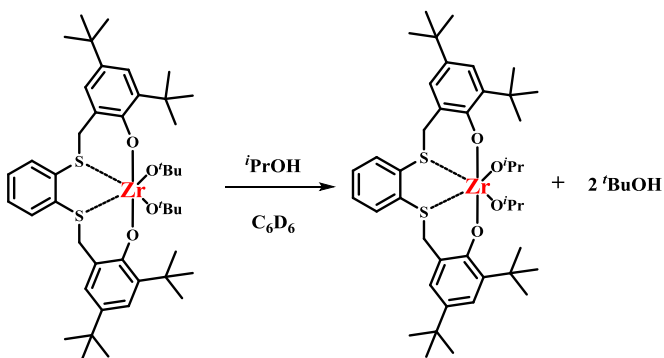
Figure 2.3.1.7 Scheme of exchange reaction between **1** and ^{i}PrOH.

The strong increase of reactivity can not be due only to the change of initiator group. Therefore, to evaluate the effective role of external alcohol, the ROP of *rac*-lactide (100 eq.) was carried out using the complex **2** in presence of ^{t}BuOH as cocatalysts, see Table 2.3.1.1 (entries 8-10); at 100°C high monomer conversion was observed in 10 min. The kinetics was of first-order with respect to the monomer concentration and the measured rate costant was $7.8 \pm 1.2 \ h^{-1}$ (Figure 2.3.1.8).
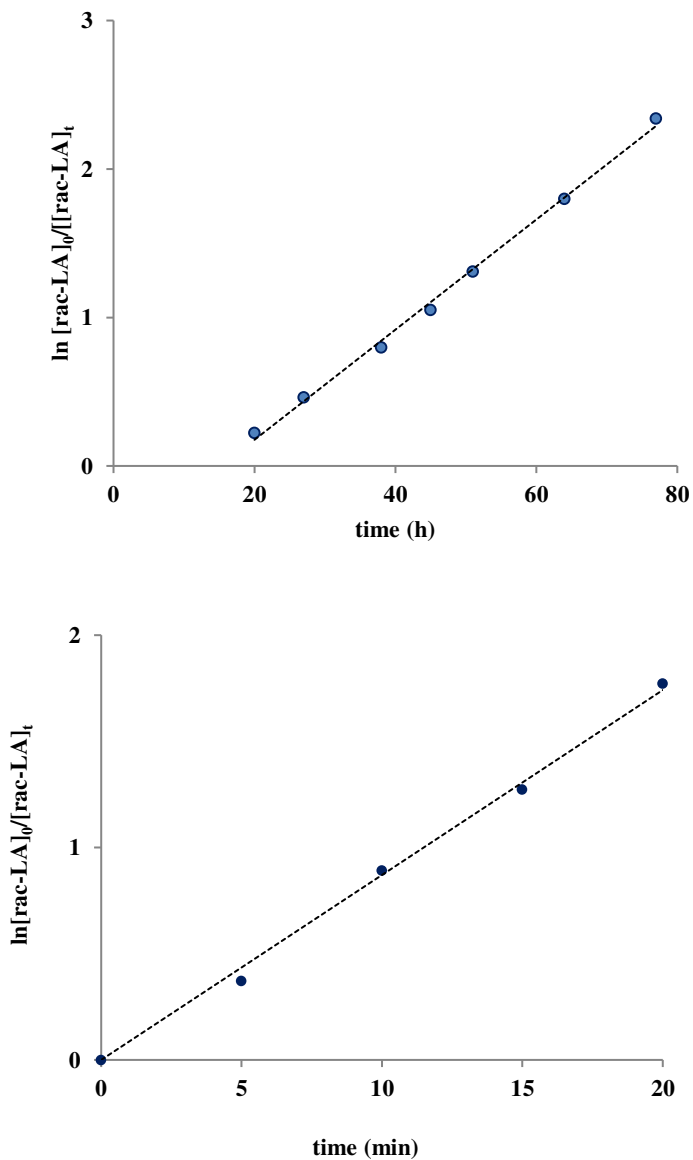
Figure 2.3.1.8. Kinetic plot for ROP of *rac*-LA promoted by **1** at 80°C in absence of alcohol *(up)* with $k_{obs} = 0.371 \pm 0.0009$ h^{-1} and in presence of ^{t}BuOH *(down)* with $k_{obs} = 7.8 \pm 1.24$ h^{-1}

The ^{1}H NMR and ESI MS analysis of the obtained PLA confirmed the formation of linear oligomers characterized by *tert*-butoxide end groups (singlet at 1.46 ppm), below Figure 2.3.1.9 and 2.3.1.10.
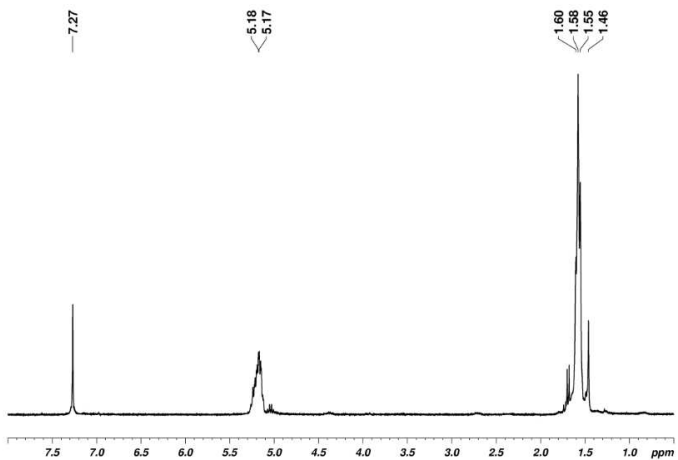
Figure 2.3.1.9. ^{1}H NMR spectrum (400 MHz, CDCl$_3$, 298 K) of PLA by **2**/^{t}BuOH
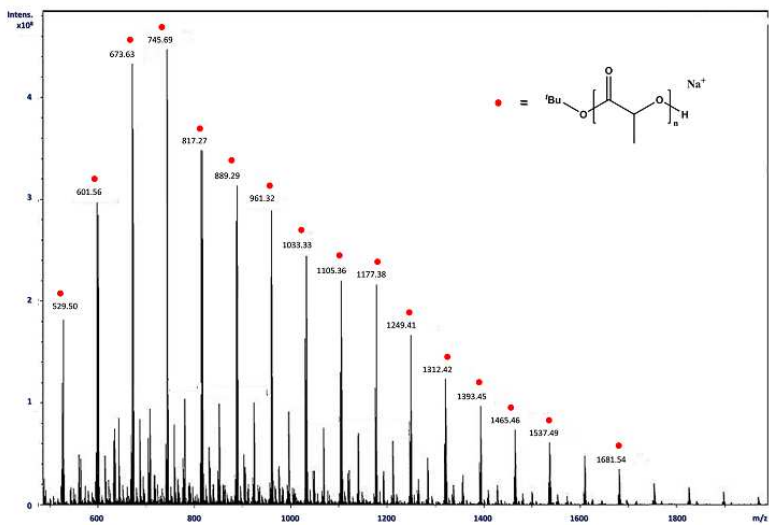
Figure 2.3.1.10. ESI-MS spectrum of PLA obtained by **2**/^{t}BuOH as initiator.

As in the case of ^{i}PrOH, the reaction of **1** with ^{t}BuOH was investigated through 2D ^{1}H−^{1}H EXSY spectroscopy. An exchange reaction between *tert*-butyl alcohol and the *tert*-butoxy ligand was detected; the process was slow with the rate constant of 1.0×10^{-3} s^{-1}.

All the experimental evidences suggest the establishment of an alternative ROP focused on the "activated monomer" mechanism. This process implies, firstly, the coordination of the lactide to the Lewis acidic metal center that actives the monomer, then the nucleophilic attack of ROH to the electrophilic carbon atom of the carbonyl group triggers the polymerization process (Figure 2.3.1.11).
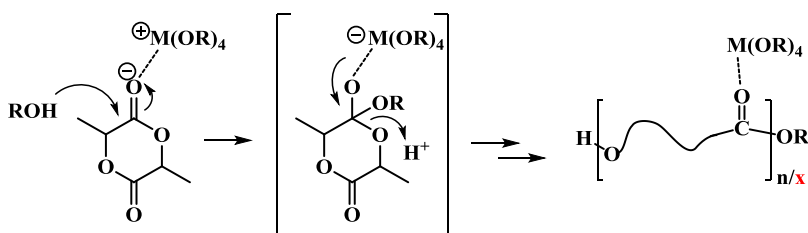
Figure 2.3.1.11. "Activated Monomer" Polymerization

2.4 Conclusions

We synthetized a new series of (OSSO)-type Group IV complexes of general formula $(OSSO_X)M(OR)_2$, by protonolysis reactions between an appropriate proligand (**L1-3**) and a metal alkoxide precursor. All complexes were obtained in good yields and fully characterized by NMR spectroscopy. ^{1}H NMR of the complexes suggested an octahedral environment with rigid C_2-symmetry as confirmed by crystallographic data of complex **2** (Figure 2.2.10), in which the *fac-fac* ligand wrapping around the metal center was observed. The titanium complex **4** showed a fluxional character at 25°C because of weaker interaction between the soft sulfur atom and the hard titanium ion. Complexes **1-5** were active in the ROP of *rac*-lactide; the best performance was observed with **2**, where the monomer was quantitatively converted into polymer in 24 h. The polymerization is characterized by long induction time and a pseudo first order kinetic with respect to the monomer. In the presence of *[i]PrOH*, the catalytic performances improved (94 % conversion, 30 minutes) and no induction time was registered. Under this condition, a linear dipendence between molecular weight and monomer conversion was observed, suggesting a living character of the polymerization. The strong increase of the polymerization reactivity can not justified only by the exchange of the initiator group. The ROP by **2** was studied in presence of 5 eq. of *[t]BuOH*; a 95 % of monomer conversion in 30 minutes was observed and the resulting polymer showed a *tert*-butoxide end group. [1]H-^{1}H EXSY experiment displayed the stability of the complex **2** in presence of *tert*-butanol. The lack of reactivity of **1-5** in presence of an exogenous alcohol, suggests that the ROP operating mechanism is the activated monomer mechanism in alternative to the common coordination-insertion process.

2.6 References

[22] Bradley, D. C.; Mehrotra, R. C.; Rothwell, I. P.; Singh, A. *Alkoxo and Aryloxo Derivatives of Metals, Academic, San Diego, CA,* **2001**.

[23] Saha, T. K.; Ramkumar, V.; Chakraborty, D. *Inorg. Chem.* **2011**, *50,* 2720-2722.

[24] Whitelaw, E. L.; Jones, M. D.; Mahon, M. F. *Inorg. Chem.* **2010**, *49*, 7176–7181

[25] Zelikoff, A. L.; Kopilov, J.; Goldberg, I.; Geoffrey W. Coates, G. W.; Kol, M. *Chem. Commun.*, **2009**, 6804-6806.

[26] Stopper, A.; Press, K.; Okuda, J.; Goldberg, I.; Kol, M. *Inorg. Chem.* **2014**, *53*, 9140−9150.

[27] Sergeeva, E.; Kopilov, J.; Goldberg, I.; Kol, M. *Inorg. Chem.*, **2010**, *49*, 3977–3979.

[28] Buffet, J.-C.; Kapelski, A.; Okuda, J. *Macromolecule*s, **2010**, *43*, 10201-10203.

[29] Lapenta, R.; Buonerba, A. De Nisi, A.; Monari, M.; Grassi, A.; Milione, S.; Capacchione, C. *Inorg. Chem.* **2017**, *56*, 3447-3458.

[30] a) Ishii, A.; Toda, T.; Nakata, N.; Asajima, K. *Organometallics,* **2011**, *30*, 2947-2956. **b)** Si, G.; Zhang, L.; Han, B.; Duan, Z.; Li, B.; Dong, J.; Li, X.; Liu, B. *Polym. Chem.* **2015**, *6*, 6372-6377. **c**) Konkol, M.; Nabika, M.; Kohno, T.; Hino, T. *Organomet. Chem.* **2011**, *696*, 1792−1802.

[31] Cohen, A.; Yeori, A.; Goldberg, I.; Kol, M. *Inorg, Chem.* **2007**, *46*, 8114-8116.

[32] Sarazin, Y.; Carpentier, J.-F. *Chem. Rev.* **2015**, *115*, 3564−3614.

Chapter 3

3.1 Bis(phenolato) Group IV metal complexes in the polymerization of α-olefins

Post-metallocene catalysts are widely used in olefin polymerization (ethylene, styrene, propylene, 1-hexene, cyclic olefins) allowing to obtain polymers and olefin copolymers with controlled microstructure.[33] Titanium and zirconium complexes of bis(phenoxy-imine) ligands developed by Fujita; known also as FI from the the japanese pronunciation of the ligand "Fenokishi-Imin Haiishi", display a catalytic activity strongly dependant of the steric and electronic encumbrance of the substituents at the phenoxide groups and nitrogen atoms. The Figure 3.1.1 shows one of the most active FI complexes in ethylene polymerization with catalyst activity of $4.3 \cdot 10^9$ $g_{polimero} \cdot mol^{-1} h^{-1}$ at 25°C and $7.2 \cdot 10^9$ $g_{polimero} \cdot mol^{-1} h^{-1}$ at 75°C, in comparison to 1×10^7 $g_{polimero} \cdot mol^{-1} . h^{-1}$ for the metallocene catalyst at room temperature.
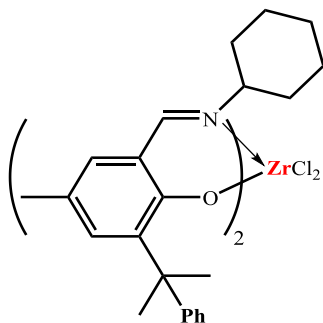
Figura 3.1.1. Dichloro Zirconium Bis(Phenoxy-Imine) complex[34]

Replacing the cyclohexyl group at the nitrogen atom with the 2,3,4,5,6-pentafluorobenzene (Figure 3.1.2), the catalytic performances descreased significantly, achieving the value of $4.08 \cdot 10^7$ $g_{polimero} \cdot mol^{-1} . h^{-1}$ at 50°C and $3 \cdot 10^7$ $g_{polimero} \cdot mol^{-1} h^{-1}$ at 75°C. Interestingly, propylene polymerization by

FI catalysts produced unexpectedly syndiotactic polymer via chain-end control mechanism.
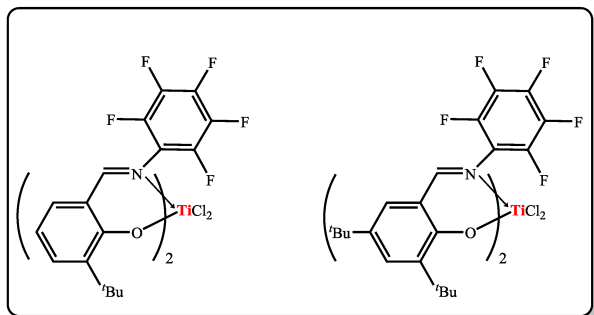
Figure 3.1.2. Titanium Complex Containing Two Phenoxy-Imine Chelate Ligands substituted with fluorine atoms. [35]

In 2000 Kol et al.[36] reported a zirconium complex of salan ligands (Chart 2), which allows isospecific and living polymerization of 1-hexene and propylene in presence of $B(C_6F_5)_3$ activator (Figure 3.1.3).
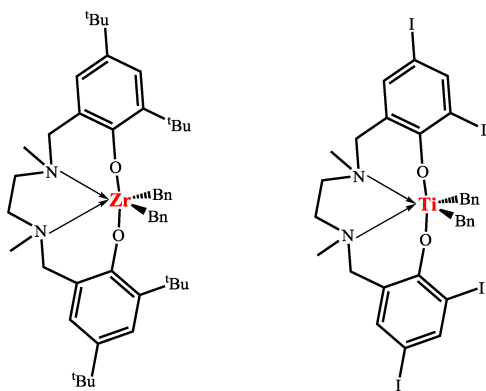
Figure 3.1.3. Titanium and Zirconium Complexes bearing salan-type ligand.

In recent decades, OSSO-type bis(phenolato) ligands were developed. They are similar to the [ONNO]-type, but the N donors are replaced with more *softer* sufur atoms. The tetradentate [OSSO]-type group 4 complexes were widely explored in the polymerization of α-olefin for their good polymerization control and high stereoselectivity. Among these, one of the most significantly example is reported in Figure 3.1.4, producing isotactic enriched polystyrene.[37]
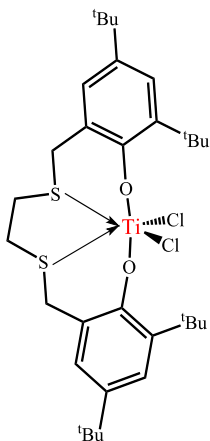
Figure 3.1.4. (OSSO)TiCl$_2$ complex

Similar (OSSO)ZrBn$_2$ complexes are displayed in Figure 3.1.5. The complex **A**, prepared by Kol,[31] resulted active in the living polymerization of 1-hexene giving atactic polymer; while **B**, prepared by Ishii,[38] provided a highly active and stereospecific catalytic system for the polymerization of 1-hexene to give isotactic poly(1-hexene)s. In this framework, we decided to explore the performances of OSSO-type titanium complexes featuring the *o*-phenylene bridged bis(phenolato) ligands. In this chapter are described the synthesis and the solution properties of two titanium complexes bearing **L1** and **L2** ligands (Chart 1); the results on the performances of these catalysts in olefin polymerization are also reported.

In order to get a more insight in the structure-activity relationship, we thought of extending the class of investigated complexes including a flexible OSSO-type titanium complex. To achieve this aim, we prepared a new OSSO ligand (**L4**) in which the sulfur atoms and the methylene groups are inverted, see Scheme 3.2.1.
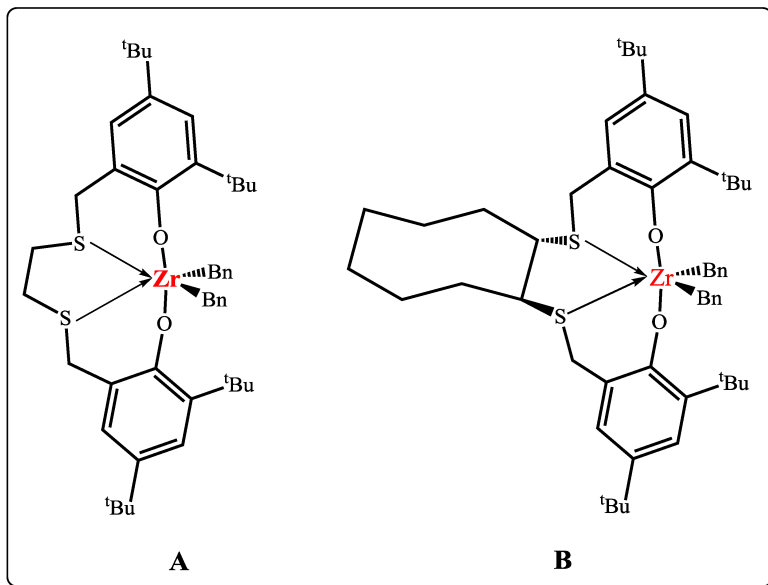
Figure 3.1.5. Zirconium complexes bearing OSSO-type bisphenolate ligand prepared by Kol (**A**) and Ishii (**B**)

3.2 Synthesis and characterization of (OSSO)TiCl₂ complexes 6-8

The **L4** ligand was prepared by reaction between 2,4-di-*tert*-butyl-6-mercaptophenol sodium salt and 1,2-bis(bromomethyl)benzene in dry THF (Scheme 3.2.1).[39]
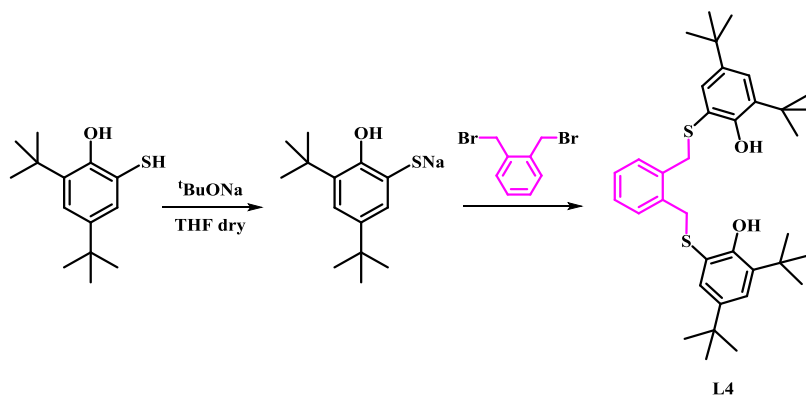
Scheme 3.2.1. Synthesis of **L4**

The **L4** ligand was fully characterized by NMR spectroscopy and element analysis. The ^{1}H NMR shows, in Figure 3.2.1, at ô 1.12 and 1.27 ppm two singlets due to the *tert*-butoxide groups (36 H). The signal of the methylene groups (s, 4H, ô 3.53 ppm) are followed by the singlet of OH (2 H) at ô 6.86 ppm. In the range between 6.75-7.20 ppm, the aromatic protons (8 H) were observed.
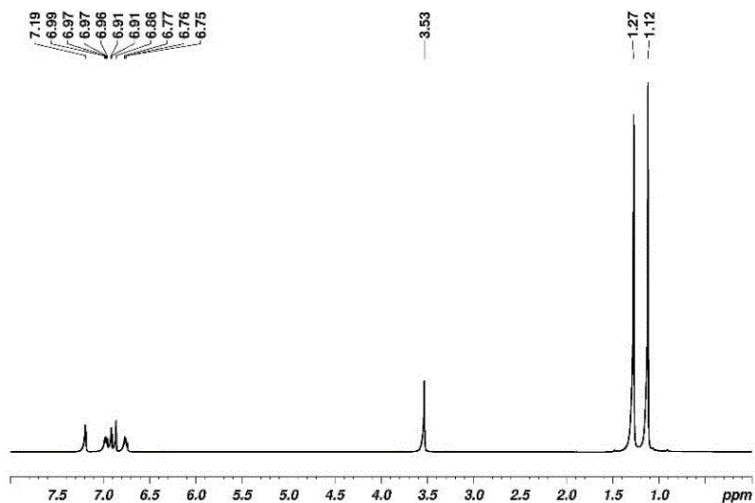
Figure 3.2.1. ^{1}H NMR of **L4** (CDCl$_3$, 300 MHz, 25°C)

To explore the influence of eletronic and steric factors of the ligands in the olefin polymerization, three new titanium complexes (**6-8**) bearing OSSO-type ligands (**L1-2** and **L4**) were synthetized through reaction between the appropriate proligand and TiCl$_4$ at room temperature (see Figure 3.2.2).
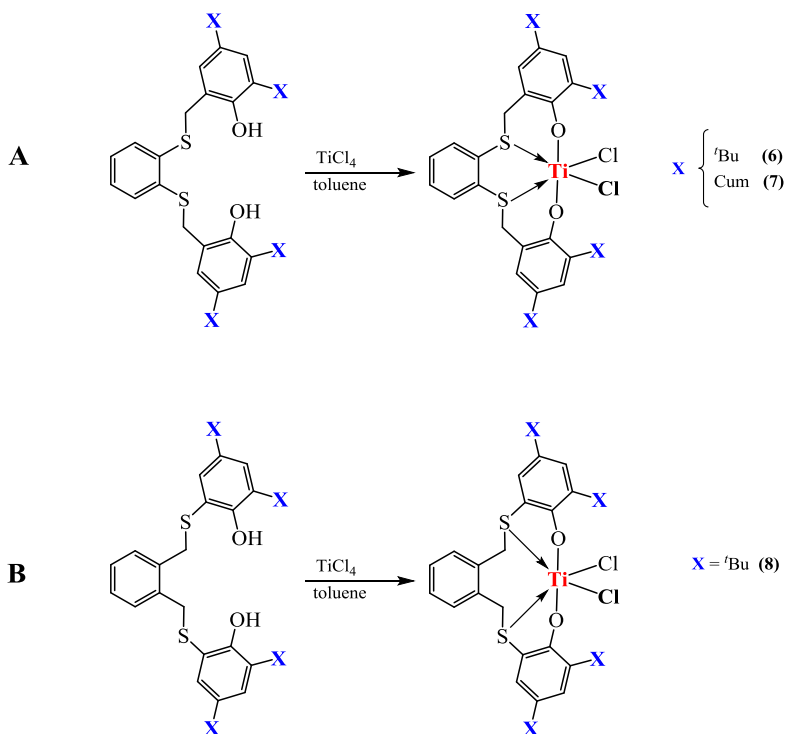
Figure 3.2.2. Schematic procedure for the synthesis of the complexes **6-8**.

The ^{1}H NMR spectrum of the complex (OSSO$_{tBu}$)TiCl$_2$ (**6**) in benzene-d$_6$ solution displays the diastereotopic methylene protons as AB pattern at 3.2 and 4.4 ppm. The resonances of *tert*-butyl substituents on the phenoxide groups result as singlets at 1.03 and 1.89 ppm accounting for 36 protons. The aromatic protons appeared in the range between 6.09-7.34 ppm (Figure 3.2.3).
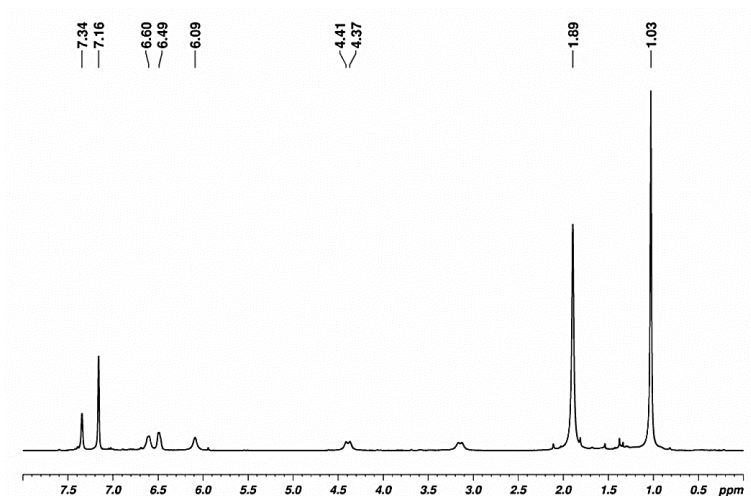
Figure 3.2.3. ^{1}H NMR of (OSSO$_{tBu}$)TiCl$_2$ (**6**) (300 MHz, C$_6$D$_6$, 25°C)

The ^{1}H NMR spectrum of the complex **6** in tetrachloroethane-d$_2$ (TCDE), at 25°C, showed broad resonances for the methylene protons bound to sulfur atoms and for the CH$_3$ protons of the *tert*-butyl groups, indicating a fluxional behavior of the complex in TCDE solution. By cooling the solution of **6** to -50 °C, the signals became narrower and well-resolved; new resonances were detected between 3.5-5.3 ppm, suggesting an equilibrium among more than one isomer (Figure 3.2.4).
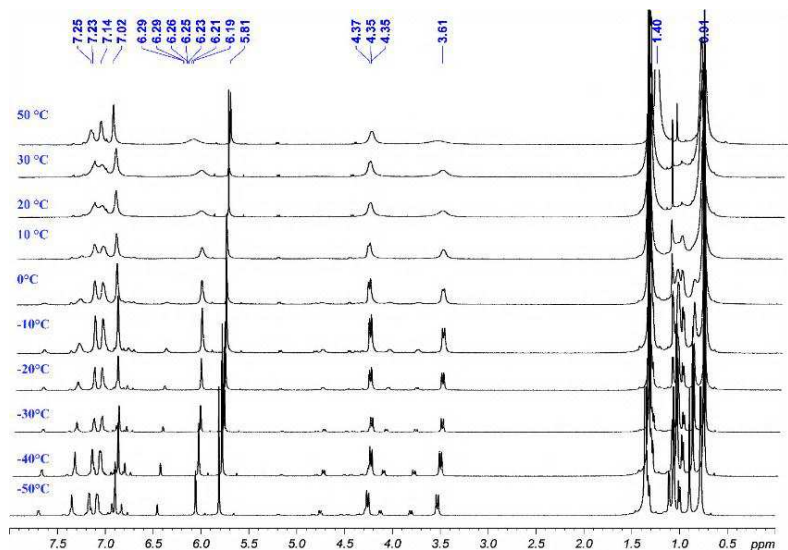
Figure 3.2.4. Variable-Temperature ^{1}H NMR spectra of complex **6** (TCDE, 600 MHz)

Thus, the exchange regime for **6** was analyzed by ^{1}H-^{1}H EXSY at -40 °C. In Figure 3.2.5, the positive cross peaks correlating the signals of the methylene groups of three species were observed. The most abundant isomer showed a C_2-symmetric structure, testified by AB pattern at 3.53 and 4.27 ppm of the methylene protons. C_1-symmetric isomer was also present, in which the not equivalent methylene protons appeared as doublets at δ 3.81, 4.12, 4.28 and 4.78 ppm, respectively. Another pattern of less intense signals, attributable to a further species in solution was detected; attempts to determinate solution structure of the latter were not successful.
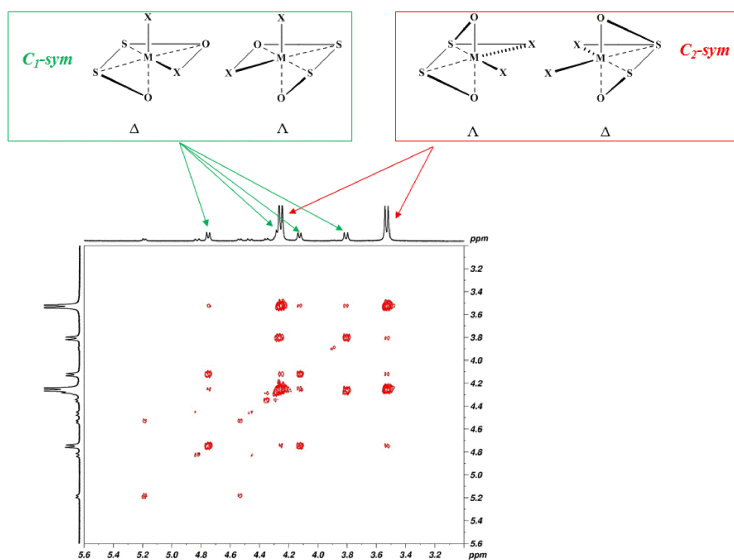
Figure 3.2.5. EXSY spectrum of **6** at -40 °C (τ_m = 0.500 s, TCDE, 600 MHz).

The single-crystal X-ray diffraction of **6**, obtained in acetonitrile-d_3 solution at 25°C, confirmed the C_2-symmetry, in which the Ti atom adopts a distorted octahedral coordination and the tetradentate ligand is in the *fac-fac* wrapping with the two oxygen in trans, the two sulfur and chlorides atoms in cis position, respectively. The structural rigidity of the OSSO ligand induces a distortion of the octahedral molecular geometry, resulting in the deviation of the O-Ti-O angle from linearity [O1-Ti-O2 161.09 (14)°]. The Ti-S distances are shorter than those found in a similar diisopropoxy Ti(IV) complex bearing an OSSO type ligand,[40] but longer than the Ti-S bond lengths in the dimeric Ti(III) complex.[38] The distance between the two chlorides was 104.89 (6)°. The ORTEP drawing of (OSSO^{t}Bu)TiCl$_2$ is reported below in Figure 3.2.6.
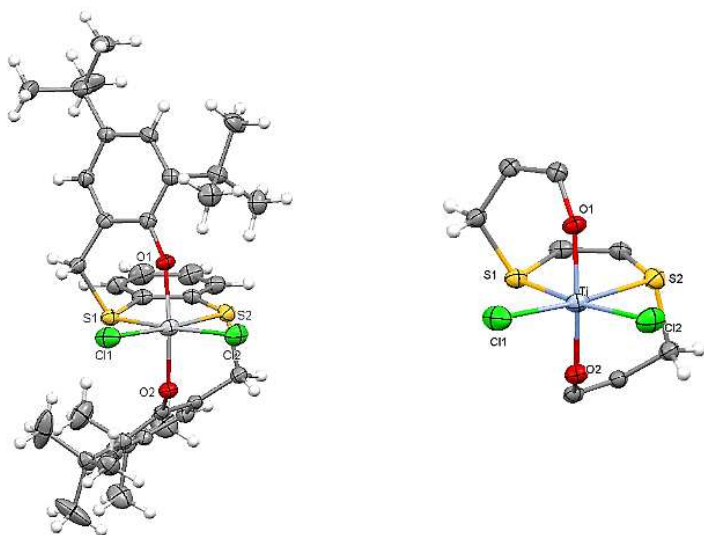
Figure 3.2.6 ORTEP deawing of (OSSOtBu)TiCl$_2$ (30% thermal ellipsoids, hydrogen atoms were omitted for clarity). Selected bond lengths [Å] and bond angles[deg]: Ti-Cl1 = 2.271 (2); Ti-Cl2 = 2.278 (2); Ti-O1 = 1.835 (3); Ti-O2 = 1.864 (3); Ti-S1 = 2.601 (2); Ti-S2 = 2.603 (2); S1-Ti-S2 = 77.88 (5); O1-Ti-O2 = 161.09 (14); Cl1-Ti-Cl2 = 104.89 (6).

As observed for the complex **6**, also (OSSO$_{Cum}$)TiCl$_2$ **7** displays in solution an equilibrium between two isomers; the C$_1$ symmetric isomer is in 3:2 molar ratio with the C$_2$ symmetric isomer (see Figure 3.2.7).
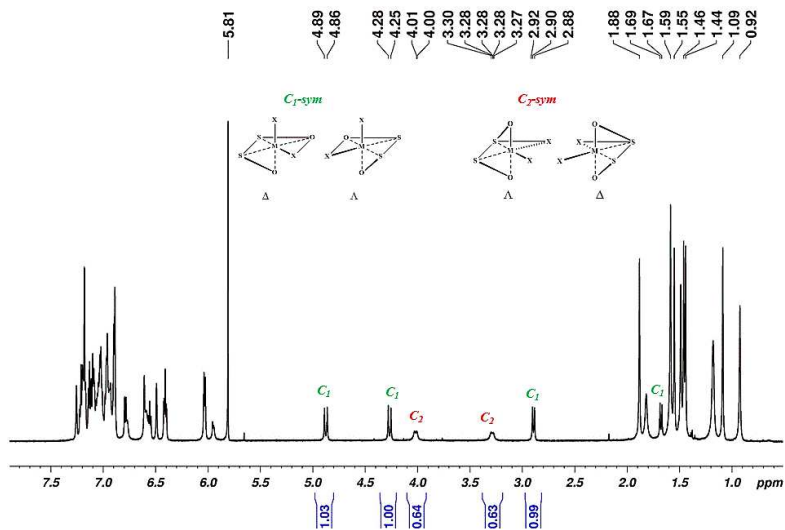
Figure 3.2.7. ^{1}H NMR of **7** (TCDE, 600 MHz, 30°C)

The variable temperature (VT) ^{1}H NMR spectroscopy, in the range of temperature from 30°C to 90°C, shows that the isomers of **7** are rigid at 30°C, but become fluxional upon warming at 50 °C and the coalescence temperature is at 70 °C (Figure 3.2.8). The coalescence event confirmed that the different resonances of S-CH$_2$ protons belong from two isomers interconverting in the fast regime. Then, the exchange of **7** was studied through EXSY experiments at 30°C; as reported in Figure 3.2.9, positive cross-peaks that correlate the methylene signals of the C$_1$- and C$_2$-symmetric structures were observed.
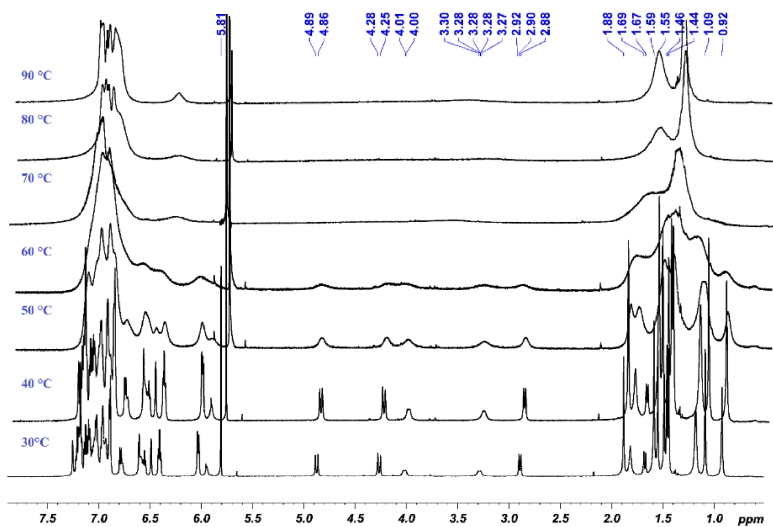
Figure 3.2.8. Variable-Temperature ^{1}H NMR spectra of complex **7** (TCDE, 600 MHz)
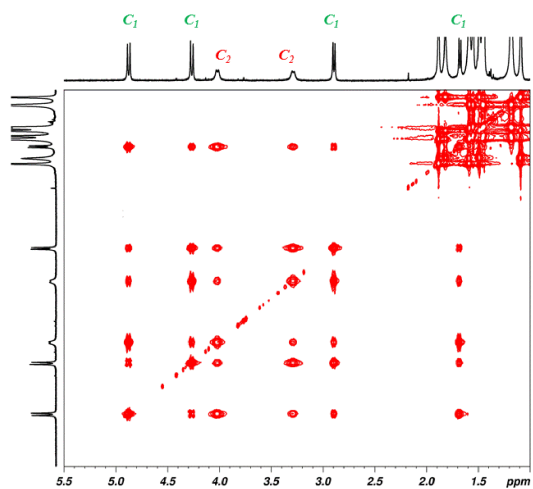
Figure 3.2.9. EXSY spectrum of **7** at 25 °C (τ_m = 0.300 s, TCDE, 600 MHz).

The titanium complex (**8**) bearing a more flexible OSSO-type ligand (**L4**) was synthetized using the same procedure previously described in the Section 2.2. The ^{1}H NMR spectra of **8**, at 25°C, in aprotic deuterated solvents (benzene, chloroform, dichloromethane) featured broaden resonances which suggest a fluxional behavior on the NMR timescale (Figure 3.2.10).
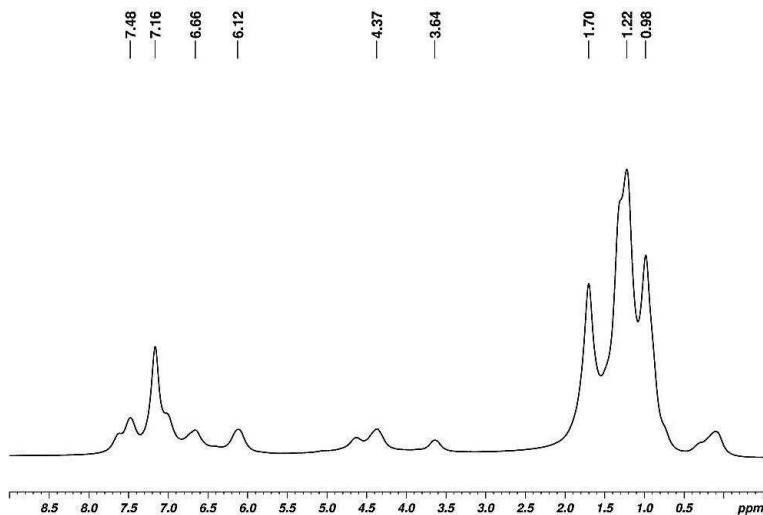
Figure 3.2.10. ^{1}H NMR of **8** (300 MHz, C$_6$D$_6$, 25°C)

3.3 Ethylene and propylene polymerization catalyzed by 6-8

The complexes $[OSSO_X]TiCl_2$ (**6-8**) were tested in ethylene polymerization under the typical reaction conditions using a 250 mL Buchi glass pressure reactor equipped with a mechanical stirrer and modified methylaluminoxane (MMAO 7 wt % in toluene) as activator. The complexes **6-8** are active in ethylene polymerization (Table 3.3.1). At [Al]/[M] molar ratio of 1000, the best catalytic performances are observed for **7** with the activity of 42 $Kg_{PE} \cdot mol_{cat}^{-1} \cdot bar^{-1} \cdot h^{-1}$ (entry 2, Table 3.3.1), followed by **6** and **8** respectively. The activity of **7** decreases when the [Al]/[MMAO] molar ratio was changed to 2000 or 500.

Table 3.3.1. Ethylene polymerization with complexes 6-8/MMAO

Entry[a]	Precatalyst	[Al]/[M]	Yield	Activity[b]	T_m^c	M_w^d	PDI
			g	$kg_P \cdot mol_{cat}^{-1} \cdot bar^{-1} \cdot h^{-1}$	°C	KDa	
1	**6**	1000	0.49	9.8	135.1	458	75.8
2	**7**	1000	2.20	42	136.3	1370	55.9
3	**8**	1000	0.33	6.6	135.3	530	70.2
4	**7**	2000	0.26	5.2	134.5	944	76.3
5	**7**	500	0.17	3.4	135.2	1341	51.4

[a]Conditions: 10 µmol precatalyst, Pethylene = 5 bar, 25°C, 100 mL toluene, 1 h; [b]kilograms of polymer·precatalyst mol^{-1}·h^{-1}·pressure of ethylene bar^{-1}; [c]Melting temperature determined by DSC.[d]Determined by GPC respect to polystyrene standard.

The PEs by **7** display a T_m of 136.3 °C suggesting the formation of highly linear polymer; the ^1H and ^{13}C NMR spectra confirmed this attribution (see Figure 3.3.1). The molecular weight distributions (M_w/M_n) show broad PDI index, probably due to a partial activation of the active species or to degradation of the catalyst when treated with alkyl aluminium excess.

a

5.82

1.17

6.5 6.0 5.5 5.0 4.5 4.0 3.5 3.0 2.5 2.0 1.5 1.0 0.5 ppm

b

74.20
73.76
73.32

29.38

85 80 75 70 65 60 55 50 45 40 35 30 25 20 15 10 5 ppm
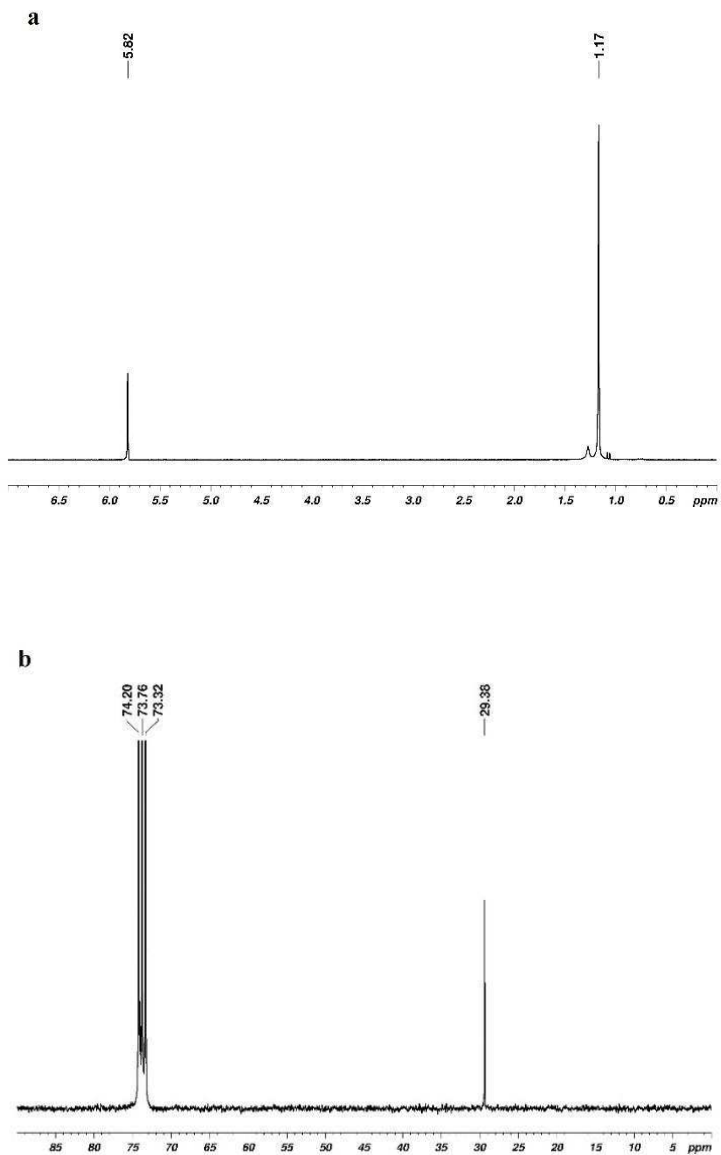
Figure 3.3.1. a) ^{1}H and b) ^{13}C NMR of PE obtained by **7** (entry 2, Table 3.3.1)

Activation of the alkyl group IV metal complexes with a $B(C_6F_5)_3$ or $(Ph_3C)[B(C_6F_5)_4]$ would lead to active (Ti^{IV}) species weakly coordinated by tetraperfluoroarylborate anion.[41]

Table 3.3.2. Ethylene and propylene polymerization with complexes **6-8/** $Al^iBu_3/(Ph_3C)[B(C_6F_5)_4]$

Entry[a]	Precatalyst	monomer	T	Yield	Activity[b]	T_m[c]	M_w[d]	PDI[d]
			°C	g	$kg_P \cdot mol_{cat}^{-1} \cdot bar^{-1} \cdot h^{-1}$	°C	KDa	
1	**6**	ethylene	25	1.48	59	133	1196	71
2	**7**	ethylene	25	5.94	238	122	107	32
3	**8**	ethylene	25	1.56	62	134	1109	77
4[e]	**7**	propylene	25	0.15	3	n.d.	-	-
5[f]	**7**	propylene	-78	-	-	-	-	-

[a]Conditions: 10 µmol precatalyst and $(Ph_3C)[B(C_6F_5)_4]$, 0.2 mmol Al^iBu_3; $P_{monomer}$ = 5 bar, 100 mL toluene, 0.5 h; [b]kilograms of polymer·precatalyst $mol^{-1} \cdot h^{-1}$·pressure of ethylene bar^{-1}; [c]Melting temperature determined by DSC; [d]Determined by GPC respect to polystyrene standards; [e]Reaction time = 1 h, 25 °C; [f]20 mL liquid propylene, 20 mL toluene, 24 h; n.d. = not determined.

The titanium complex **7** is the most active in ethylene polymerization (238 $Kg_{PE} \cdot mol_{cat}^{-1} \cdot bar^{-1} \cdot h^{-1}$) after activation with $(Ph_3C)[B(C_6F_5)_4]$ and $Al(^iBu)_3$. The complexes **6** and **8** show moderate[42] activity with calculated TOF values of 59 and 62 $Kg_{PE} \cdot mol_{cat}^{-1} \cdot bar^{-1} \cdot h^{-1}$ respectively.

The DSC analysis of the polyethylenes (PEs) suggested the formation of highly linear polymers with T_m of about 122 °C for **7** and of about 130°C for **6** and **8**. The NMR analysis confirmed the linear nature of the obtained polymers. The ^1H NMR spectrum of PE by **7** shows a singlet due to the polymethylene sequence at δ 1.16 ppm; a unique signal at δ 28 ppm in the ^{13}C NMR spectrum was parallely observed (Figure 3.3.2). The same occurs for the polymers by the runs 1 and 3 (Table 3.3.2). The molecular weight distributions of PEs are monomodal and PDI values are large, probably as a result of different active species.

a) ——5.80 ——1.15

b) ⌐72.61 ⌐72.17 ⌐71.73 ——27.78
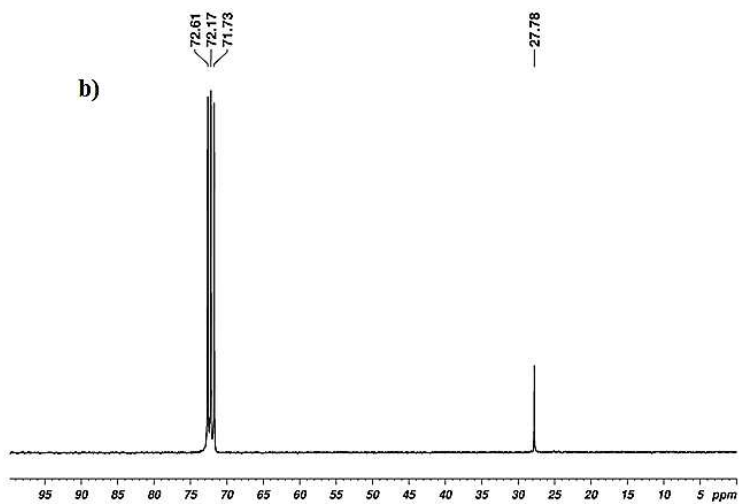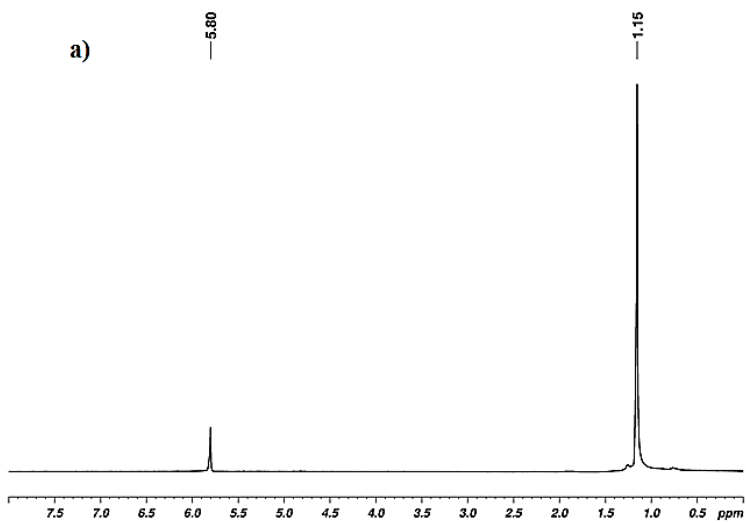
Figure 3.3.2. a) ^{1}H NMR and b) ^{13}C NMR of PE obtained by 7 (TCDE, 250 MHz, 90 °C).

The complex **7** was also active in propylene polymerization (entry 4, Table 3.3.2) with 3 Kg$_{PP}$·mol$_{cat}^{-1}$·bar^{-1}·h^{-1} at 25°C, but become inactive at low temperature. The oligomeric nature of the products is clearly showed in the ^{1}H and ^{13}C NMR spectra (Figure 3.3.4 and 3.3.6). The NMR analysis of oligopropylene sample, in fact, provides useful information about the polymerization mechanism, tacticity and end groups. When polymerization is terminated by β-hydride or β-methyl transfer to the metal center, producing vinylidene, allyl or 2-butenyl terminal groups (Figure 3.3.3).[43]

vinylidene   **allyl**

cis-**2-buthenyl**   **3-butenyl**
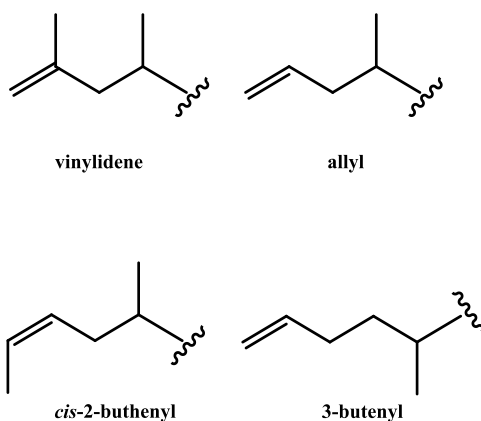
Figure 3.3.3. Possible terminations of the propylene polymerization.

The ^{1}H NMR of polypropylene by entry 4 (Table 3.3.2), in Figure 3.3.4, showed two broad signals at δ 4.57 (s) and 4.65 (s) ppm and singlet at 1.60 ppm typical of a vinylidene end group due to β-hydride transfer from the last 1,2 inserted propylene unit. In addition, the presence of allyl termination produces signals at δ 4.88 (s), 4.93 (d) and 5.71 (m) ppm, whereas the *cis*-2-butenyl end-group yields resonances at δ 5.37 (m) ppm due to the β-methyl transfer and the 3-butenyl signals in the range of δ 5.0- 6.0 ppm. Among these terminations, the vinylidene end group represented about of

44 %, while the allyl and the remaining *cis*-2-butenyl end-group to 39 % and 14 %, respectively. The 3-butenyl end group was around the 3%.
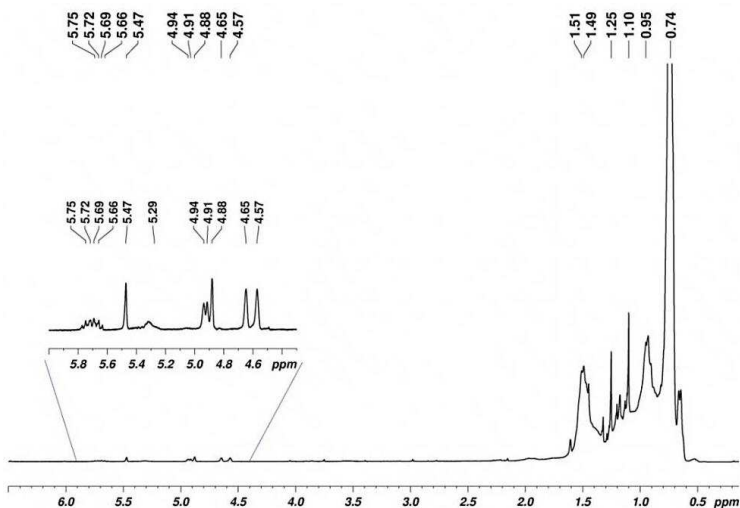
Figure 3.3.4. ^{1}H NMR spectrum (CDCl₃, 25 °C, 300 MHz) of PP oligomers by **7**

In addition, ^{13}C NMR analysis permitted to identify the regioirregular stereosequences and to estimate the percentage of regioinversion, analyzing the spectral range of the aliphatic region (Figure 3.3.6). The regioirregular stereosequences by 2,1-insertion can produce head-tail, head-head, tail-tail or single inverted unit in the head-to tail.[41]

Head-to tail sequence
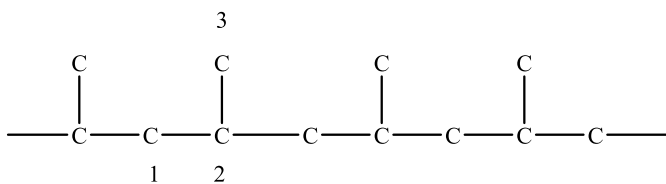
Isolated head-to-head regioerror
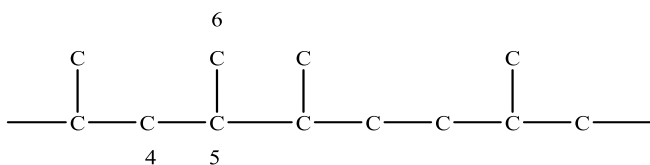
Isolated tail-to-tail regioerror
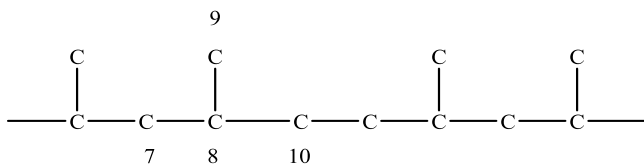
Single inverted unit in the head-to tail sequence
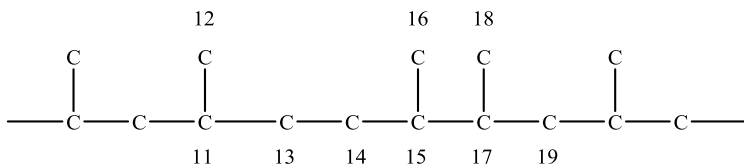
Figure 3.3.5. Regioirregular stereosequences of 2,1-insertion in the propylene polymerization.

The methyl region of ^{13}C NMR spectrum suggested the atactic nature of the PP with 27 % of regioinversions, calculated by the comparison of the integral value of the signals in the spectral range between δ 34.4-35.6 ppm due to the regioirregular 2,1-units versus the integral of the area between δ 45.9-47.5 ppm relative to 1,2-insertion.[44]
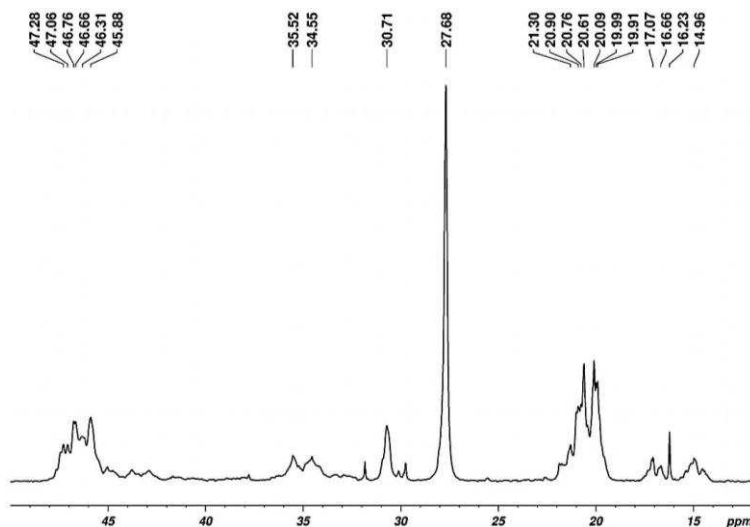
Figure 3.3.6. Aliphatic region of ^{13}C NMR spectrum (CDCl$_3$, 25 °C, 75 MHz) of PP oligomers by **7**

A careful screening of the olefin region in the range between δ 110-150 ppm, confirmed also the effective presence of unsaturated chain end anticipated by ^{1}H NMR.[45]

The Figure 3.3.7 shows the presence of vinylidene, allylic, *cis*-2-butenyl and 3-butenyl terminations. The trityl chloride (Ph$_3$CCl), resulting from (Ph$_3$C)[B(C$_6$F$_5$)$_4$] cocatalyst, was also detected and the relative signals appeared at δ 126.39, 128.02, 130.89 and 142.50 ppm.
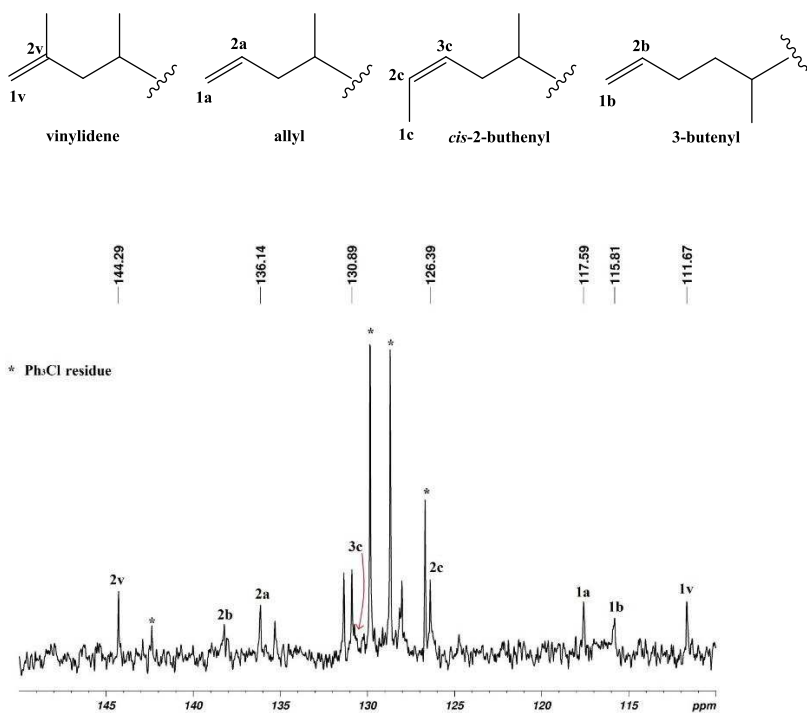
Figure 3.3.7 Olefinic region of ^{13}C NMR spectrum (CDCl$_3$, 25 °C, 75 MHz) of PP oligomers by **7**

3.4 Conclusions

The dichloro titanium complexes of tetradentate [OSSO]-type ligands (**6-8**) were prepard and completely characterized by NMR spectroscopy. The complexes **6** and **7** showed in solution at 25°C an equilibrium between C_2- and C_1-symmetric stereo-isomers; in the case of the complex **6**, the C_2-symmetric structure is favorite, whereas **7** is mainly detected in C_1-symmetry. At room temperature, the ^{1}H NMR spectrum of **8** displayed broad resonance for the methylene protons of the ligand bridge, suggesting a fluxional character of the complex on the NMR timescale.

The complexes **6-8** are poorly active in the polymerization of ethylene using MMAO as cocatalyst, probably for a partial decomposition of the catalyst or inefficient activation of the precatalysts. Activation of **7** with $(Ph_3C)[B(C_6F_5)_4]$ leads to a high catalytic activity of 238 $Kg_{PE}\cdot mol_{cat}^{-1}\cdot bar^{-1}\cdot h^{-1}$; linear polyethylene with a T_m of 122°C and M_w of 107 KDa was obtained under these conditions. The catalysts **6** and **8** displayed a moderate activity of 59 and 62 $Kg_{PE}\cdot mol_{cat}^{-1}\cdot bar^{-1}\cdot h^{-1}$, respectively. The PE are linear with a T_m of 134°C and M_w is about of 1200 KDa. GPC analysis showed a very large distributions of the polymer molecular weights, indicating a low control of the polymerization process, probably due to the presence of different active species in solution.

The precatalyst **7** was also active under propylene flow at room temperature, producing atactic oligomers terminated with unsatured end-groups.

3.5 References

[33] Matsugi, T.; Fujita, T. *Chem. Rev.* **2008**, *37*,1264.

[34] Makio, H., Kashiwa, N.; Fujita, T. *Adv. Synth. Catal.* **2002**, *344*, 477-493

[35] a) Saito, J.; Mitani, M.; Mohri, J.-i.; Yoshida, Y.; Matsui, S.; Ishii, S.-I.; Kojoh, S.- I.; Kashiwa, N.; Fujita, T. *Angew. Chem. Int. Ed.*, **2001**, *40*, 2918. b) Makio, H.; Terao, H.; Iwashita, A.; Fujita, T. *Chem. Rev.*, **2011**, *111*, 2363.

[36] Tshuva, E. T.; Goldberg, I.; Kol, M. *J. Am. Chem. Soc.* **2000**, *122*, 10706–10707.

[37] a) Capacchione, C.; Proto, A.; Ebeling, H.; Mülhaupt, R.; Spaniol, T. P.; Möller, V.; Okuda, J. *J. Am. Chem. Soc.* **2003**, *125*, 4964–4965. b) Capacchione, C.; De Carlo, F.; Zannoni, C.; Okuda, J.; Proto, A. *Macromolecules* **2004**, *37*, 8918–8922. c) Proto, A.; Avagliano, A.; Saviello, D.; Capacchione, C. *Macromolecules* **2009**, *42*, 6981–6985.

[38] Ishii, A.; Toda, T.; Nakata, N.; Matsuo, T. *J. Am. Chem. Soc.* **2009**, *131*, 13566-13567.

[39] Ma, H.; Spaniol T. P.; Okuda, J. *Inorg. Chem.*, **2008**, *47*, 3328–3339.

[40] Cohen, A.; Goldberg, I.; Venditto, V.; Kol M. *Eur. J. Inorg. Chem.*, **2011**, *46*, 5219-5223.

[41] Milione, S.; Bertolasi, V.; Cuenca, T.; Grassi, A. *Organometallics* **2005**, *24*, 4915-4925

[42] Britovsek, G. J. P.; Gibson, V. C.; Wass, D. F. *Angew. Chem. Int. Ed.* **1999**, *38*, 428 – 447.

[43] Carvill, A.; Zetta, L.; Zannoni, G.; Sacchi, M. C. *Macromolecules*, **1998**, *31*, 3783-3789.

[44] Asakura, T.; Nishiyama, Y.; Doi, Y. *Macromolecules* **1987**, *20*, 616–620.

[45] Resconi, L.; Cavallo, L.; Fait, A.; Piemontesi, F. *Chem. Rev.* **2000**, *100*, 1253-1345.

Chapter 4

4.1 Calixarenes as alternative ligands for Group IV metal complexes

The term calixarene indicates macrocycle containing phenol groups linked by a methylene bridge at the 2,6-positions.[46] In 1978 cyclic oligomers derivated by condensation reaction between formaldehyde and *p*-substitued phenols were obtained for the first time.[47] The total number of "repetitive units" is shown as number in brackets between "calix" and "arene"; e.g. *p-tert*-butylcalix[8]arene. Calixarenes show basket shape in which many type of molecules can be encapsulated through van der Waals or hydrogen bond interactions generating structures with four different conformations: cone, partial cone, 1.3 alternate and 1.2 alternate (Figure 4.1.1); the most stable conformation is the cone.
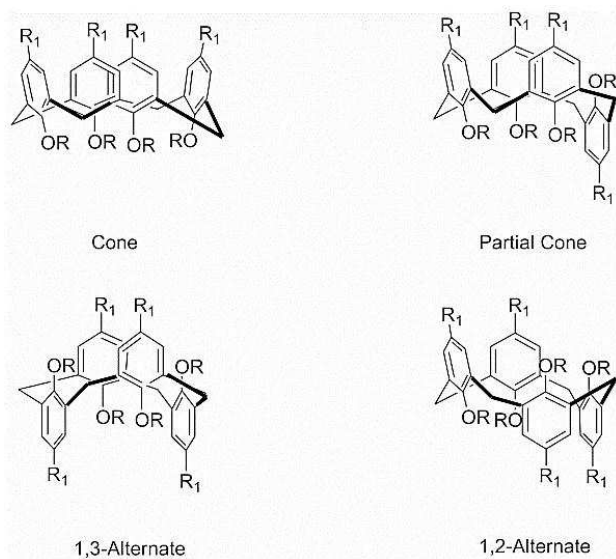
Figure 4.1.1. Four conformations of calix[4]arene

Calixarenes are able to coordinate transition metals, producing metal complexes with interesting chemical and electronical properties. The first transition-metal complexes of calixarenes were reported by Olmstead et al., in 1985, from the reaction of *p-tert*-butylcalix[4]arene (TBC[4]) with Ti(IV), Co(II) and Fe(III) amides.[48] To date, the Cambridge Structural Database (CSD) contains over 200 calix[4]arene complexes with transition metals. Calixarenes have also been explored as suitable macrocycle ligand to achieve efficiente metal catalysts;[49] a rapresentative example is given by the *cone*-25,27-dipropyloxy-26,28-dioxo-calix[4]arene titanium (IV) dichloride (Figure 4.1.2) which is active in the ROP of *rac*-lactide under bulk conditions (88 % conv. of 1000 equiv. in 3 h at 130°C). This complex showed a "cone" conformation, in which two phenolate and two ether groups are in an octahedral environment.[50]
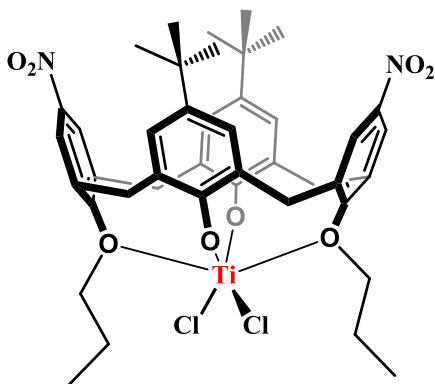
4.1.2. Representative drawing of calix[4]arene titanium(IV) dichloride

4.2 Cyclic aliphatic polyesters derived from renewable sources

Cyclic polymers are emerging as interesting materials with unique physical properties. The absence of chain end and the cyclic topology impart properties that are different from those of the corresponding linear polymers, as e.g. increased glass transition temperatures, smaller hydrodynamic volumes and lower intrinsic viscosities.[51] Cyclic aliphatic polyesters are biodegradable and biocompatible; advantages for a range of biomedical applications could come from cyclic polylactides or polycaprolactones. However, the synthesis and purification of these compounds are challenging. The ring closure is conventionally carried out through the coupling of end-groups in a linear chain using diluted solutions in the presence of a metal complex (Figure 4.2.1).[52]
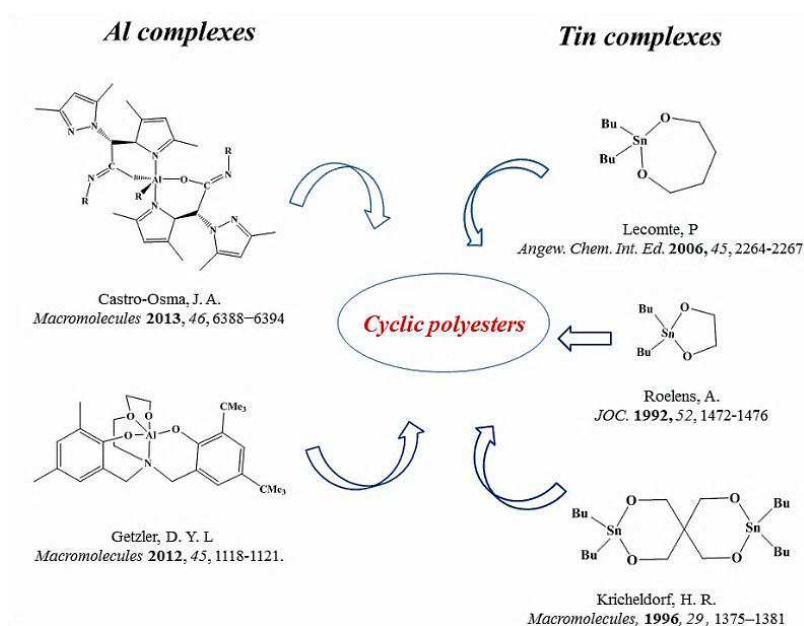
Figure 4.2.1. Catalysts employed for the cyclopolymerization of various lactones

Alternatively, the ring-expansion technique can be used; this approach implies the insertion of cyclic monomers into an activated cyclic polymer chain. A remarkable example of ring-expansion technique is the zwitterionic polymerization of lactide in presence of N-heterocyclic carbenes (NHCs) as organocatalysts to produce cyclic PLA.[53]
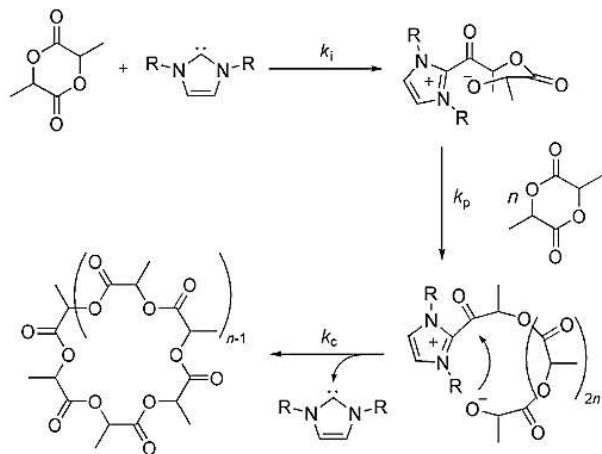
Figure 4.2.2. Zwitterionic polymerization of lactide promoted by NHC.

Cyclic polyesters have also been synthesized taking advantage of the intramolecular transesterification reactions during the polymerization of cyclic esters using cyclic polylactides anchored to a polymeric support.[54] In this system, the catalyst is bound to a polystyrene resin having benzylamine groups. The living polymerization of lactide leads to a growing polymer bound to the heterogeneous support and the intrachain transesterification yields cyclic oligomers in solution, see Figure 4.2.3.
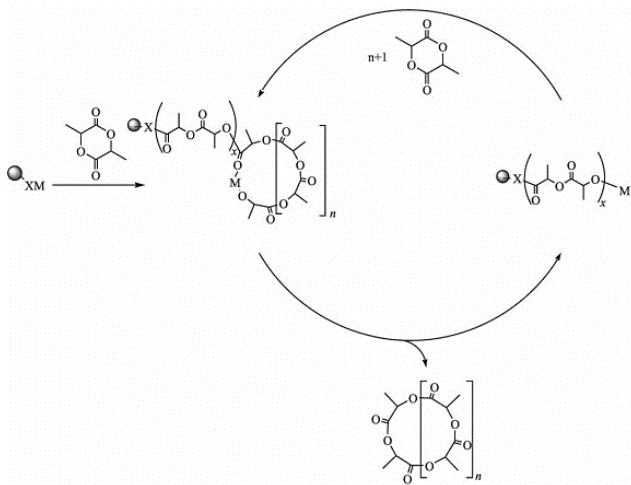
Figure 4.2.3. Synthesis of cyclic polylactides from solid supported catalyst

4.3 ROP of rac-lactide promoted by dinuclear zirconium complex bearing a 1,5-bridged calix[8]arene ligand (9)

In recent times bimetallic complexes are emerging as a new class of catalysts with promising performances in the ROP of cyclic esters. These complexes display different catalytic performances in comparision to the analogous monometallic species because of two reactive metals in close proximity which can influence each other.

Tolman et al.[55] reported the synthesis of a new dizinc–monoalkoxide complex bearing bis(phenoxy diamine) ligand as an efficient catalyst for the controlled polymerization of LA. Williams et al.[56] studied a new family of mono and bimetallic zinc complexes with bis(imino)diphenylamido ligands, observing that the bimetallic catalysts are much more active than the monometallic clearly proving that a cooperative interaction between the two zinc ions is determinant for a controlled polymerization mechanism (Figure 4.3.1).
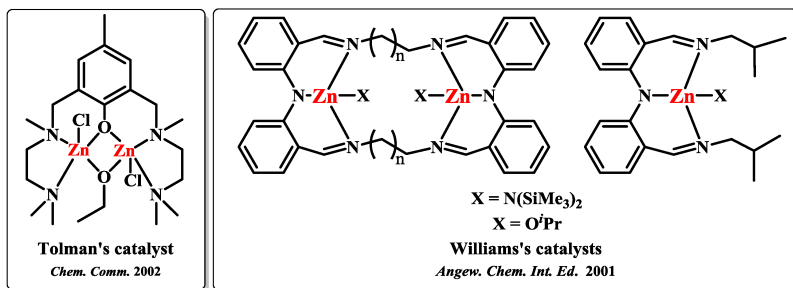
Figure 4.3.1. Mono- and dinuclear zinc catalysts active in the ROP of lactones

Although group IV metal complexes are of particular interest in the ROP of cyclic esters, few bimetallic Group IV complexes have been reported for the polymerization of LA until now. Kol et al.[25] reported that dinuclear

titanium and zirconium complexes of phenylenediamine bis(phenolate) resulted extremely active in the *rac*-lactide polymerization, leading to heterotactically-enriched PLAs. Bochmann[57] and Lin[58] observed that heterobimetallic Ti complexes bearing ONNO and ONSO-type bisphenolate ligands displayed a better performances compared to the mononuclear Ti complex. The same catalytic behavior was described by Tseng[59] with bimetallic titanium complexes coordinated by hydrazine-bridging schiff base ligands.

Aiming to design novel bimetallic Group IV metal catalysts, we turned our attention to large calix[n]arene (with n $\geq$ 6), which are able to coordiante more than one metal atom in close proximity. In 2016, a tetranuclear titanium complex bearing *p-tert*-butylcalix[8]arene ligand was prepared by McIntosh and studied in the polymerization of *rac*-lactide.The complex is composed by two *anti*-oriented *p-tert*-butylcalix[4]arene-like substructures; each unit, assumimg a *cone* conformation; coordinates two metal centers bounded by two bridging propoxides (Figure 4.3.2).[60] Another example is represented by an anionic Ti-*p-tert*-butylcalix[8]arene complex; in this last case, the ligand shows a 'tennis-ball' conformation (Figure 4.3.3).
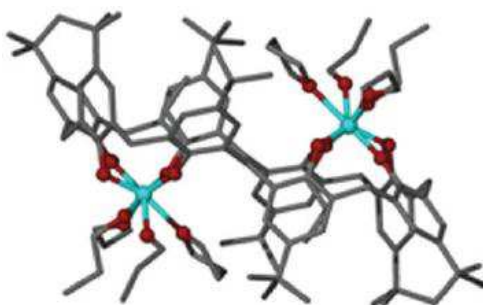
Figure 4.3.2. Ti$_4$TBC[8](O^{n}Pr)$_8$(THF)$_2$ complex in double-cone conformation
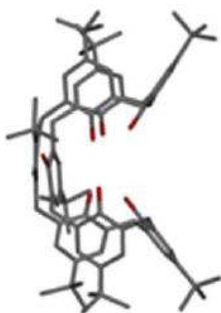
Figure 4.3.3. "Tennis-ball" conformation of *p-tert*-butylcalix[8]arene

To reduce the number of possible conformations that the macrocycle can assume and to induce coordination of metal atoms in strategic positions for catalysis, we have chosen a calix[8]arene bridged between phenolic rings at 1,5-positions with *m*-xylene-diyl group, as ligand for the synthesis of the dinuclear zirconium *p-tert*-butylcalix[8]arene complex (**9**), in Figure 4.3.4. This project was carried out in collaboration with the group of Prof. Neri of our Departament.
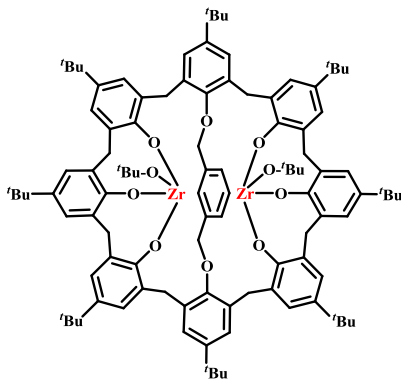
9

Figure 4.3.4. Schematic representation of complex **9**

The complex **9** displayed a folded calix[8]arene conformation in which each calix[4]arene substructure binds one zirconium atom (see Figure 4.3.5).
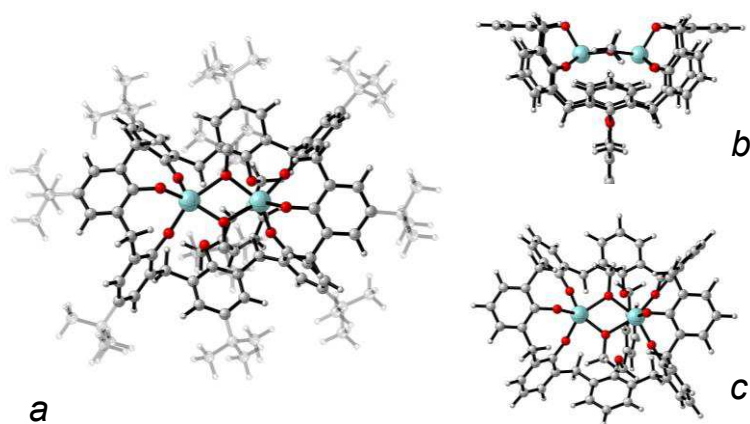
Figure 4.3.5. Minimum-energy structure for C (a). Top (b) and front views (c) of the minimum-energy structure for the simplified model complex of **9**.

The complex **9** was tested in the ROP of *rac*-LA in toluene solution using a monomer/initiator molar ratio of 100 (entries 1-4, Table 4.3.1). At 100 °C, the complete monomer conversion was observed in only 30 minutes with turnover frequency of 194 h^{-1} (see entry 4, Table 4.3.1). This activity is comparable to those of the most performing Group IV catalysts active in the ROP of lactide.[20] In Figure 4.3.6, ^1H NMR spectrum of PLAs obtained by complex **9** at 100°C shows typical resonances relative to methine group at 5.20 ppm and methyl protons at 1.58 ppm. The methine resonance in the homonuclear decoupled ^1H NMR spectrum revealed an atactic microstructure (P_r = 0.49-0.57).

Table 4.3.1. ROP of rac-LA, ε-CL and β-BL.

Entry[a]	Monomer	Monomer/C (molar ratio)	T (°C)	t (min)	Conversion[b] (%)	TON[c]	TOF[d] (h^{-1})	$M_{n(exp)}$[e] (DA)	$M_{n(th)}$[f] (DA)	PDI[e]
1 [g]	rac-LA	100	25	1440	50	50	2	629	3603	1.10
2	rac-LA	100	50	660	90	90	8	686	6486	1.14
3	rac-LA	100	80	108	93	93	52	629	6702	1.28
4	rac-LA	100	100	30	97	97	194	705	6990	1.23
5	rac-LA	250	100	40	93	233	349	3209	16755	1.28
6	rac-LA	500	100	60	96	480	480	8579	34591	1.27
7	rac-LA	750	100	80	98	735	551	15760	52968	1.30
8	rac-LA	1000	100	100	98	980	588	26619	70624	1.47
9	ε-CL	100	100	3	97	97	3233	621	5536	1.23
10	β-BL	100	100	840	90	90	6.4	599	3874	1.25

[a]Reaction conditions: Complex **9** (4.6 µmol, 7.8 mg) and toluene (2.4 mL). [b]Determined by ^{1}H NMR spectroscopy (CDCl$_3$ as solvent, 25 °C). [c]Turnover number (*mol* of polymerized *rac*-Lactide per *mol* of catalyst). [d]Turnover frequency (TON per reaction time). [e]Experimental molecular weight ($M_{n(exp)}$) and polydispersity index (PDI, M_w/M_n) determined by GPC in THF using polystyrene standards and corrected using a factor of 0.58. [f]Calculated molecular weight using: $M_{n(th)}$ (kg mol^{-1}) = 144.13×[([*rac*-LA]$_0$/[C])/2]×(*rac*-LA conversion). [g]Dichloromethane as solvent.
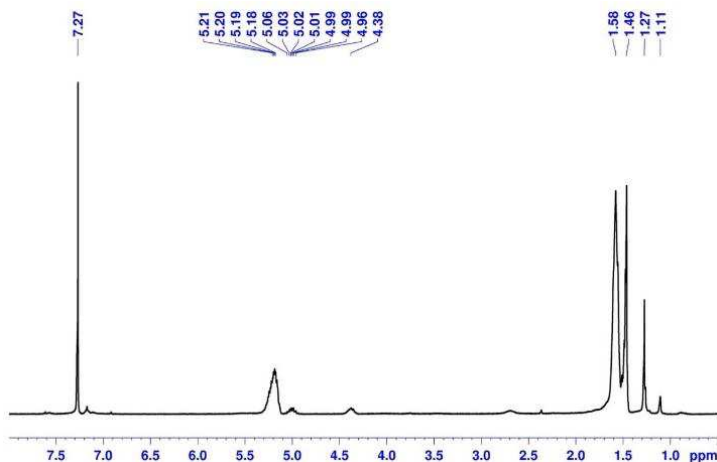
Figure 4.3.6. ^{1}H NMR spectrum of PLA, entry 4 of Table 4.3.1 (CDCl$_3$, 300 MHz, 25°C)

The molecular weight distributions of the PLAs are narrow (PDI = 1.10-1.30) and monomodal, but the experimental molecular weights (M$_{n(exp)}$) are lower than the calculated values (M$_{n(th)}$).

To further explore the catalytic ability of **9**, the influence of the monomer to initiator molar ratio was investigated in the range from 100 to 1000 (entries 4-8, Table 4.3.1). In presence of 1000 eq. of *rac*-lactide and polymerization time of 100 min (entry 8, Table 4.3.1), the M$_{n(exp)}$ increase linearly with the monomer to initiator ratio, and the M$_{n(exp)}$ and M$_{n(th)}$ increase linearly; the slope suggests that the transesterification reactions are progressively more important with respect to the propagation steps as the monomer to intiator molar ratio increases (Figure 4.3.7).
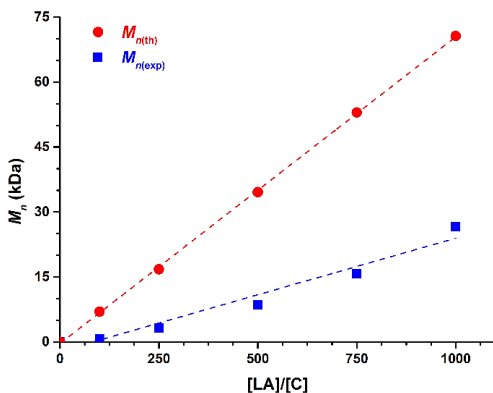
Figure 4.3.7. Linear dipendence of Mn (KDa) vs monomer concentration.

The MALDI TOF mass spectra of polyesters allows to investigate the polymerization mechanism by inspection of the nature of the end groups. The MALDI TOF spectrum of obtained PLA (Figure 4.3.8 a, entry 4, Table 4.3.1) revealed the presence of cyclic oligomers as K^+ and Na^+ adducts with formula $[OCH(CH_3)C=O]_nK^+$ and $[OCH(CH_3)C=O]_nNa^+$, formed by intramolecular transesterification process. Linear chains of PLA terminated with *tert*-butoxide group were also observed, but they are less abundant; the cyclic/linear molar ratio is of 70/30. All the peaks in the mass spectrum were half-integer multiples of the lactide unit (72 m/z) suggesting inter-chain transesterification. Moreover, cyclic polylactides showed an average number of monomer units of 7 and linear PLAs of 7.5 units (see Figure 4.3.8 (a) on the right).
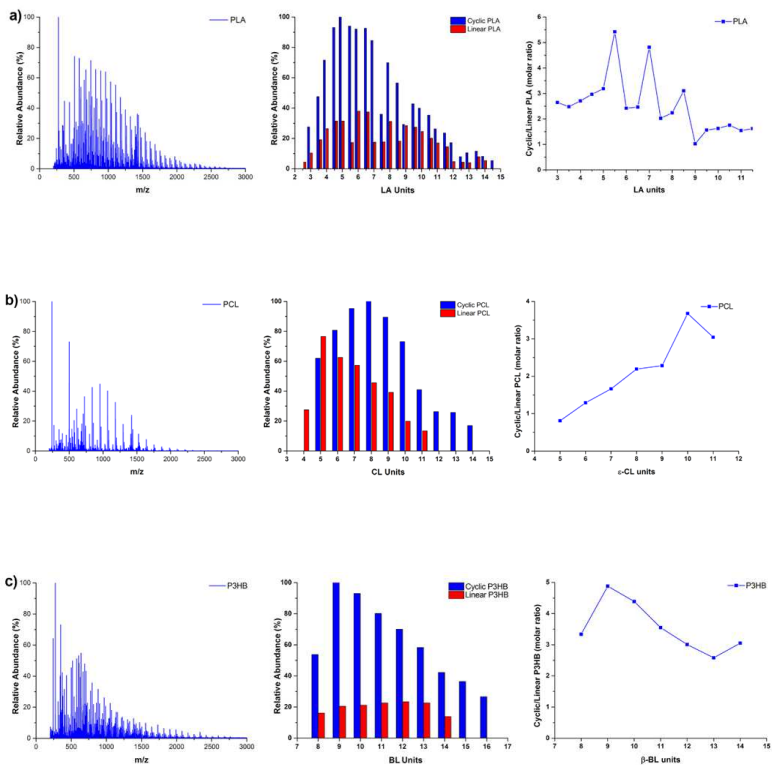
Figure 4.3.8. MALDI-TOF-MS spectra of PLA (a), PCL (b) and PHB (c) on the left and their molecular weight distribution profiles depending for linear and cyclic polyester chains, in the middle. The last graphs, on the right, described the cyclic/linear ratio as function of inserted monomer units.

4.4 Kinetic studies

To achieve insight into the polymerization mechanism, kinetic studies were performed. Taking costant the concentration of the monomer at 80°C and varing the concentration of the initiator, the reaction profiles were obtained analysing aliquots of the reaction mixture at different reaction time by ^{1}H NMR spectroscopy (CDCl$_3$, 250 MHz). The monomer conversion showed exponential decays and the semilogarithmic plots of $\ln([LA]_t/[LA]_0)$ versus polymerization time are linear, indicating a first order kinetics in lactide concentration (Figure 4.4.1). At monomer to initiator ratio of 100, the apparent polymerization rate constant (k_{app}) was 0.121±0.003 min^{-1}.

To calculate the reaction order with respect to the complex **9**, the k_{app} values were plotted against the concentrations of the catalyst ([**9**]); a linear increase of k_{app} versus [**9**] was observed. Furthermore the log-log plot of k_{app} ($\ln (k_{app})$) or of the reaction rate ($\ln (r)$) versus the molar concentration of complex **9** ($\ln$[**9**]) are linear and the gradient, in both case, is close to one, confirming that the polymerization is first-order in the initiator (Figure 4.4.1). In conclusion, L-LA polymerization catalyzed by **9** proceeds according the following kinetic law:

$$-d[LA]/dt = k_{app} \, [LA] = k_p[\mathbf{9}] \, [LA]$$

with a kinetic constant k_p of 0.26±0.05 M^{-1}s^{-1}. The proposed reation path is reported in Scheme 4.4.1. The transterification reactions are secondary reaction that are competitive with the propagation step. In our specific case, probably, the presence of two zirconium centres in the complex **9** promoted the folding of the growing chain in order to allocate one of the carboxyl group near to the metal centre; thus the intrachain transterification is favoured and cyclic oligomers are preferentially formed respect to the linear ones.
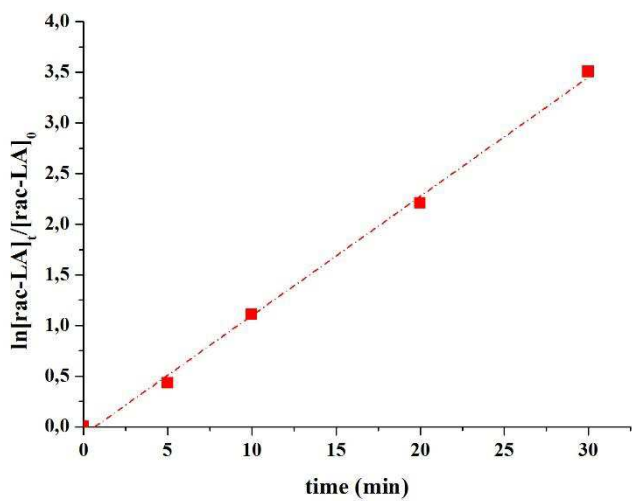
Figure 4.4.1. Kinetic study of rac-LA polymerization promoted by complex **9** at 100 °C (k_{app} = 0.121±0.003 min^{-1}).
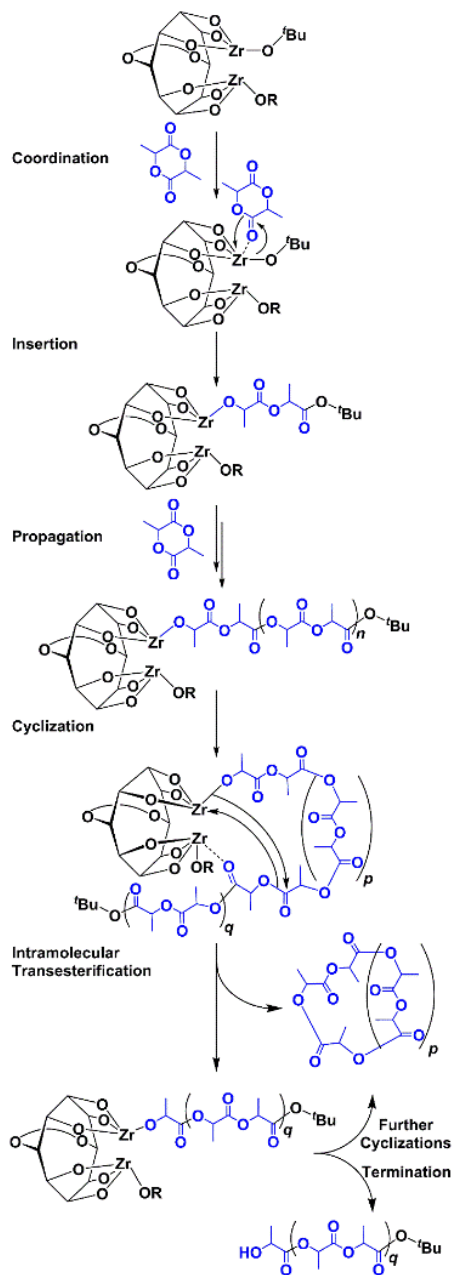
Scheme 4.4.1. Ring opening polymerization mechanism promoted by **9**

Table 4.3.3. Reaction rate as a function of catalyst concentration for ROP of LA with 9.

Entry	[C] (M)	[rac-LA]/[C] (molar ratio)	r (M s⁻¹)
S1	$1.42 \cdot 10^{-2}$	50	$2.7 \cdot 10^{-3} \pm 1.5 \cdot 10^{-4}$
S2	$7.07 \cdot 10^{-3}$	100	$1.7 \cdot 10^{-3} \pm 1.3 \cdot 10^{-4}$
S3	$4.72 \cdot 10^{-3}$	150	$1.2 \cdot 10^{-3} \pm 6.3 \cdot 10^{-}$
S4	$3.53 \cdot 10^{-3}$	200	$7.3 \cdot 10^{-4} \pm 3.7 \cdot 10^{-5}$

Reaction conditions: [rac-LA] = 0.706 M, TCE-d_2 = 0.6 mL, T = 80 °C.
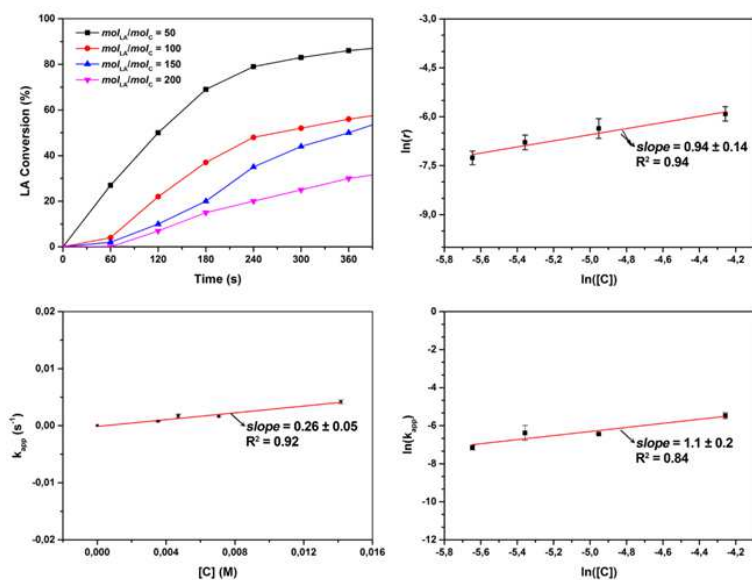
Figure 4.4.2. Kinetic plots for determination of reaction order with respect to the catalyst for ROP of rac-LA.

4.5 Polymerization of ε-caprolactone (ε-CL) and β-butyrolactone (β-BL)

The polymerization study was extended to ε-CL and β-BL monomers, possessing a seven-and four-member ring. The results are summerized in the Table 4.3.1, entries 9 and 10. The catalyst **9** quantitatively converted ε-CL in 3 minutes, while high monomer conversions of β-BL were observed in 14 h. For both polymers, the distribution of molecular weights was monomodal with narrow PDI (~1.20). The experimental molecular weigths were lower than the theorical ones. The PCL and P3HB polymers were analyzed by MALDI-TOF-MS. The formation of cyclic polyesters was observed also in these cases (Figure 4.3.5 b and c). The averange number of ε-CL units was 8 for the cyclic polymers and 7 for linear ones; The cyclic/linear molar ratio resulted of 69:31 for the ε-CL polymerization. The averange number of BL units was 11 for both cyclic and linear polymers; the molar ratio between cyclic and linear chains was 80/20 (Table 4.5.1).

Table 4.5.1. Cyclic/linear molar ratio determined by MALDI-MS analysis

Polymer	Cyclic/Linear [molar ratio]	Average number of monomers	
		Cyclic	Linear
PLA	70/30	7	7.5
PCL	69/31	8	7
P3HB	80/20	11	11

4.6 Conclusions

In this study we report the synthesis of a dinuclear zirconium complex bearing a 1,5-bridged-calix[8]arene ligand (**9**), obtained by protonolysis reaction of Zr(O^{t}Bu)$_4$ (two equivalents) with 1,5-m-xylene-diyl-bridged calix[8]arene (one equivalent) in THF at room temperature. The complex **9** showed catalytic activities comparable to those of the most performing catalysts reported in literature in the ROP of rac-LA, ε-CL and β-BL, giving macrolactones with high selectivity through a coordination-insertion mechanism. The cooperative effect of the zirconium metal centers promoted an improvement of the catalytic activities and, at the same time, the intramolecular transesterification reaction with respect to the chain propagation reaction leading to the selective production of macrocyclics.

4.7 References

[46] David, G. C. Calixarenes (Royal Soc Chem, Cambridge) *1989*, 1-2.

[47] Gutsche, C. D.; Muthukrishnan, R. *J. Org. Chem.*, **1978**, *43*, 25, 4905-4906.

[48] Olmstead, M. M.; Sigel, G.; Hope, H.; Xu, X.; Power, P. P. *J. Am. Chem. Soc.*, **1985**, *107*, 8087-8091.

[49] a) Redshaw, C. *Dalton Trans.* **2016**, *45*, 9018-9030; b) Floresta, G.; Talotta, C.; Gaeta, C.; De Rosa, M.; Chiacchio, U.; Neri, P.; Rescifina, A. *J. Org. Chem.* **2017**, *82*, 4631-4639; c) De Rosa, M.; La Manna, P.; Soriente, A.; Gaeta, C.; Talotta, C.; Hickey, N.; Geremia, S.; Neri, P. *Chem. Eur. J.* **2017**, *23*, 7142-7151; d) Talotta, C.; Gaeta, C.; De Rosa, M.; Ascenso, J. R.; Marcos, P. M.; Neri, P. *Eur. J. Org. Chem.* **2016**, *2016*, 158-167; e) De Rosa, M.; La Manna, P.; Soriente, A.; Gaeta, C.; Talotta, C.; Neri, P. *RSC Adv.* **2016**, *6*, 91846-91851; f) Capacchione, C.; Neri, P.; Proto, A. *Inorg. Chem. Commun.* **2003**, *6*, 339-342.

[50] Frediani, M.; Sémeril, D.; Mariotti, A.; Rosi, L.; Frediani, P.; Rosi, L.; Matt, D.; Toupet, L. *Macromol. Rapid Commun.* **2008**, *29*, 1554–1560.

[51] Semlyen, J. A. *Cyclic Polymers,* Kluwer Academic, Dordrecht, The Netherlands, 2nd edn, **2000**.

[52] Hoskins, J. N.; Grayson, S. M. *Polym. Chem.*, **2011**, *2*, 289–299.

[53] Culkin, D. A.; Jeong, W.; Csihony, S.; Gomez, E. D.; Balsara, N. P.; Hedrick, J. L.; Waymouth, R. M. *Angew. Chem., Int. Ed.*, **2007**, 46, 2627–2630.

[54] Chisholm, M. H.; Gallucci, J. C.; Yin, H. *Proc. Natl. Acad. Sci.* **2006**, *103*, 15315-15320.

[55] Williams, C. K.; Brooks, N. R.; Hillmyer, M. A.; Tolman, W. B. *Chem. Commun.*, **2002**,*0*, 2132-2133.

[56] Thevenon, A.; Romain, C.; Bennington, M. S.; White, A. J. P.; Davidson, H. J.; Brooker, S.; Williams, C. K. *Angew. Chem. Int. Ed.* **2016**, *55*, 8680-8685.

[57] Sarazin, Y.; Howard, R. H.; Hughes, D. L.; Humphrey, S. M.; Bochmann, M. *Dalton Trans.* **2006**, 340−350.

[58] Chen, H.-Y.; Liu, M.-Y.; Sutar, A. K.; Lin, C.-C. *Inorg. Chem.* **2010**, *49*, 665−674.

[59] Tseng, H.-C.; Chen, H.-Y.; Huang, Y.-T.; Lu, W.-Y.; Chang, Y.-L.; Michael Y. Chiang, M. Y.; Lai, Y.-C.; Chen, H.-Y. *Inorg. Chem.*, **2016**, *55*, 1642–1650.

[60] Ryan, J. D.; Gagnon, K. J.; Teat, S. J.; McIntosh, R. D. *Chem Comm* **2016**, *52*, 9071-9073.

Chapter 5

5.1 Polyesters by copolymerization of epoxides with anhydrides

In the recent years, an alternative approach to the synthesis of biodegradable and biocompatible aliphatic polyesters is the ring-opening copolymerization (ROCOP) of cyclic anhydrides and epoxides, derivated by sustainable sources. The most common polymers are poly(propylene succinate) [P(PO-SA)], poly(cyclohexene succinate) [(PCSu) or P(PO-CHO)], poly(propylene maleate) [P(PO-MA)]. (Figure 5.1.1); these materials are interesting for the potential applications in medical field as drug delivery agents, fibers and medical sutures/stents.[61]
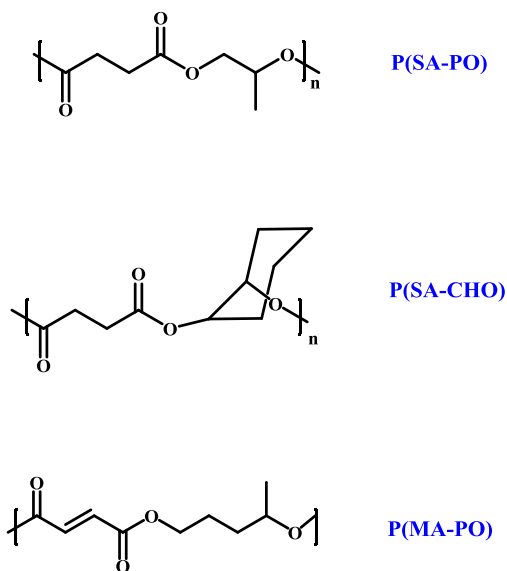
Figure 5.1.1. Rapresentation of biodegradable polyesters obtained by ROCOP of epoxides/anhydrides.

ROCOP allows to modulate the polymer structure using different combination of monomers. Until now, in literature, have been reported approximately 20 anhydrides and 20 epoxides, useful to generate about 400 new polymer structures.[62] Despite the variety of epoxides, cyclohexene oxide (CHO) and propylene oxide (PO) are widely studied for their ability to provide many possible combinations with anhydrides, leading to new polymer structures potentially interesting in medical devices (Figure 5.1.2 and 5.1.3). Generally, anhydrides and epoxides are classified by their number of ring (mono-, bi-, tricyclic) and side chains. Among these the most employed epoxides are monosubstitued monocyclic epoxides (e.g., epichlorohydrine or 1-butene oxide).
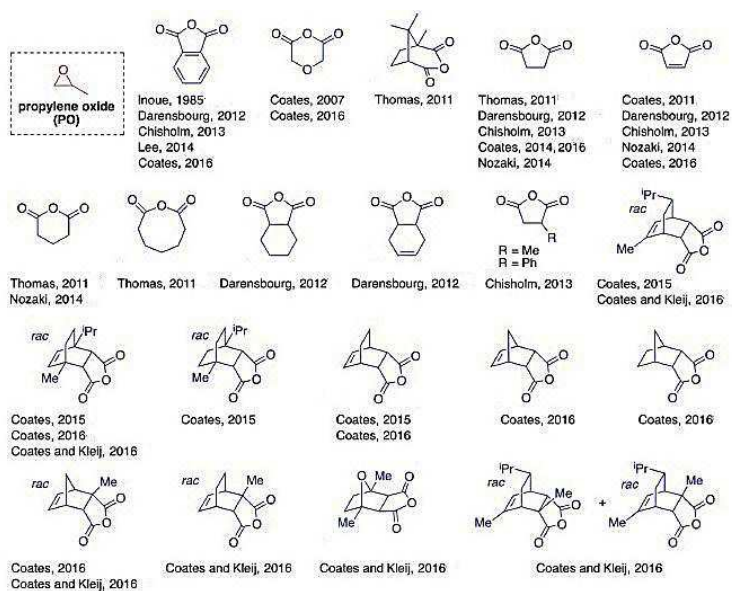
Figure 5.1.2. Anhydride copolymerized with propylene oxide[62]

Figure 5.1.3. Anhydride copolymerized with cyclohexene oxide[62]

Ring opening copolymerization allows also to prepare polymeric materials with a modulable glass transition temperature, depending on the epoxide/anhydride combination used. The Tg values increase in the order propylene < styrene < cyclohexene oxide for a definite anhydride and in the order succinic < maleic < cyclohexane < phtalic < cyclohexene anhydride, considering a specific epoxide and are found in the range from 39°C to 95°C.[63]

Wang et al. observed that aromatic polyesters, such as poly(propylene phtalate), showed a tensile strength of 23.5 MPa respect to aliphatic polyester, as poly(propylene succinate), with a tensile strength of 19.1 MPa.[64]

5.2 Ring-opening copolymerization (ROCOP) of epoxide and anhydride

The ring opening copolymerization (ROCOP) of epoxides and anhydrides is a polymerization process similar to the classical ROP of cyclic esters, which leads to polyesters with a range of chemical and physical properties easily modified through a variaty of co-monomers (Figure 5.2.1).[65]
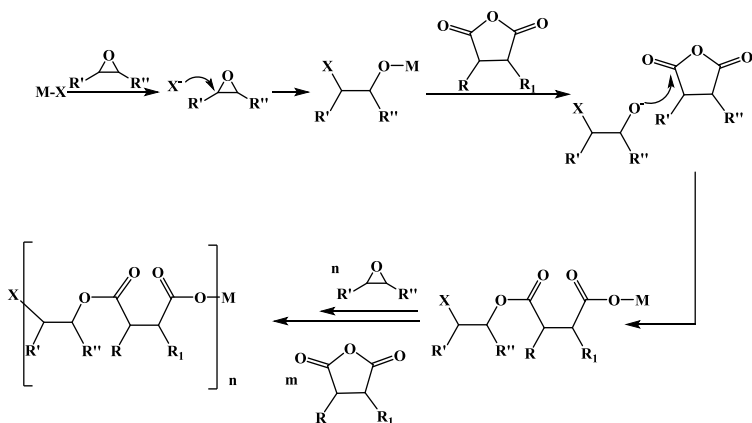
Figure 5.2.1. Elementary steps of ROCOP between epoxides and anhydrides.

The first alternating copolymerization between epoxide and anhydride was reported in 1960 by Fischer[66] using tertiary amines or tetrabutyl tin as cocatalyst. This process resulted poorly controlled and low molar mass products were obtained. In the next twenty years, various new catalyst systems (such as $ZnEt_2$, $LZnEt_2$ and R_3Al) have been studied and many of which displayed good catalytic performances in presence of a nucleophilic cocatalysts. Among the common co-catalysts, there are Lewis bases, as 4-dimethylaminopyridine (DMAP) or methyl imidazole), quaternary ammonium salts (tetrabutylammonium chloride (TBACl)) and phosphine (as bis(triphenylphosphine)-iminium salts).

The well-controlled polymerization of epoxide with anhydride was first reported in 1985 by Aida[67] and Inoue[68] using porphyrin aluminum complexes in combination with tetralkyl ammonium halide cocatalyst that yields alternating copolymer of propylene oxide and styrene oxide with phthalic anhydride (TOF = 5 h^{-1}). Analogous chromium complex produced perfectly alternatate copolymers with molar mass of 1-20 k$_g$mol^{-1} (see Figure 5.2.2). Changing the chromium metal center for cobalt or manganese, the activity decreased.[69]
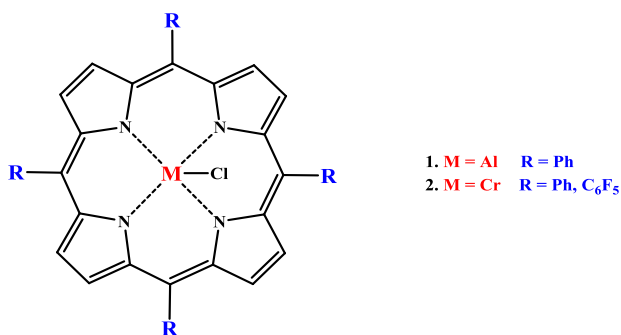
Figure 5.2.2. Porphyrin catalysts for the copolymerization epoxides and anhydrides

In 2007, Coates and al.[70] tested a series of substituted 2-cyano-β-dikitiminato zinc complexes in the ROCOP of epoxide/anhydride and epoxide/CO_2, obtaining perfectly alternating polyesters with molecular weight of 55 K$_g$·mol^{-1}.
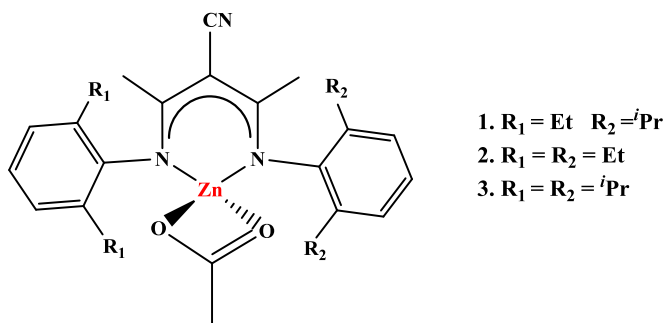
Figure 5.2.3. β-dikitiminato zinc acetate complexes

1. R_1 = Et R_2 = ^{i}Pr
2. R_1 = R_2 = Et
3. R_1 = R_2 = ^{i}Pr

Salan-type and salen-type (see Chart 2) metal complexes are efficient initiators in epoxides-anhydrides copolymerization. In 2011, Coates et al.[71] studied the polymerization of the maleic anhydride (MA) with many epoxides using salen Cr complexes; Duchateau reported a series of Al, Co and Cr salen complexes active in this catalysis. The best performances were achieved by chromium complexes in presence of bis(triphenylphosphine)iminium chloride (PPNCl) cocatalyst.[72]

M = Al, Co, Cr

R_1, R_2 = H, Ph, cyclohesyl
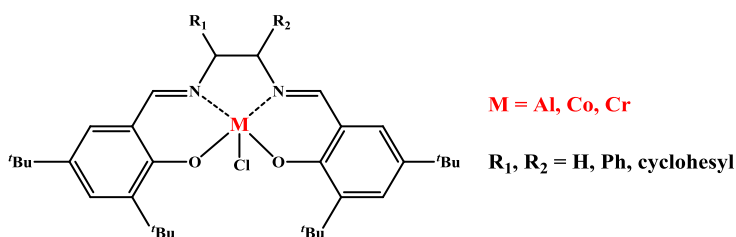
Figure 5.2.4. Salen catalysts active in ROCOP

Recently, much attention is focused on the bimetallic complexes, which show higher performances with respect to the monometallic analogues. Indeed, dinuclear Cr(III) salan complexes are efficient initiators for the copolymerization of maleic anhydride and epichlorohydrin (TOF = 7.8 h^{-1}),

producing alternating polyester with M_n of 32 $K_g \cdot mol^{-1}$ (Figure 5.2.5). The monometallic analogue displayed, in the same conditions, a TOF value of 0.9 h^{-1} and the obtained polymer showed an average molecular weight of 5 $K_g mol^{-1}$.[73] Trinuclear zinc salen and salan complexes are extremely active in the copolymerization reactions.[74]
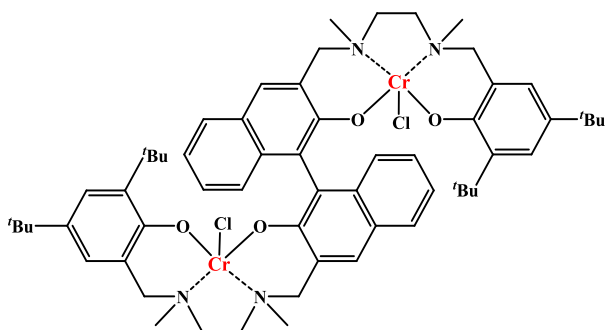
Figure 5.2.5. Salan catalyst

Nozaki et al. prepared a bi- and mono-nuclear manganese or iron-corrole complexes, that combined with PPNCl, are highly versatile catalysts for the polymerization of epoxides, yielding a wide range of polyesters (Figure 5.2.6).[75]
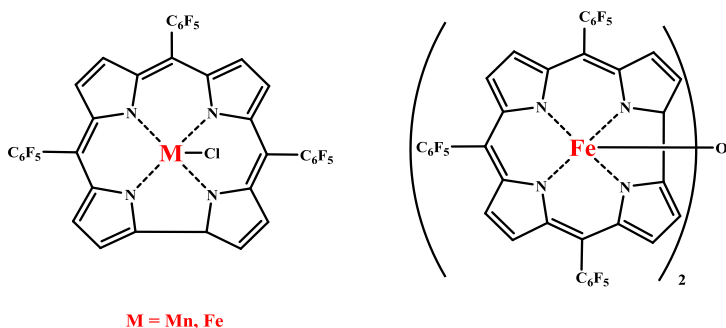
Figure 5.2.6. Structure of corrole Mn and Fe complexes.

Other bimetallic complexes are dizinc and dimagnesium catalysts bearing macrocyclic ancillary ligand. These catalysts, schematically reported in Figure 5.2.7, displayed good polymerization control and activities with TOF of 97 h^{-1}.[76]
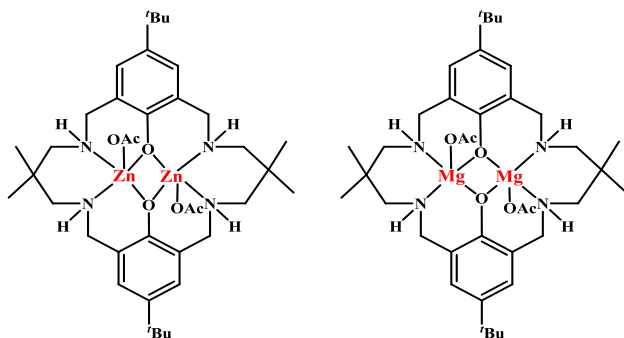
Figure 5.2.7. Di-zinc and magnesium catalysts tested in the PA and CHO copolymerization

Although poorly studied, dinuclear zinc *N*-Heterocyclic carbene (NHCs) complexes are of great interest. In 2004, Buchmeiser et al. synthetized mono(1,3-bis(2,4,6-trimethylphenyl)imidazol-2-ylidene) zinc (II) complex that showed low activity and high selectivity in the copolymerization of cyclohexene oxide with CO_2.[77] An other bidentate zinc complexes bearing pyridyl-NHC ligands were reported by Tolman. Dinuclear NHC complexes bearing 2,4,6-trimethylphenyl substituents (Figure 5.2.8, **A**) were found active in ROP of *rac*-lactide with good control of molecular weight, yielding polymers with an heterotactic-enriched structure. In 2014, Dagorne studied similar complexes in which the NHC ligands have methyl and *n*-butyl groups at the nitrogen atoms, respectively (Figure 5.2.8, **B**). These catalysts displayed a good efficiency in the controlled ROP of lactide and trimethylene carbonate under mild polymerization conditions.[78] In this Chapter, we report our results in exploring the catalytic performances of these complexes in the copolymerization reactions of cyclohexene oxide or propylene oxide with succinic anhydride.
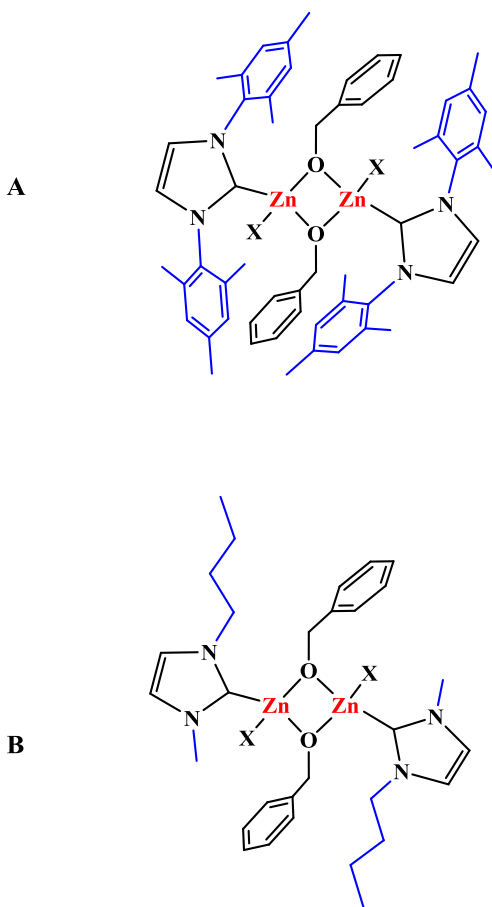
Figure 5.2.8. Di-zinc catalysts reported by Tolman (**A**) and Dagorne (**B**)

5.3 Copolymerization mechanism for epoxide and anhydride

The copolymerization mechanism consists of three pathways involving different pentacoordinate and hexacoordinate species. The general sequence starts with the epoxide activation through interation with the metal center followed by the attack to the carboxylate unit. The resulting alkoxide reacts with the anhydride to generate new ester and a metal carboxylate bond is able to proceed in the copolymerization.

In cycle 1 of Scheme 5.3.1, the polymerization provides the formation of hexacoordinate monoalkoxide monocarboxylate intermediate, indicated with AC, which evolves in the hexacoordinate bis(alkoxide) species, namely AA. In cycle 2 and 3, the fundamental intermediate is represented by a bis(carboxylate) (CC); starting from the hexacoordinate monoalkoxide monocarboxylate specie (AC); the dissociation into alkoxide (cycle 2) or a carboxylate (cycle 3) can be observed (Scheme 5.3.1).[62]

Epoxide homopolymerization is possible in presence of strongly electrophilic metal center, differently there are not examples of anhydride homopolymerization because it is disfavored thermodynamic process.
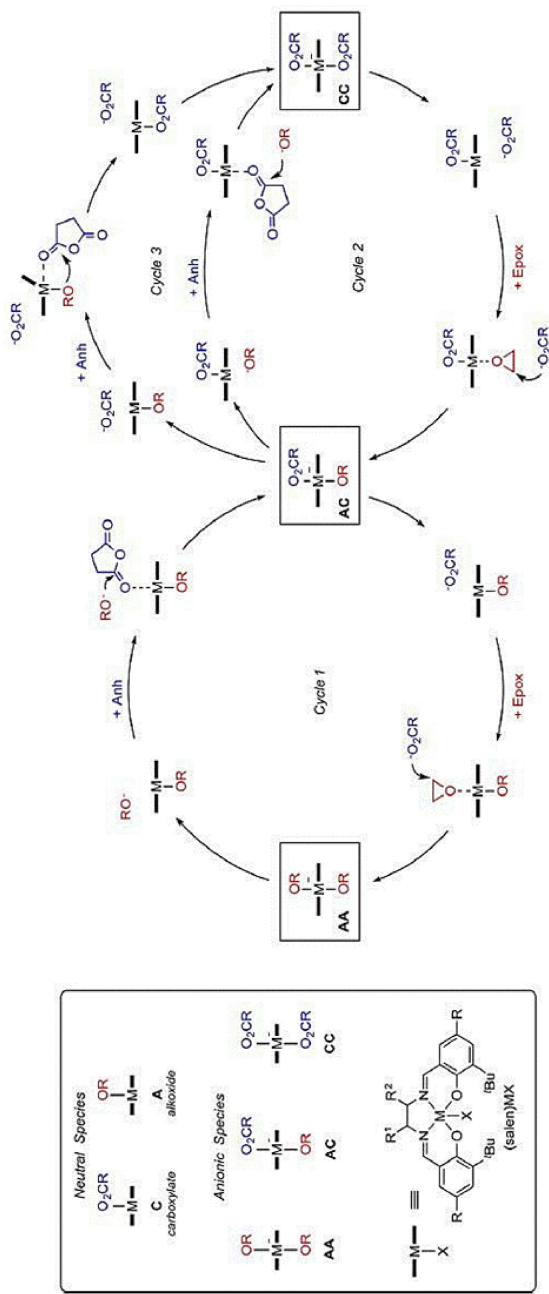
Scheme 5.3.1. Mechanistic possibilities in the ROCOP epoxide/anhydride.

5.4 Synthesis of dinuclear zinc-N-heterocyclic carbene complexes

The zinc complexes $[(R_1,R_2\text{-}C_{NHC})ZnX(OBn)_2]$ (**10**. $R_1 = R_2$ = Mesityl, X = Cl; **11**. R_1 = Me, R_2 = ^{n}butyl, X = Br; **12**. $R_1 = R_2$ = methyl and X = I) bearing monodentate N-heterocyclic carbenes (NHCs) used in this study are reported in Figure 5.4.1.
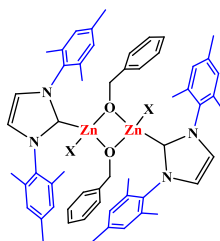
(10)
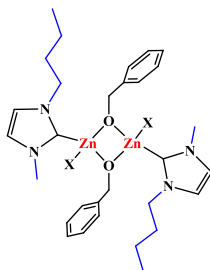
(11)
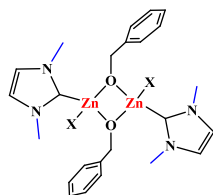
(12)

Figure 5.4.1. Synthesis of $(C_{NHC})ZnX(OBn)_2$ (**10-12**).

The complexes **10** and **11**, previously reported by Tolman and Dagorne, were synthetized according to the literature by alcoholysis of $[(R_1,R_2\text{-}$

C_{NHC})ZnClEt] precursor.[79] In particular, the reaction between the commercial imidazolium salts with two equivalent of diethylzinc (ZnEt$_2$) yields selectively the ethylchloride-zinc intermediates [(R$_1$,R$_2$-C$_{NHC}$)ZnClEt] that, in presence of one equivalent of benzyl alcohol, give the desired complexes (Scheme 5.4.1). The complex **10** appeared as a yellow powder, while **11** was precipitated in a mixture CH$_2$Cl$_2$/pentane (1:3) at -30°C and recovered as light brown solid.

It is noteworthy that the excess of ZnEt$_2$ promotes the formation of a single intermediate; differently the reaction of the imidazolium salt with one equivalent of ZnEt$_2$ leads to the equimolar mixture of biscarbene and monocarbene Zn-derivates.[80]

10. **R** = Mes, Mes
11. **R** = ^{n}Bu, Me
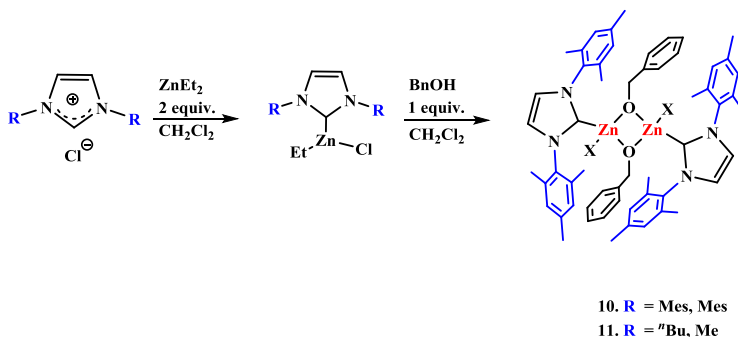
Scheme 5.4.1. Synthetic procedure of **10** and **11** from the corresponding imidazolium salts.

The complexes **10** and **11** were characterized by NMR spectroscopy. The ^{1}H NMR spectrum in CDCl$_3$ of **10** displayed at δ 1.96 and 2.02 the singlets of CH$_3$ relative to the mesityl groups and the methylene protons appeared at 3.74 and 4.32 ppm as broad doublet (AB spin system). The CH=CH resonances were detected at 5.78 and 6.52 ppm, respectively. The remaining signals between 7.08-7.58 ppm were due to the aromatic ring protons (Figure 5.4.2).
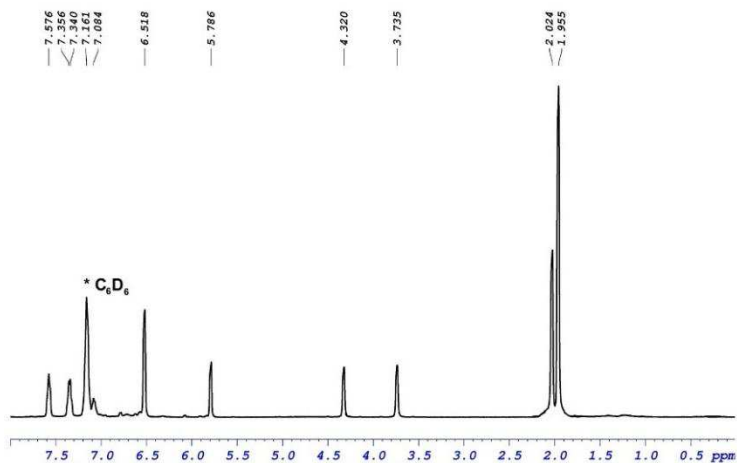
Figure 5.4.2. ^{1}H NMR (C_6D_6, 400 MHz, 25°C) of **10**.

Differently, the complex **11** showed, in the ^{1}H NMR spectrum, a broad signals at δ 4.68 assigned to CH_2-benzyl groups, suggesting a fluxional character of the complex in solution (Figure 5.4.3).
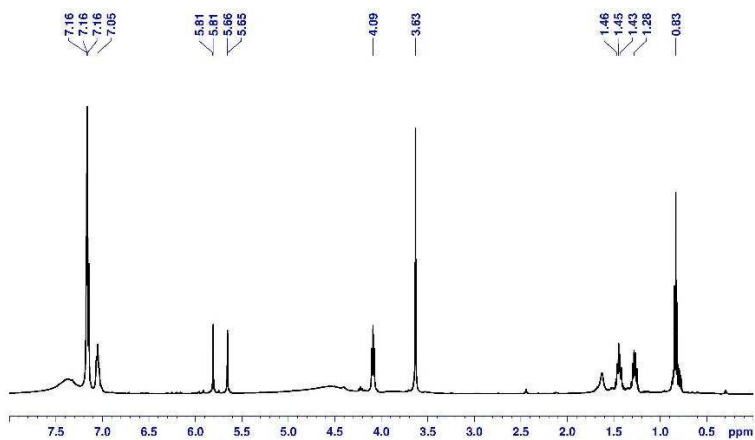
Figure 5.4.3. ^{1}H NMR ($CDCl_3$, 500 MHz, 25°C) of **11**.

Both the complexes **10** and **11** were stable in chlorinated solvents with a good stability in inert atmosphere, and in air for many hours in solid state

The synthetic procedure, described for the complexes **10** and **11**, was unsuccessful for **12**. In fact, the reaction between the imidazolium iodide salt and excess of $ZnEt_2$ yields a white precipitate insoluble in THF, ether, CH_2Cl_2 and benzene. So, the imidazolium iodide salt (IMe) was deprotonated by sodium bis(trimethylsilyl)amide (NaHMDS), yielding the corresponding free carbene that led to **12** (Figure 5.4.4) through the reactions with $ZnEt_2$ and, subsequently, with two equivalents of BnOH.
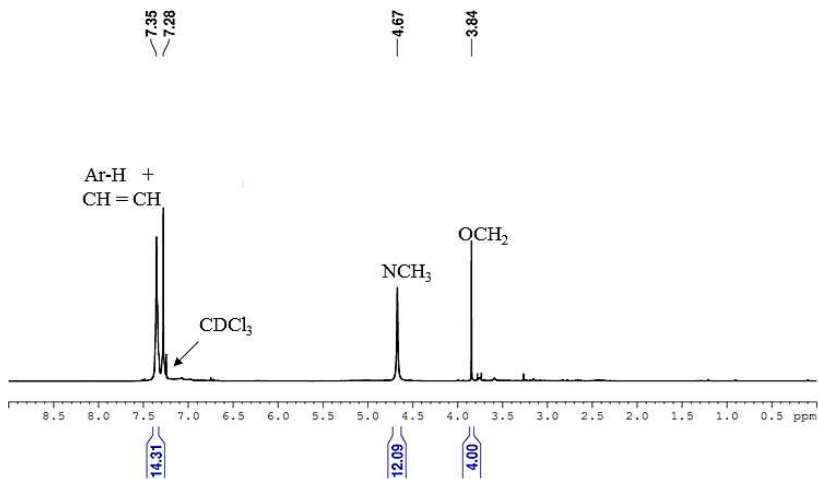
Figure 5.4.4. ¹H NMR (CDCl₃, 500 MHz, 25°C) of **12**.

The ¹H NMR spectrum (in CDCl₃) of the complex **12** displayed at 3.84 ppm a singlet that integrated for 4 protons relative to the two OCH_2Ph groups and at 4.67 ppm the NCH_3 resonances; all the aromatic resonances were observed in the range between δ 7.28 and 7.35.

5.5 Copolymerization of CHO with SA catalyzed by 10-12

The catalytic performances of **10-12** were explored in the copolymerization of cyclohexene oxide and succinic anhydride under solvent free and at high tempertature; the main results are reported in the Table 5.5.1.

Table 5.5.1. ROCOP of CHO with SA using the complexes 10-12.

entry[a]	Initiator	time h	CHO conv. %[b]	SA conv. %[b]	Ester link. %[b]	$M_{n(GPC)}$[c] g/mol	PDI[c]
1	**10**	4	78	95	75	2249	1.79
2	**11**	3	91	96	83	1711	1.54
3	**12**	2	88	86	87	1191	1.46
4[d]	**10**	24	94	99	91	830	1.25
5[d]	**11**	24	89	90	95	971	1.28
6[d]	**12**	24	67	97	86	1010	1.82

[a]Reaction conditions: [I] = 19.4 μmol, [I]/[CHO]/[SA] = 1:100:100, T = 110 °C, neat; [b]Determined by ^{1}H NMR analysis of crude reaction mixture; [c]Determined by GPC analysis using polystyrene standards; [d]Entry 4. Solvent = toluene (1 mL), T = 90°C.

The complex **10** converted about 78 % CHO and 95 % SA in 4 h (Entry 1, Table 5.5.1). Swictching from complex **10** to complexes **11** and **12** (N_1-Me, N_2-Me), the catalytic activities significantly increased probably due to the decrease of the steric hindrance (88 % PCHO and 86 % PSA in 2 h, entry 3 Table 5.5.1). These results indicate a catalytic behavior comparable to the most active complexes reported in the ROCOP.

The complex **10**, in toluene solution, converted both the monomers in 24 h at 90°C with a slight increment of the ester linkage (91%, entry 4 in Table 5.5.1) respect to the run explored in neat conditions (entry 1, Table 5.5.1). The monomer conversion of the reaction mixture and the percentage of ester linkage in the isolated polymer were determined by ^{1}H NMR using DMSO as solvent. This allows to distinguish the chain end signals of the poly(cyclohexene succinate) from the polyether signals. All polymers

displayed a monomodal molecular weight distributions and narrow polydispersity (PDI = 1.25-1.82), but the M_n values are low for the presence of transesterification reactions as suggested by MALDI-TOF-MS analysis (Figure 5.5.2).

^{1}H NMR spectrum of P(CHO-SA) by **10** confirmed the effective formation of the copolymer; traces of polyether linkages at 3.4 ppm were also detected (Figure 5.5.1).
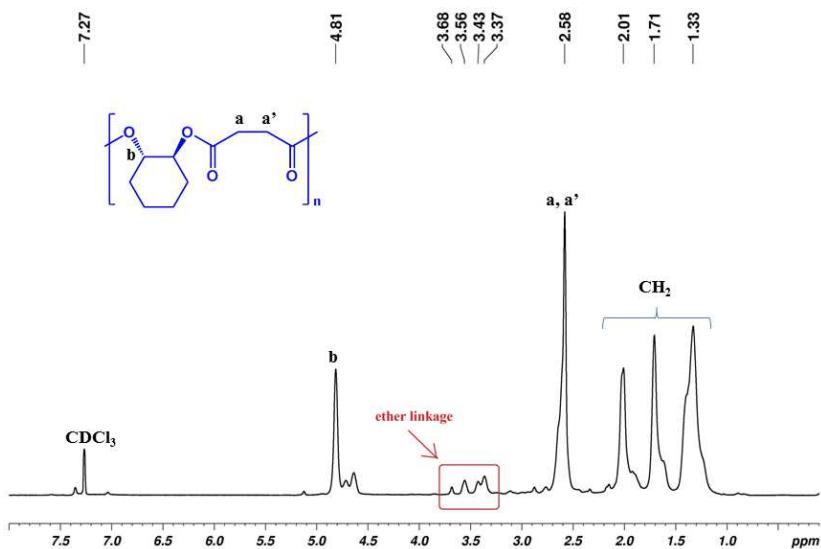
Figure 5.5. 1. ^{1}H NMR (CDCl$_3$, 500 MHz, 25°C) of P(CHO-SA) obtained by **10** (entry 1, Table 5.5.1).

The MALDI-TOF-MS analysis displayed two principal distributions (Figure 5.5.2.); the more abundant one indicates a linear polymer in which the peaks are separated by 198 m/z, corresponding to repeating units [CHO-

SA]. The second one is attributed to a cyclic product, probably due to the intermolecular transesterification process.[11]
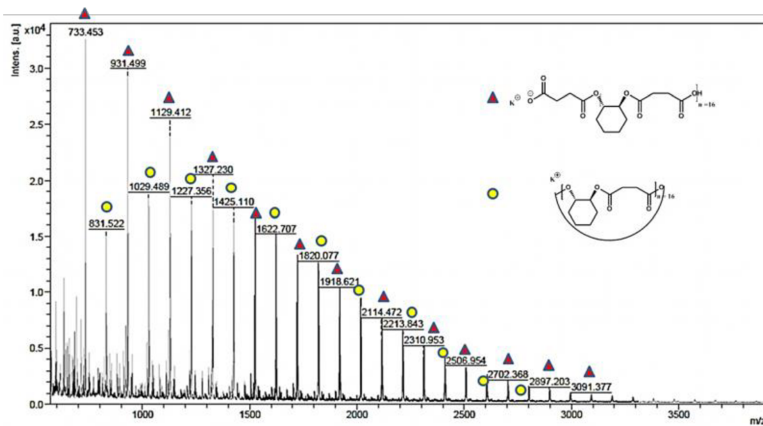
Figure 5.5.2. MALDI-TOF-MS spectrum of P(CHO-PSA) obtained by **10** (entry 1, Table 5.5.1).

Recently, Darensbourg et al.[81] published one of the most relevant paper about the copolymerization of CHO with carbon dioxide, in which a benefical effects from the addition of an external cocatalysts, like a quaternary ammonium salts or Lewis bases, was observed. The cocatalyst provides a better initiator group for the ring opening of epoxide, reducing drastically the induction period. So, the copolymerization of CHO with SA were carried out in presence of one equivalent of TBACl (tetrabutylammonium chloride) in absence of solvent at 110°C. All complexes showed a significant increase of the catalytic activities in neat conditions (entries 1, 3, 4; Table 5.5.2). The complex **12** showed the best performances, incorporating the 80% of cyclohexene oxide into a polymer in only 30 minutes. The catalytic trend changed drastically in toluene and for the complex **12**, only the 51 mol % of SA and 38 mol % of CHO were converted (entry 7, Table 5.5.2). The complex **10** appeared poorly active under solvent free conditions (entry 1, Table 5.5.2), it displayed a very

interesting behavior in solution. All succinic anhydride and 50 mol % of cyclohexene oxide (entry 5, Table 5.5.2) were converted in 5 h. For both cases, the ester linkage amounted to 90 %. To improve the catalytic activities of **10-12**, the polymerizations were carried out using two equivalents of TBACl, in the same conditions used previously; unfortunately none significant catalytic variations were observed. In the presence of 4-Dimethylaminopyridine (DMAP) as cocatalyst, **10** showed a moderate activity with only the 22 mol % of CHO conversion and 62 mol % of PSA (entry 2, Table 5.5.2). GPC analysis displayed monomodal molecular weight distribution and moderately narrow polidispersivity indices (PDI = 1.21-1.40).

Table 5.5.2. ROCOP of CHO with SA using the complexes 10-12 in presence of cocatalyst

entry[a]	Initiator	Cocat	time h	CHO conv. %[b]	SA conv. %[b]	Ester link. %[b]	$M_{n(GPC)}$[c] g/mol	PDI[c]
1	**10**	TBACl	0.5	41	89	87	1004	1.26
2	**10**	DMAP	0.5	22	62	83	1645	1.11
3	**11**	TBACl	0.5	62	90	90	1199	1.21
4	**12**	TBACl	0.5	80	93	91	1435	1.69
5[d]	**10**	TBACl	5	49	96	98	722	1.21
6[d]	**11**	TBACl	5	42	80	98	728	1.40
7[d]	**12**	TBACl	5	38	51	92	986	1.26

[a]*Reaction conditions*: [I] = 19.4 μmol, [I]/[CHO]/[SA] = 1:100:100, T = 110 °C, neat; [b]Determined by ^{1}H NMR analysis of crude reaction mixture; [c]Determined by GPC analysis using polystyrene standards; [d] addition of 19.4 μmol TBACl or DMAP.

To investigate the copolymerization mechanism, kinetic studies were carried out in toluene solution. At 90°C an induction period of 4 h for SA and 8 h for CHO was observed in presence of the complex **10**; after this time, the polymerization proceeded following a first order kinetic in monomer concentration ($k_{sa} > k_{CHO}$) (see Figure 5.5.3). Thus, in presence of

one equivalent of TBACl, the activity of the complex **10** increased considerably and a reduction of the induction time (1 h for SA and 2 h for CHO) was detected (Figure 5.5.3).
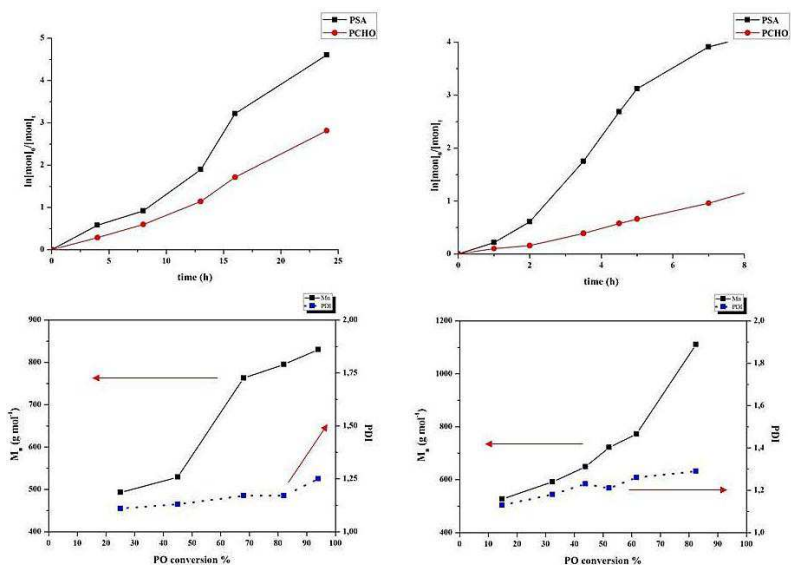
Figure 5.5.3. (Left) Kinetic of CHO and PSA in the ROCOP using **10** at 90°C in toluene (1mL) and below the development of Mn (black) and PDI (blu) vs CHO conversion %. (Right) Kinetic of CHO and PSA after addition of TBACl and below, relation between Mn, CHO conversion % and PDI.

5.6 Copolymerization of PO with SA catalyzed by 10-12

The copolymerization of propylene oxide (PO) with succinic anhydride (SA) was performed under neat conditions at 110°C (entries 1-3, Table 5.6.1) and toluene at 90°C (entries 4-6, Table 5.6.1). The results were summarized in Table 5.6.1.

Table 5.6.1. ROCOP of PO with SA catalyzed by 10-12

entry[a]	Initiator	time h	PO conv. %[b]	SA conv. %[b]	Ester link. %[b]	$M_{n(GPC)}$[c] g/mol	PDI[c]
1	**10**	4	68	98	73	2587	1.05
2	**11**	4	99	61	85	720	1.24
3	**12**	4	76	32	38	645	1.14
4[d]	**10**	4	20	60	88	1277	1.09
5[d]	**11**	24	90	89	80	978	1.25
6[d]	**12**	24	96	50	39	965	1.32

[a]Reaction conditions: [I] = 19.4 µmol, [I]/[PO]/[SA] = 1:100:100, T = 110 °C, neat; [b]Determined by ^1H NMR analysis of crude reaction mixture; [c]Determined by GPC analysis using polystyrene standards; [d]Entry 4. Solvent = Toluene (1 mL), T = 90°C.

The complex **10** promoted a fast consumption of anhydride, as previously seen in the copolymerization of CHO with SA, while in the case of the catalysts **11** and **12**, higher conversions of the PO compared to SA were observed, probably for the less steric encumbrance of the ancillary substituents on NHC ligands. The copolymers produced using the complexes **10** and **11** exhibited comparable percentages of ester linkages of about 70-80 %. In solution the complex **10** displayed the highest catalytic activity, converting 60 mol % of SA and 20 mol % of PO in 4 h. In the case of complex **12**, the homopolymerization of PO was favored in comparison to the copolymerization (entry 6, Table 5.6.1). The perfect combination of activity and selectivity ester was obtained with complex **11**, in which the different steric encumbrance of nitrogen position favors the competition of anhydride or the epoxide in the coordination-insertion step. All the

polyesters were analyzed by GPC. The PDI values were narrow and the molecular weights (Mn) were low.

The ^{1}H NMR spectrum of the poly(propylene succinate) obtained by complex **10** is reported in Figure 5.6.1. The PPO appeared at 1.26 (CH$_3$), 4.17 (CH$_2$) and 5.15 (CH) ppm; while methylene resonances of PSA were detected at 2.64 ppm. The benzylic end-group was also observed.
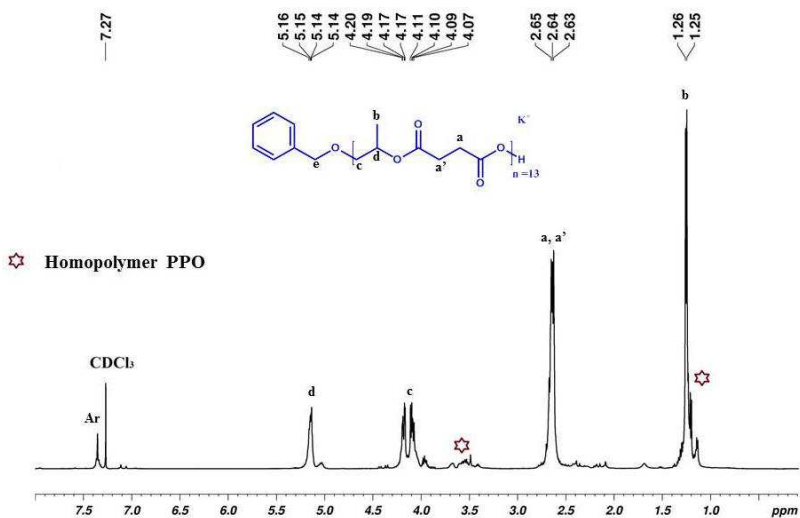
Figure 5.6.1.^{1}H NMR of poly(propylene succinate) obtained by complex **10** in CDCl$_3$.

The ^{13}C NMR signals for the benzylic group were clearly observed at 66.38, 128.42, 128.42, 128.50, 128.78 ppm. The regioselectivity of PO ring opening was assessed from the methine or methylene carbon signals in the range between 28 and 30 ppm, typical of the regiosequences (tail-tail (T-T), head-head (H-H) and head-tail (HT)). Depending on the ratio between the TT, HH and HT areas, same information about the regioselectivity of the poly(propylene succinate) were detected.[69] In our specific case all the polyesters are regioirregular (Figure 5.6.3).
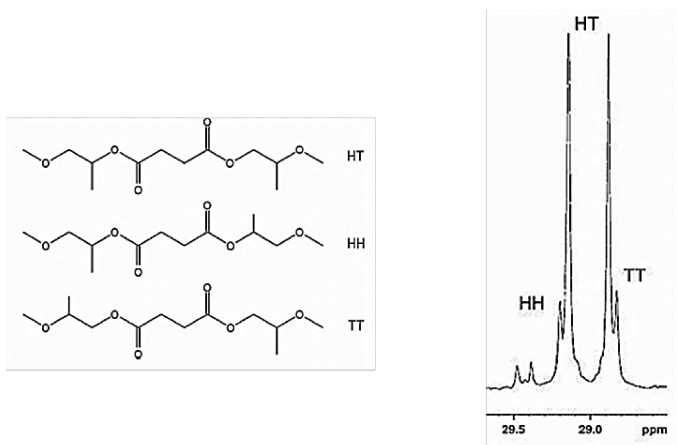
Figure 5.6.2. Regioselectivity of polypropylene succinate reported by Chisholm.
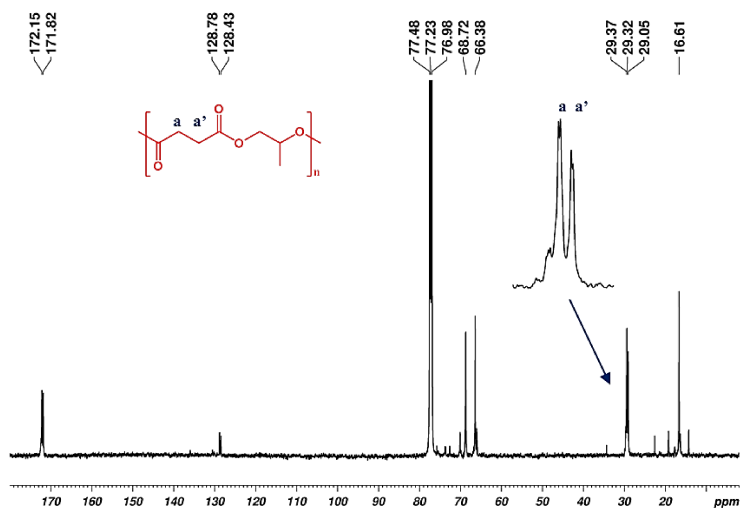
Figure 5.6.3. ^{13}C NMR of P(PO-SA) obtained by complex **10**

Finally, a further confirmation of the copolymer microstructure was offered by MALDI-TOF-MS analysis using the 2,5-dihydroxybenzoic acid (DHB)

matrix and dichloromethane as solvent. The main pattern of signals comprises peaks separated by m/z of 158 corresponding to [PO-SA] unit terminated with PhCH$_2$O$^-$ and H$^+$ stabilized with potassium ion (Figure 5.6.4.).
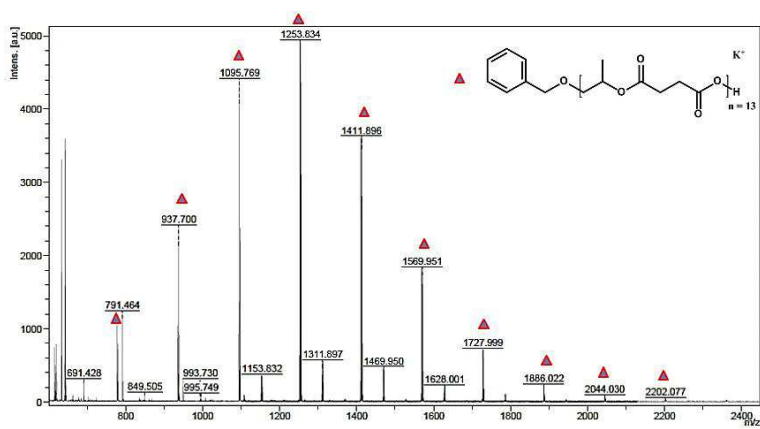
Figure 5.6.4. MALDI-TOF-MS of poly(propylene succinate), entry 1 Table 5.4.1.

The role of the cocatalyst in the copolymerization of PO with SA was investigated in presence of one equivalent of TBACl. In only 30 min, **11** converted 87 mol % of PO and 70 mol % of SA (entry 3 Table 5.6.2). The addition of DMAP (entry 2, Table 5.6.2) did not produce benefits. In toluene solution the best performance was showed by complex **12** and complete conversion of both the monomers was detected after 5 h. The ester linkage (mol %) remained also low. The GPC analysis reveals oligomers with M$_n$ of 600-900 Da and a narrow molecular weight distributions (PDI = 1.04-1.40).

Table 5.6.2. ROCOP of CHO with SA using 10-12 in presence of cocatalysts.

Entry[a]	Initiator	Cocat	time h	PO conv. %[b]	SA conv. %[b]	Ester link. %[b]	$M_{n(GPC)}$[c] g/mol	PDI[c]
1	**10**	TBACl	0.5	52	63	83	770	1.04
2	**10**	DMAP	0.5	4	10	−	574	1.30
3	**11**	TBACl	0.5	87	72	80	903	1.08
4	**12**	TBACl	0.5	44	20	74	612	1.12
5[d]	**10**	TBACl	4	45	62	94	630	1.04
6[d]	**11**	TBACl	5	63	80	98	728	1.40
7[d]	**12**	TBACl	5	99	93	37	711	1.20

[a]Reaction conditions: [I] = 19.4 μmol, [I]/[cocat]/[PO]/[SA] = 1:1:100:100, T = 110 °C, 0.5 h, neat; [b]Determined by ^{1}H NMR analysis of crude reaction mixture; [c]Determined by GPC analysis using polystyrene standards. [d]Solvent = Toluene (1 mL), T = 90°C.

The reaction kinetics in the PO polymerization catalyzed by **11** was explored at 90°C in toluene. At the beginning, the polymerization started slowly showing an induction period of 7 h; then, a pseudo first-order kinetics in monomer concentration was observed for this monomer. By addition of a Lewis base (TBACl), the performances improved and a sensible reduction of the induction period (around 3 h) was recorded (Figure 5.6.5).
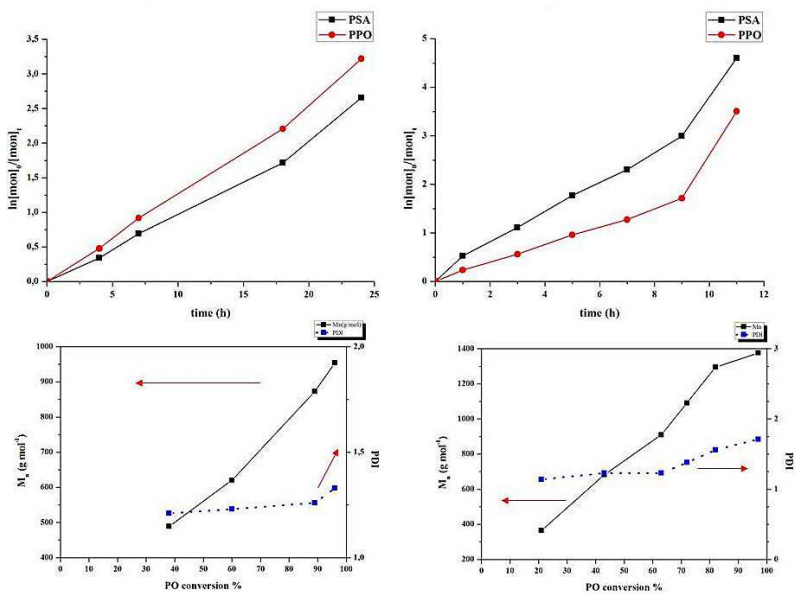
Figure 5.6.5. (Left) Kinetic of PPO and PSA in the ROCOP using **11** at 90°C in toluene (1mL) and below the development of Mn (black) and PDI (blu) vs PPO conversion %. (right) Kinetic of PPO and PSA after addition of TBACl and below, relation between Mn, PPO conversion % and PDI.

5.7 Scale up of copolymerization reaction of CHO with SA by 10-12

The catalytic performances of **10-12** were also tested in presence of 250 eq. of the CHO and SA respectively. The main results were reported in Table 5.7.1. In 4 h the catalyst **12** showed the best activity, but the ester selectivity remained low. Good activity and selectivity control was observed using the complexes **10** and **11**. The molecular weight of the polyesters remained low, probably for the transesterification reactions, but the relative polydispersity indices were moderately narrow (Table 5.7.1).

The complex **10**, in presence of TBACl, showed a significant increase of the catalytic activity and the ester linkage percentage remained also high. The molecular weight was about 2.1 KDa and PDI of 1.66, estimated by GPC.

Table 5.7.1. ROCOP of CHO with SA catalyzed by 9-11

Entry[a]	Initiator	CHO conv. %[b]	SA conv. %[b]	Ester link. %[b]	$M_{n(GPC)}$[c] g/mol	PDI[c]
1	**10**	63	78	79	1412	1.46
2	**11**	84	98	81	1764	1.63
3	**12**	93	97	64	1740	1.55
4[b]	**10**	81	99	83	2149	1.66
5[c]	**10**	96	99	85	1473	1.32

[a]Reaction conditions: [I] = 19.4 μmol, [I]/[CHO]/[SA] = 1:250:250, T = 110 °C, 4 h, neat; [b]T= 110 °C, 4 h, neat, 1 eq. TBACl; [c]T= 90 °C, 48 h, toluene.

5.8 Conclusion

In this chapter, a series of dinuclear zinc-*N*-heterocyclic carbenes complexes (**10-12**) differently substituted on the nitrogen atoms of the NHC ligands were investigated in the copolymerization of succinic anhydride (SA) with cyclohexene oxide (CHO) or propylene oxide (PO) under solvent free and high tempertature. The complex **12** (N_1-Me, N_2-Me) was the most active in the ROCOP of succinic anhydride with both propylene oxide and cyclohexene oxide, but its ester selectivity resulted very low. In the case of the polymerization between SA and CHO, the polymerization reaction was dominated by a continue competition of the two monomers to the metal center, testified by a similar conversion at different times. In the case of PO, the small size of the epoxide promoted the rapid coordination to the zinc, suggesting a tendency to obtain a block copolymer. Conversely, in presence of complex **10** (N_1-Mes, N_2-Mes), SA was consumed faster than epoxide. The addition of a Lewis bases, in particular TBACl, produced a positive effect on the catalytic performances, but the molecular weights were low (1 KDa). The oligomeric nature of the obtained polyesters was confirmed by MALDI-TOF-MS analysis, in which the linear and the cyclic polyesters were detected.

5.9 References

[61] Lecomte, P.; Jérôme, C. Recent Developments in Ring-Opening Polymerization of Lactones. In Synthetic Biodegradable Polymers; Rieger, B., Künkel, A., Coates, G. W., Reichardt, R., Dinjus, E., Zevaco, A. T., Eds.; Advances in Polymer Science, Vol. 245; Springer-Verlag: Berlin and Heidelberg, Germany, **2012**; 173−217; DOI: 10.1007/978-3-642-27154-0

[62] Longo, J. M.; Sanford, M. J.; Coates, G. W. *Chem. Rev.* **2016**, *116*, 15167−15197.

[63] **a)** Longo, J. M.; DiCiccio, A. M.; Coates, G. W. *J. Am. Chem. Soc.,* **2014**, *136*, 15897–15900. **b)** Darensbourg, D. J.; Poland, R. R.; Escobedo, C. *Macromolecules* **2012**, *45*, 2242−2248.

[64] Wang, D.; Zhang, G.; Zhang, Y.; Gao, Y.; Zhao, Y.; Zhou, C.; Zhang, Q.; Wang, X. *J. Appl. Polym. Sci.*, **2007**, *103*, 417–424.

[65] Paul, S.; Zhu, Y.; Romain, C.; Brooks, R.; Saini, P. K.; Williams, C. K., *Chem. Commun.* **2015**, *51*, 6459-6479.

[66] Fischer, R. F., *J. Polym. Sci.* **1960**, *44*, 155-172.

[67] **a)** Aida, T.; Inoue, S., *J. Am. Chem. Soc.* **1985**, *107*, 1358-1364; **b)** Aida, T.; Sanuki, K.; Inoue, S., *Macromolecules* **1985**, *18*, 1049-1055.

[68] Asano, S.; Aida, T.; Inoue, S. *Macromolecules*, **1985**, 18, 2057–2061.

[69] Bernard, A.; Chatterjee, C.; Chisholm, M. H. *Polymer*, **2013**, *54*, 2639-2646.

[70] Jeske, R. C.; DiCiccio, A. M.; Coates, G. W. *J. Am. Chem. Soc.*, **2007**, 129, 11330–11331.

[71] DiCiccio, A. M.; Coates, G. W., *J. Am. Chem. Soc.* **2011**, *133*, 10724-10727.

[72] a) Nejad, E. H.; van Melis, C. G. W.; Vermeer, T. J.; Koning, C. E.; Duchateau, R., *Macromolecules* 2012, *45*, 1770-1776. b) Huijser, S.; HosseiniNejad, E.; Sablong, R.; de Jong, C.; Koning, C. E.; Duchateau, R., *Macromolecules* **2011**, *44*, 1132-1139.

[73] Liu, J.; Bao, Y.-Y.; Liu, Y.; Ren, W.-M.; Lu, X.-B., *Polym. Chem.* **2013**, *4*, 1439-1444.

[74] Liu, D.-F.; Wu, L.-Y.; Feng, W.-X.; Zhang, X.-M.; Wu, J.; Zhu, L.-Q.; Fan, D.-D.; Lu, X.-Q.; Shi, Q., *J. Mol. Catal. A: Chem.* **2014**, *382*, 136-145.

[75] Robert, C.; Ohkawara, T.; Nozaki, K., *Chem. - Eur. J.* **2014**, *20*, 4789-4795.

[76] Saini, P. K.; Romain, C.; Zhu, Y.; Williams, C. K., *Polym. Chem.* **2014**, *5*, 6068-6075.

[77] Wang, D.; Wurst, K.; Buchmeiser, M.R. *J. Organomet. Chem.* **2004**, *689*, 2123–2130.

[78] a) Fliedel, C.; Mameri, S.; Dagorne, S.; Avilés, T. *Appl. Organometal. Chem.* **2014**, *28*, 504–511. b) Fliedel, C.; Vila-Viçosa, D.; Calhorda, M. J.; Dagorne, S.; Avilés, T. *Chem.Cat.Chem.* **2014**, *6*, 1357 – 1367.

[79] Jensen, T. R.; Schaller, C. P.; Hillmyer, M. A.; Tolman, W. B. *J. Organomet. Chem.*, **2005**, *690*, 5881.

[80] Fliedel, C.; Mameri, S.; Dagorne, S.; Avilés, T. *Appl. Organometal. Chem.* **2014**, *28*, 504–511.

[81] Darensbourg, D. J.; Mackiewicz, R. M. *J.AM. CHEM. SOC.* **2005**, *127*, 14026-14038.

Chapter 6: Experimental Part

6.1 Materials and methods

All manipulations were performed under a dry nitrogen or argon atmosphere using a Braun single station drybox or standard Schlenk techniques. Glassware and vials for the reactions were dried overnight at 120°C in the oven. The solvents (hexane, tetrahydrofuran, toluene, dichloromethane), purchased by Sigma Aldrich, were appropriately anhydrated and purified by distillation under inert atmosphere. Isopropyl and *tert*-butyl alcohol were distilled over magnesium turnings. Ligands and monomers (racemic-lactide and succinic anhydride) were purified by crystallization and stored in vacuum under P_2O_5. Liquid monomers (racemic β-butyrolactone, ε-caprolactone, cyclohexene oxide and propylene oxide) were dried with CaH_2 and distilled under reduced pressure. mMAO (7 wt% Aluminium in toluene, Sigma Aldrich), diethylzinc and trityl tetrakis(pentafluorophenyl)borate were used as received and stored in the glovebox. Deuterated solvents were dried with molecular sieves. Ethylene was purchased from Rivoira. All other chemicals were commercially available and used as received unless otherwise stated.

6.2 Instruments and measurements

NMR spectra were recorded on Bruker Advance 250, 300, 400, 500 and 600 MHz spectrometers at 25 °C, unless otherwise stated. Chemical shifts for ^1H NMR were reported in δ (parts per million) and coupling constants (J) in hertz. NMR spectra are referenced using the residual solvent peak (7.27 for ^1H and 77.23 for ^{13}C in $CDCl_3$; 7.16 for ^1H and 128.06 for ^{13}C in C_6D_6; 5.8 for ^1H and 73.78 for ^{13}C in TCDE). Variable-temperature ^1H NMR experiments were performed in J. Young NMR tube using toluene-d_8 as solvent at Bruker Avance 600 spectrometer. Mn and Mw values and the

polidispersivity index (Mw/Mn) of polyesters were estimated by gel permeation chromatography (GPC) at 30 °C, using THF as solvent and polystyrene standards as reference. Mn was corrected using the factor of 0.58 for PLA, 0.56 for PCL and 0.54 for PHB, according to the literature.[82] The polyethylene samples were analyzed also by thermal analysis (DSC) using TA Instrument DSC Q2000 in nitrogen flow with a heating and cooling rate of 10 °C min^{-1} in the range 100 to +200 °C. Mass spectra were registered by Bruker solariX XR Fourier transform ion cyclotron resonance mass spectrometer, in the range 1000-8000 m/z, using 2,5-dihydroxybenzoic acid (DHB) as matrix for MALDI. The laser power was 15% and the acquisition was in positive mode. For the preparation of the samples, 10 μL of polymer solutions (1mg/mL in CH_2Cl_2) were mixed to 10 μL of a saturated solution of matrix prepared at the concentration of 30 mg/mL. The final solution was deposed on the MALDI target for the acquisition.

6.3 Experimental part of Chapter 2

6.3.1 Synthesis of 2-(bromomethyl)-4,6-bis(2-phenylpropan-2-yl)phenol

A round-bottomed flask with a magnetic stirrer bar was charged with c.a. 100 mL of acetic acid, 2,4-bis(2-phenylpropan-2-yl)phenol (10.0 g, 30.3 mmol) and paraformaldehyde (1.0 g, 33.3 mmol, 1.1 eq.). The suspension was left under stirring at room temperature. After 2 h, a solution of HBr 33% in acetic acid (34 mL, 194.3 mmol, 6.4 eq) was added dropwise to the mixture, producing a yellow solution. After 90 minutes, the reaction was stopped through the addition of cold water and the reaction mixture was extracted with CH_2Cl_2 to recover the bromo derivative. Finally, the organic solvent was removed under reduced pressure, obtaining an orange viscous oil that in petroleum ether at -20°C precipitated as a white solid (77% yield).

Spectroscopic data: ^{1}H NMR (300 MHz, CDCl$_3$, 25°C) = δ 7.37-7.25 (m, 10H, Ar), 7.22-7.18 (m, 1H, Ar), 7.14 (d, J_{HH} = 2.2 Hz, 1H, Ar), 4.60 (br, 1H, O*H*), 4.45 (s, 2H, C*H$_2$*), 1.75 (s, 6H, C(C*H$_3$*)$_2$Ph), 1.63 (s, 6H, C(C*H$_3$*)$_2$Ph). ^{13}C NMR (75.4 MHz, CDCl$_3$, 25 °C) = δ 150.8, 150.3, 147.9, 142.7, 135.4, 129.5, 128.2, 127.8, 127.5, 126.9, 126.2, 126.1, 125.9, 125.4, 42.8 and 42.2 (C(CH$_3$)$_2$Ph), 31.2 (C(CH$_3$)$_2$Ph), 30.5 (CH$_2$), 29.8 (C(CH$_3$)$_2$Ph).

6.3.2 Synthesis of L2

In a round-bottomed flask with a magnetic stirrer bar, a THF solution (20 mL) of sodium tert-butoxide (0.68 g, 7.08 mmol, 2 eq.) was added dropwise to a THF solution (10 mL) of 1,2-benzenedithiol (0.50 g, 3.51 mmol), producing a white suspension of the corresponding sodium salt. Then, 2-(bromomethyl)-4,6-bis(2-phenylpropan-2-yl)phenol (2 eq.) in 20 mL of THF was added to the reaction mixture at room temperature. The reaction was left under stirring overnight. After this time, the solvent was removed in vacuum and the crude product washed with CH$_2$Cl$_2$. Finally, the organic solvent was removed under reduced pressure, recovering a viscous oil that crystallized in petroleum ether at rt. Yield = 78%. Single crystals were grown from toluene/THF (1:1 v/v). Spectroscopic data: ^{1}H NMR (300 MHz, CDCl$_3$, 25°C) = δ 7.32-7.25 (m, 12H, Ar), 7.19 (m, 10H, Ar), 7.01 (m, 4H, Ar), 6.86 (m, 2H, Ar), 4.88 (s, br, 2H, O*H*), 3.96 (s, 4H, C*H$_2$*), 1.61 (s, 24 H, C*H$_3$*). ^{1}H NMR (250 MHz, C$_6$D$_6$, 25°C) = δ 7.51-7.31 (m, 26H, Ar), 7.01-7.00 (d, J_{HH} = 2.2 Hz, 2H, Ar), 5.03 (s, 2H, O*H*), 4.11 (s, 4H, C*H$_2$*), 1.76 (s, 24 H, C*H$_3$*). ^{13}C NMR (62.9 MHz, C$_6$D$_6$, 25°C) = δ 202.40, 201.39, 200.27, 193.23, 188.32, 186.59, 182.38, 180.23, 179.25, 178.92, 178.05, 177.27, 176.81, 176.00, 174.85, 93.82 (CH), 93.29 (CH), 85.11 (CH$_2$), 82.30 (CH$_3$), 80.99 (CH$_3$). Elemental analysis calcd (%) for C$_{56}$H$_{58}$O$_2$S$_2$: C,

81.31; H, 7.07; S, 7.75. Found: C, 81.58; H, 7.29; S, 7.51. $[M + Na]^+ = 848.9$ m/z

6.3.3 Synthesis of L1

L1 was prepared following the same procedure of **L2** (6.3.2). Yield: 75%. ^{1}H NMR (250 MHz, CDCl$_3$, 25 °C) = δ 7.37-7.33 (m, 2H, Ar), 7.22 (d, J_{HH} = 2.3 Hz, 2H, Ar), 7.16-7.10 (m, 2H, Ar), 6.87 (d, J_{HH} = 2.4 Hz 2H, Ar), 6.10 (s, 2H, O*H*), 4.14 (s, 4H, C*H*$_2$), 1.42 (s, 18H, C*H*$_3$), 1.22 (s, 18H, C*H*$_3$). ^{1}H NMR (250 MHz, C$_6$D$_6$, 25°C) = δ 7.39 (m, 2H, Ar), 7.10-7.06 (t, J_{HH} = 8.6 Hz, 2H, Ar), 6.84 (s, 2H, O*H*), 6.71-6.59 (t, J_{HH} = 8.6 Hz, 2H, Ar), 6.27 (s, 2H, Ar), 3.82 (s, 4H, C*H*$_2$), 1.57 (s, 18H, C*H*$_3$), 1.23 (s, 18H, C*H*$_3$). ^{13}C NMR (75.4 MHz, CDCl$_3$, 25°C) = δ 151.63, 142.64, 137.24, 137.06, 132.92, 128.29, 125.58, 124.08, 121.82, 37.34 (CH), 35.16 (CH), 34.39 (CH$_2$), 31.71 (CH$_3$), 30.05 (CH$_3$). $[M + Na]^+ = 601.7$ m/z

6.3.4 Synthesis of L3

Yield: 50%. Spectroscopic data: ^{1}H NMR (300 MHz, CDCl$_3$, 25 °C) = δ 7.27-7.24 (m, 4H, Ar), 7.19-715 (m, 2H, Ar), 7.02 (d, J_{HH} = 2.6 Hz, 2H, Ar), 5.87 (s, br, O*H*), 4.11 (s, 4H, C*H*$_2$). ^{1}H NMR (250 MHz, C$_6$D$_6$, 25°C) = δ 7.05-7.01 (m, 2H, Ar), 6.88-6.84 (dd, J_{HH} = 10.9 Hz, 4H, Ar), 6.77-6.73 (m, 2H, Ar), 5.50 (s, 2H, O*H*), 3.78 (s, 4H, C*H*$_2$). ^{13}C NMR (62.9 MHz, C$_6$D$_6$, 25°C) = δ 149.19, 137.87, 131.69, 129.72, 128.18, 127.90, 126.96, 125.68, 121.34, 33.45. Elemental analysis calcd (%) for C$_{20}$H$_{14}$Cl$_4$O$_2$S$_2$: C, 48.80; H, 2.87; S, 13.03. Found: C, 48.94; H, 2.96; S, 12.94. $[M + Na]^+ = 515.2$ m/z

6.3.5 Synthesis of the complex 1

Zr(O^{t}Bu)$_4$ (0.33 g, 0.86 mmol) was dissolved in toluene (5 mL) and added dropwise to a toluene solution (5 mL) of **L1** (0.50 g, 0.86 mmol) at room temperature. The yellow solution was left under stirring for 2 h. Then, the volatiles were removed in vacuum and the desired complex **1** was washed with hexane (0.46 g, 66 % - yellow solid). Spectroscopic data: ^{1}H NMR (600 MHz, Tol-d$_8$, 25°C) = δ 7.29 (d, J_{HH} = 2.6 Hz, 2H, Ar), 6.90-6.88 (m, 2H, Ar), 6.66-6.63 (m, 2H, Ar), 6.06 (d, J_{HH} = 2.5 Hz, 2H, Ar), 4.19 (d, J_{HH} = 12.7 Hz, 2H, CH-H), 3.30 (d, J_{HH} = 12.7 Hz, 2H, CH-H), 1.77 (s, 18H, CH_3), 1.57 (s, 18H, OC(CH_3)$_3$), 1.08 (s, 18H, CH_3). ^{13}C NMR (75.4 MHz, CD$_2$Cl$_2$, 25°C) = δ 159.81, 139.05, 137.57, 136.71, 136.39, 130.55, 126.04, 123.95, 121.17, 77.47, 41.96, 35.71, 33.17, 33.00, 31.83, 30.86. Elemental analysis calcd (%) for C$_{44}$H$_{66}$O$_4$S$_2$Zr: C, 64.90; H, 8.17; S, 7.88. Found: C, 65.05; H, 8.19; S, 7.84.

6.3.6 Synthesis of the complex 2

The complex **2** was obtained in good yield (70%) starting from **L2** (0.50 g, 0.61 mmol) and Zr(O^{t}Bu)$_4$ (0.23 g, 0.61 mmol) using the same approach reported for the complex **1**. ^{1}H NMR (600 MHz, Tol-d$_8$, 25°C) = δ 7.38-7.36 (m, 4H, Ar), 7.19-7.04 (m, 18H, Ar), 6.94-6.88 (m, 2H, Ar), 6.72-6.70 (m, 2H, Ar), 5.95 (d, J_{HH} = 2.6 Hz, 2H, Ar), 4.00 (d, J_{HH} = 12.7 Hz, 2H, CH-H), 3.13 (d, J_{HH} = 17.7 Hz, 2H, CH-H), 2.29 (s, 6H, CH_3), 1.71 (s, 6H, CH_3), 1.39 (s, 12H, CH_3), 1.33 (s, 18H, OC(CH_3)$_3$). ^{13}C NMR (75.4 MHz, CD$_2$Cl$_2$, 25°C) = δ 151.60, 150.59, 149.57, 142.46, 137.43, 135.74, 131.53, 129.33, 128.40, 128.17, 127.31, 127.22, 127.02, 126.47, 125.94, 125.13, 124.13, 69.34, 42.97, 42.46, 34.22, 31.55, 31.24, 29.95. Elemental analysis calcd (%) for C$_{64}$H$_{74}$O$_4$S$_2$Zr·C$_7$H$_8$: C, 73.85; H, 7.16; S, 5.55. Found: C, 73.70; H, 7.14; S, 5.56.

6.3.7 Synthesis of the complex 3

Zr(O^{t}Bu)$_4$ (0.19 g, 0.50 mmol) was dissolved in toluene (5 mL) and added dropwise to a toluene solution (5 mL) of **L3** (0.50 g, 1.01 mmol) at 25°C. The solution was left under stirring for 2 h. Then, the volatiles were removed under reduced pressure and the desired complex **3** was washed with hexane (0.62 g, 57%). Spectroscopic data: ^{1}H NMR (600 MHz, Tol-d$_8$, 25°C) = δ 7.04 (d, J_{HH} = 2.7 Hz, 4H, Ar), 6.75-6.73 (m, 4H, Ar), 6.60-6.58 (m, 4H, Ar), 5.88 (d, J_{HH} = 2.6 Hz, 4H), 5.59 (d, J_{HH} = 12.8 Hz, 4H, CH-H), 3.19 (d, J_{HH} = 12.9 Hz, 4H, CH-H). ^{13}C NMR (75.4 MHz, CD$_2$Cl$_2$, 25°C) = δ 157.40, 136.66, 135.52, 131.08, 129.10, 127.83, 126.95, 124.61, 122.70, 41.40. Elemental analysis calcd (%) for C$_{40}$H$_{24}$Cl$_8$O$_4$S$_4$Zr: C, 44.83; H, 2.26; S, 11.97. Found: C, 44.92; H, 2.28; S, 11.93.

6.3.8 Synthesis of the complex 4

Ti(O^{i}Pr)$_4$ (0.17 g, 0.61 mmol) was dissolved into 5 mL of toluene and added dropwise to a toluene solution (5 mL) of **L2** (0.50 g, 0.61 mmol). The reaction mixture was stirred for 2 h at room temperature. After this period, the volatiles were removed in vacuum and the complex **4** was isolated as a yellow solid (0.30 g, 64%). Spectroscopic data: ^{1}H NMR (600 MHz, CD$_2$Cl$_2$, 25°C) = δ 7.34-7.33 (m, 2H, Ar), 7.24-7.04 (m, 20H, Ar), 6.89-6.87 (m, 4H, Ar), 6.03 (d, J_{HH} = 2.5 Hz, 2H, Ar), 4.38 (m, 2H, OCH), 3.61 (brs, 4H, CH_2), 1.78 (brs, 12H, CH_3), 1.38 (s, 12H, CH_3), 1.05 (d, J_{HH} = 5.4 Hz, 12H, CH(CH_3)$_2$). ^{13}C NMR (62.9 MHz, CD$_2$Cl$_2$, 25°C) = δ 161.42, 152.44, 151.98, 138.91, 137.65, 137.58, 135.46, 130.52, 128.18, 127.69, 127.64, 127.02, 126.80, 125.88, 125.56, 125.03, 122.00, 79.40, 42.60, 41.18, 31.13, 25.99. Elemental analysis calcd (%) for C$_{62}$H$_{70}$O$_4$S$_2$Ti: C, 75.13; H, 7.12; S, 6.47. Found: C, 75.29; H, 7.14; S, 6.44.

6.3.9 Synthesis of the complex 5

Hf(O^{t}Bu)$_4$ (0.28 g, 0.61 mmol) was dissolved into 5 mL of toluene and added dropwise to a toluene solution (5 mL) of **L2** (0.50 g, 0.61 mmol). The reaction mixture remained in stirring at 25 °C. Then, the volatiles were removed using a vacuum pump and the desired complex **5** recovered (0.37 g, 68%). Single crystals of the complex were grown from toluene at -20 °C. Spectroscopic data: ^{1}H NMR (600 MHz, Tol-d$_8$, 25°C) = δ 7.38-7.36 (m, 2H, Ar), 7.15-7.13 (q, J_{HH} = 6.1 Hz, 2H, Ar), 7.07-6.92 (m, 20H, Ar), 6.75-6.73 (m, 2H, Ar), 5.95 (d, J_{HH} = 2.4 Hz, 2H, Ar), 4.05 (d, J_{HH} = 12.6 Hz, 2H, CH-H), 3.20 (d, J_{HH} = 12.6 Hz, 2H, CH-H), 2.24 (s, 6H, CH_3), 1.74 (s, 6H, CH_3), 1.36 (s, 12H, CH_3), 1.33 (s, 18H, OC(CH_3)$_3$). ^{13}C NMR (75.4 MHz, CD$_2$Cl$_2$, 25°C) = δ 159.47, 152.37, 152.04, 138.22, 138.02, 136.78, 136.46, 130.76, 128.17, 127.83, 127.03, 126.84, 125.54, 125.18, 121.30, 76.85, 42.91, 42.41, 41.66, 33.10, 32.79, 31.42, 30.85, 28.29. Elemental analysis calcd (%) for C$_{64}$H$_{74}$HfO$_4$S$_2$: C, 66.85; H, 6.49; S, 5.58. Found C, 66.97; H, 6.51; S, 5.54.

6.3.10 Lactide Polymerization

A typical polymerization procedure is herein reported. In a Braun Labmaster glovebox, a Schlenk flask (10 cm^3) was charged sequentially with a toluene solution (2.4 mL) of the precatalyst (12.5 μmol) and rac-lactide (0.180 g, 1.25 mmol). The mixture was thermostated at the required temperature for a defined time. At specified time, aliquots of the polymerization mixture were sampled by a pipette and quenched in CDCl$_3$ to assess the monomer conversion by ^{1}H NMR spectroscopy. The polymerization was stopped with wet n-hexane. The obtained polymer was recovered by filtration and dried in vacuum at 40 °C for 16 h.

6.3.11 Lactide Polymerizations in the Presence of isopropanol

A typical polymerization procedure in presence of alcohol is herein reported. In a Braun Labmaster glovebox, a Schlenk flask (10 cm^3) was charged sequentially with a toluene solution (2.4 mL) of the precatalyst (12.5 µmol) and rac-lactide (0.180 g, 1.25 mmol). So, sequential additions of alcoholic solution in toluene (0.30, 0.75 or 1.5 mL of a 0.083 M) were made. The mixture was stirred with the magnetic bar and thermostated at the required temperature for a defined time. At specified time, an aliquot of the mixture was sampled by a pipette and quenched in CDCl$_3$ to determinate the monomer conversion by ^{1}H NMR. The polymerization was stopped with wet n-hexane. The obtained polymer was recovered by filtration and dried in vacuum at 40 °C for 16 h and, finally, characterized by NMR spectroscopy and GPC analysis.

6.4 Experimental part of Chapter 3

6.4.1 Synthesis of L4

In 15 mL of THF solution containing 2,4-di-*tert*-butyl-6-mercaptophenol (10 g, 41.95 mmol) and sodium *tert*-butoxide (2.01 g, 20.98 mmol) was added dropwise a THF solution (5 mL) of 1,2-bis(bromomethyl)benzene (5.53 g, 20.98 mmol). The resulting mixture was left under stirring for 3 h at room temperature. After this time, the volatiles were removed by rotary evaporated and the residue extracted with methylene chloride, obtaining a yellow oil. Finally, the oil was recrystallized with MeOH at 25°C to afford colorless crystals. Yield: 82%. Spectroscopic data: ^{1}H NMR (300 MHz, CDCl$_3$, 25 °C): δ 7.20-7.18 (m, 2H, Ar), 6.99-6.96 (m, 2H, Ar), 6.91 (s, 1H, Ar), 6.86 (s, 1H, Ar), 6.77-6.74 (m, 2H, Ar), 3.53 (s, 4H, CH$_2$), 1.27 (s, 9H,

CH$_3$), 1.12 (s, 9H, CH$_3$). ^{13}C NMR (75.4 MHz, CDCl$_3$, 25 °C): δ 153.58, 142.21, 135.98, 135.17,131.18, 130.72, 127.84, 126.21, 117.45, 37.62, 35.37, 34.38, 31.67, 29.60. MS (m/z): [M + Na]$^+$ = 601.315

6.4.2 Synthesis of the complex 6

A solution of TiCl$_4$ (1 eq., 0.86 mmol, 0.09 mL) in toluene (4 mL) was added dropwise to a toluene solution (6 mL) of **L1** (0.50 g; 0.86 mmol) at 25°C. The mixture was left under stirring for 2 h and the solvent distilled off in vacuum. The red residue was crystallized from acetonitrile at 25 °C (0.41 g, 82%). Spectroscopic data: ^{1}H NMR (250 MHz, C$_6$D$_6$, 25 °C): δ 7.34 (m, 2H, Ar), 6.60- 6.50 (m, 4H, Ar), 6.09 (m, 2H, Ar), 4.38 (d, 2H, CH$_2$), 3.15 (d, 2H, CH$_2$), 1.89 (s, 18H, CH$_3$), 1.03 (s, 18H, CH$_3$). ^{1}H NMR (250 MHz, CD$_2$Cl$_2$, 25 °C): δ 7.45-7.35 (m, 4H, Ar), 7.20 (m, 2H, Ar), 6.37 (m, 2H, Ar), 4.94 (d, 2H, CH$_2$), 3.84 (d, 2H, CH$_2$), 1.58 (s, 18H, CH$_3$), 1.06 (s, 18H, CH$_3$). ^{13}C NMR (62.5 MHz, CD$_2$Cl$_2$, 25 °C): δ = 162.20, 144.60, 137.50, 136.34, 135.22, 131.76, 126.19, 124.71, 122.88, 43.19, 35.84, 34.68, 31.51, 30.86.

6.4.2 Synthesis of the complex 7

A solution of TiCl$_4$ (1 eq., 1.11 mmol, 0.12 mL) in toluene (8 mL) was added dropwise to a toluene solution (12 mL) of **L2** (0.92 g; 1.11 mmol) at 25°C. The mixture was stirred for 2 h and the solvent distilled off in vacuum. The red residue was crystallized from acetonitrile at 25 °C (0.81 g, 89%). Spectroscopic data: ^{1}H NMR (250 MHz, C$_6$D$_6$, 25 °C): δ 7.47 (d, 2H, Ar), 7.27-7.09 (m, 18H, Ar), 6.86 (d, 2H, Ar), 6.57 (d, 4H, Ar), 5.98 (d, 2H, Ar), 4.12 (d, 2H, CH$_2$), 2.90 (d, 2H, CH$_2$), 2.25 (s, 12H, CH$_3$), 1.34 (s, 12H, CH$_3$). ^{1}H-NMR (300 MHz, CD$_2$Cl$_2$, 25 °C): δ 7.33-6.51 (m, 24H, Ar), 6.19-6.06 (m, 2H, Ar), 4.99 (d, 1H, C*H*-H), 4.39 (d, 1H, CH-*H*), 4.11 (d, 1H, C*H*-H), 3.43 (d, 1H, CH-*H*), 1.94-0.84 (m, 24H, CH$_3$).

6.4.3 Synthesis of the complex 8

A solution of $TiCl_4$ (0.15 mL, 1.38 mmol) in toluene (3 mL) was added dropwise to a toluene solution (5 mL) of **L4** (0.800 g; 1.38 mmol) was added. The mixture was stirred for 2 h and the solvent distilled off in vacuum. The red residue was washed with pentane (0.59 g, 73 %). Spectroscopic data: ^{1}H NMR (250 MHz, C_6D_6, 25 °C): δ 7.65-6.11 (m, 6H, Ar), 6.12 (m, br, 2H, Ar), 4.61 (m, br, 1H, CH-*H*), 4.39 (m, br, 2H, CH_2), 3.64 (m, br, 1H, C*H*-H), 1.71-1.07 (m, 36H, CH_3).

6.4.4 Procedure for Ethylene and Propylene polymerization using MMAO

The typical polymerizations were carried in a 250 mL Buchi glass pressure reactor equipped with a mechanical stirrer. The toluene solution (100 mL) of MMAO (7 wt% in Al, 4.30 mL toluene solution, 10 mmol) was charged into the reactor and equilibrated with the monomer feed at the appropriate temperature under mechanical stirring. The polymerization started with the addition of a toluene solution (10 mL) containing the precatalyst (10 µmol). The operating monomer pressure was 5 bar. After a definite time, the polymerization reaction was quenched in methanol acidified and the polymer recovered by filtration and dried in vacuum at 50 °C for 18 h.

6.4.5 Procedure for Ethylene and Propylene polymerization using(Ph₃C)[B(C₆F₅)₄]

The typical polymerizations were carried in a 250 mL Buchi glass pressure reactor equipped with a mechanical stirrer. The toluene solution (100 mL) of Al^iBu_3 (40 mg, 0.2 mmol) was charged into the reactor and equilibrated with the monomer feed at the appropriate temperature under mechanical stirring. The polymerization started with the addition of a toluene solution (10 mL) containing the precatalyst (10 µmol) and $(Ph_3C)[B(C_6F_5)_4]$ (5.6 mg, 10 µmol). The operating monomer pressure was 5 bar. After a definite time,

the polymerization reaction was quenched in methanol acidified and the polymer recovered by filtration and dried in vacuum at 50 °C for 18 h.

6.5 Experimental part of Chapter 4

6.5.1 Synthesis of the complex 9

Zr(O^{t}Bu)$_4$ (0.27 g, 0.71 mmol) was dissolved in THF (3 mL) and added to a THF solution (5 mL) of proligand LH$_6$ (0.50 g, 0.36 mmol) at 25°C. The reaction mixture was left under stirring for 30 min and, then, the volatiles were removed under reduced pressure. The crude product was washed twice with pentane (10 mL) and a pale-green solid was isolated in good yield (60 %).

6.5.2 Ring-opening polymerization of cyclic esters

In a typical polymerization, in a glovebox, a Schlenk flask (10 mL) was charged sequentially with monomer (0.46 mmol) and the precatalyst (4.6 µmol, 7.8 mg) in 2.4 mL of dry toluene. The mixture was thermostated at the required temperature. At specified time intervals, a small quantitate was quenched in CDCl$_3$ and analyzed by ^{1}H NMR to evaluate the relative monomer conversions. Finally, the reaction mixture was quenched with wet n-hexane and the polymers precipitated into methanol. The obtained polyesters were dried in a vacuum at 40 °C for 16 h.

6.6 Experimental part of Chapter 5

6.6.1 Synthesis of Zinc ethyl chloride adduct

A solution of $ZnEt_2$ (360 mg, 2.92 mmol, 2 equiv.) dissolved in CH_2Cl_2 (4 mL) was added dropwise, under stirring, to a CH_2Cl_2 solution (6 mL) of the appropriate imidazolium chloride salt (500 mg, 1.46 mmol, 1 equiv.) at room temperature. After 2 h, the volatiles were removed in vacuum and the residue washed with pentane (2x10 mL), obtained a light oil. Yield: 90%. ^1H NMR (400 MHz, C_6D_6, 25°C) = δ 7.11 (s, 2H, CH=CH), 7.00 (s, 4 H, Ar-H), 0.84 (t, J = 8.5 Hz, 3H, $ZnCH_2CH_3$), 0.22 (q, J = 8.0 Hz, 2 H, $ZnCH_2CH_3$).

6.6.2 Synthesis of the complex 10

A solution of BnOH (0.30 mL, 316 mg, 2.92 mmol) in CH_2Cl_2 (4 mL) was added dropwise to a solution of ZnClEt-adduct (500 mg, 1.46 mmol) in CH_2Cl_2 (6 mL) at room temperature. The reaction mixture was stirred at RT for 2 h. The volatiles were then removed in vacuum and the residue washed with pentane. Complex **10** was isolated as a yellow solid after recrystallization from a CH_2Cl_2/pentane solution. Yield: 65%. ^1H NMR (500 MHz, C_6D_6, 25°C) = δ 7.58 (m, 2H, Ar-H), 7.35 (m, 2H, Ar-H), 7.08 (s, 1H, Ar-H), 6.52 (s, 4H, Ar-H), 5.79 (s, 2H, CH=CH), 4.32 (br, d, 1H, OCH_2), 3.73 (br, d, 1H, OCH_2), 2.02 (s, 6H, CH_3), 1.96 (s, 12H, CH_3). ^{13}C NMR (125 MHz, C_6D_6, 25°C) = δ 148.33, 141.67, 138.51, 135.17, 129.31, 126.85, 126.58, 125.61, 124.25, 122.45, 64.52, 20.89, 17.57.

6.6.3 Synthesis of the complex 11

A solution of BnOH (0.38 mL, 395 mg, 3.65 mmol) in CH_2Cl_2 (5 mL) was added dropwise to CH_2Cl_2 solution (6 mL) of ZnBrEt-adduct (572 mg, 1.83 mmol) at 25°C. The reaction mixture was stirred at RT for 2 h. The volatiles were then removed in vacuum and the oil residue was washed with pentane

(10 mL). Complex **11** was recovered by recrystallization at -40°C from a CH$_2$Cl$_2$/pentane solution (1:2 v/v). Yield: 75%. ^{1}H NMR (500 MHz, C$_6$D$_6$, 25°C) = δ 7.05-7.42 (m, 5H, Ar-*H*), 5.81 (s, 1H, CH=C*H*) and 5.66 (s, 1H, CH=CH), 4.59 (br, 2H, OC*H*$_2$Ph), 4.09 (t, J = 7 Hz, 2H, C*H*$_2$CH$_2$CH$_2$CH$_3$), 3.63 (s, 3H, NC*H*$_3$), 1.45 (m, J = 8 Hz, 2H, CH$_2$C*H*$_2$CH$_2$CH$_3$), 1.28 (m, J = 8 Hz, 2H, CH$_2$CH$_2$C*H*$_2$CH$_3$), 0.83 (t, J = 7 Hz, 3H, CH$_2$CH$_2$CH$_2$C*H*$_3$). ^{13}C NMR (125 MHz, C$_6$D$_6$, 25°C) = δ 172.44 (NCN), 143.90, 137.70, 127.89, 127.71, 122.07, 120.36, 65.66, 50.55, 38.32, 34.20, 20.29, 14.36.

6.6.4 Synthesis of the complex 12

A solution of BnOH (0.32 mL, 335 mg, 3.10 mmol) in CH$_2$Cl$_2$ (5 mL) was added to a dichloromethane solution (5 mL) of ZnIEt-adduct (492 mg, 1.55 mmol) at room temperature. The reaction mixture was stirred for 2 h at 25°C. Then, the volatiles were removed in vacuum and the oil residue washed with hexane (10 mL). Complex **12** appeared as a yellow solid after crystallization from a CH$_2$Cl$_2$/pentane solution (1:2 v/v). Yield: 84%. ^{1}H NMR (500 MHz, CDCl$_3$, 25°C) = δ 7.37-7.32 (m, 5H+2H, Ar-*H*+C*H*=C*H*), 4.67 (s, 3H, NC*H*$_3$), 3.84 (s, 2H, OC*H*$_2$Ph). ^{13}C NMR (125 MHz, CDCl$_3$, 25°C) = δ 136.90, 128.46, 127.39, 127.09, 123.42, 65.17, 36.77.

6.6.5 Representative Copolymerization Epoxides and Anhydride Procedure

A Schlenk tube (10 mL), with a magnetic stirring bar, was charged sequentially with CHO (190 mg, 1.94 mmol), SA (194 mg, 1.94 mmol) and the zinc complex (19.4 µmol). The reaction mixture was stirred at 110°C for a desired time. At the beginning the mixture appeared heterogeneous, but the reaction system began homogeneous for high monomers conversions. After this time, an aliquot of the crude polymerization mixture was checked by ^{1}H NMR spectroscopy to evaluate the monomer

conversions. The polymer was precipitated in MeOH and dried in vacuum overnight.

6.6.7 References

[82] Biela, T.; Duda, A.; Penczek, S.; *Macromol. Sym*p., **2002**, *183*, 1.

PUBLICATIONS ON THE PhD PROJECT

- ➢ "Stereorigid OSSO-Type Group 4 Metal Complexes in the Ring-Opening Polymerization of *rac*-Lactide". Lapenta, R.; Buonerba, A.; De Nisi, A.; Monari, M.; Grassi, A.; Milione, S. and Capacchione, C. *Inorg. Chem.*, **2017**, *56*, 3447–3458.

- ➢ "Dinuclear Zirconium Complex Bearing 1,5-Bridged-Calix[8]arene Ligand as Effective Catalyst for the Synthesis of Macrolactones". Lapenta, R.; De Simone, N. A.; Buonerba, A.; Talotta, C.; Gaeta, C.; Neri, P.; Grassi, A.; Milione, S. *submitted.*

OTHER PUBLICATIONS

- ➢ "Brain insulin resistance impairs hippocampal synaptic plasticity and memory via FoxO3a/zDHHC3-dependent enhancement of GluA1 palmitoylation". Spinelli, M.; Fusco, S.; Mainardi. M.; Scala, F.; Natale, F.; Lapenta, R.; Mattera, A.; Rinaudo, M.; Li Puma, D. D.; Ripoli, C.; Grassi, A.; D'Ascenzo, M.; Grassi, C. *Nature Communications*, **2017**, *8*.

- ➢ "A Comprehensive Depiction of the Furan-Maleimide Coupling via Kinetic and Thermodynamic Investigations of the Diels-Alder Reaction of Poly(styrene–co-2-vinylfuran) with Maleimides" Buonerba, A.; Lapenta, R.; Ortega Sánchez, S.; Capacchione, C.; Milione, S. and Grassi, A. *ChemistrySelect* **2017**, *2*, 1605 – 1612.

➢ "Monoamidinate titanium complexes: highly active catalysts for the polymerization and copolymerization of L-lactide and ε-caprolactone". Lapenta, R.; Mazzeo, M. and Grisi. F. *RSC. Adv*., **2015**, *5*, 87635-87644.

CONTRIBUTION TO CONFERENCES

- Stereorigid OSSO-Type Group 4 Metal Complexes in the Polymerization of Olefins and Polar Monomers *(Lapenta, R.; Buonerba, A.; De Nisi, A.; Monari, M.; Grassi, A.; Milione, S. and Capacchione, C.).* In: XXVI Congresso Nazionale della Società Chimica Italiana, 10-14 September 2017- Paestum (SA). (**ORAL COMMUNICATION**)

- Copolymerization of Propylene Oxide with Succinic Anhydride using Dinuclear Zinc-N-heterocyclic carbene complexes (*Lapenta, R; Milione, S.; Grassi, A. and Dagorne, S.).* In: XXVI Congresso Nazionale della Società Chimica Italiana, 10-14 September 2017- Paestum (SA). (**POSTER**)

- New [OSSO]-type group 4 complexes as catalysts for the polymerization of *rac*-lactide *(Lapenta, R.; Buonerba, A.; De Nisi, A.; Monari, M.; Grassi, A.; Capacchione, C. and Milione, S.).* In: 4th Blue Sky Conference on Catalytic Olefin Polymerization (Sorrento, Italy), 27 June – 1 July 2016. (**POSTER**)

- Monoamidinate titanium complexes: highly active catalysts for the polymerization and copolymerization of L-lactide and ε-caprolactone *(Lapenta, R.; Mazzeo, M. and Grisi. F.).* In: XIX Congresso Nazionale della Divisione di Chimica Industriale organizzato dalla Società Chimica Italiana (Salerno), 14-16 September 2015. (**POSTER)**